Coexistence in a size-structured model of marine ecosystems

– M.Sc. Thesis Report

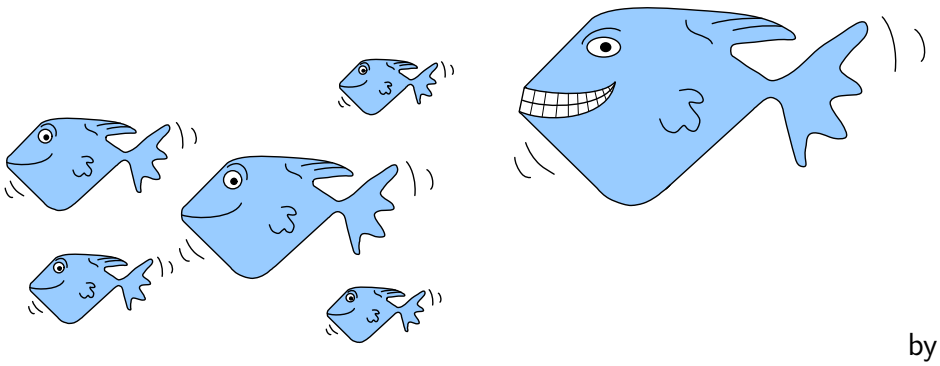

by

Martin Pedersen

Student ID: s991237

Supervisors:

Ken H. Andersen
Department of Marine Fisheries
Danish Institute for Fisheries Research (DIFRES)

Tomas Bohr
Department of Physics (FYS)
Technical University of Denmark (DTU)

Friday 28th July, 2006

Abstract

A simple size-structured dynamic population model focusing on the higher trophic levels of marine ecosystems is presented. The model encapsulates a high degree of ecological realism in its construction since it is based on a description of individual-level physiology, and it is denoted *simple* since only one trait, the ultimate body weight w_∞, is used to characterise a species.

The key component in the model is an individual-level bioenergetic growth model that allocates the acquired energy from size-dependent food intake into somatic growth, maintenance, and reproduction. The environment of an individual is completely determined by the spectra of all species and a background spectrum that provides resources to smaller individuals. From the environment the food intake is calculated, and from this the mortality and reproduction of the individuals are obtained.

Smaller species can reach the size of maturation solely on the background resources, whereas larger species need larger food items as i.e. the smaller species to reach maturation and thus sustain their populations. This mechanism, denoted the *trophic ladder*, is shown to make coexistence possible in the setting of a completely mixed environment where everybody is capable of eating everybody if they are of a suitable size.

A framework is provided that allows the model to be used for size-structured food webs. All species have preferences in [0; 1] to other species and the background spectrum. The preferences times the size-selection function, that individuals use for prey selection, correspond to interaction strengths in classical unstructured food webs. It is shown that both the food web *structure* and the *preference strengths* are important for coexistence.

Coexistence is moreover demonstrated using a third mechanism denoted switching, where individuals constantly switch their diet to the species that provides the largest amount of suitable food items.

Resumé

En simpel størrelsesstruktureret dynamisk populationsmodel, der fokuserer på de øvre trofiske niveauer i marine økosystemer, præsenteres. Modellen udviser en høj grad af økologisk realisme i dens udformning, da den er baseret på individers fysiologi, og betegnes *simpel*, da kun ét karaktertræk, den højst opnåelige individvægt w_∞, bruges til at karakterisere en art.

Hovedkomponenten i modellen er en individbaseret bioenergetisk vækstmodel, der allokerer den optagede energi fra størrelsesafhængigt fødeindtag til somatisk vækst, maintenance, og reproduktion. Miljøet, som et individ befinder sig i, er komplet beskrevet af alle arters spektre og et baggrundsspektrum, der forsyner de mindste individer med ressourcer. Fra miljøet beregnes fødeindtag, og fra dette bestemmes individernes dødelighed og reproduktion.

Mindre arter kan nå gydemodenhedsstørrelsen alene på baggrundsressourcer, hvorimod store arter kræver større fødeemner, som f.eks. de mindre arter, for at nå gydemodenhedsstørrelsen og derved opretholde deres populationer. Denne mekanisme, der betegnes en *trofisk stige*, muliggør sameksistens i et fuldstændigt blandet miljø, hvor alle kan spise alle, hvis blot de har en passende størrelse.

Modellen kan bruges til beskrivelse af størrelsesstrukturerede food webs. Alle arter har præferencer i [0; 1] til andre arter og baggrundsspektret. Præferencerne multipliceret med størrelsesselektionsfunktionen, som individerne bruger til byttedyrsudvælgelse, svarer til interaktionstyrker i klassiske ikke-strukturerede food webs. Det vises, at både *strukturen* og *præferencestørrelserne* i et food web er vigtige for sameksistens.

Sameksistens er desuden demonstreret med en tredje mekanisme kaldet switching, hvor individer konstant skifter deres fødeindtag til den art, der tilbyder den største mængde passende fødeemner.

Preface

This thesis has been submitted to obtain the Master of Science degree at the Technical University of Denmark (DTU). The project was carried out at the Department of Physics (FYS), and the Danish Institute for Fisheries Research (DIFRES) under supervision by Tomas Bohr and Ken H. Andersen. The thesis work was carried out with DIFRES as my location in the period from August 2005 to July 2006.

The presented work marks my transition from engineering (i.e. Hales & Pedersen (2002), Fléron et al. (2003), Pedersen et al. (2003)) into theoretical ecology. Since I have had no prior training in the field I attended three workshops as part of the project: SICC's *Analysis of Innovation and Competition Processes* (Milan, Italy, May 16-18, 2005), NMA's *Modelling Marine Populations from Physics to Evolution* (4 ECTS, Bergen, Norway, October 10-16, 2005), and SENSE's *Community Ecology: Processes, Models and Applications* (2 ECTS, Zeist, the Netherlands, November 6-11, 2005).

I would like to thank my supervisors Ken and Tomas for allowing me to do this thesis. Especially I acknowledge the huge amount of time Ken has invested in my project. I am grateful for your inspiration, and the many fruitful discussions we have had. Also I am thankful for your assistance in the search of a Ph.D. position, which resulted in a really interesting position at the Department of Theoretical Ecology at Lund University. I am looking forward to do more research with you. Thank you!

Thanks to everybody in the study group at DIFRES for many interesting sessions, our librarians Gitte and Carina, and Oticon Fonden for providing me with a scholarship that allowed me to participate in the three workshops, buy the laptop this thesis is written on, and for assisting me in not taking up too many loans to support myself during the work of my thesis. Iben, Lotte, Jeppe, and Jacob: thanks for our time in the student room. My good friends Thomas, Steve-O, Soda, Søren, Anders, and Rasmus thanks for your support, patience and understanding the last months. To the rest of you: may we soon meet again for good times. I also wish for good times and health in my family, which have been suffering too much from illnesses the last years.

My friend in life, Carlos, I am grateful for our friendship and hopefully we will soon again find *The Way of a Trout with a Fly*. Mathilde, thanks for your love and support – I am looking forward to your return from Canada.

Martin Pedersen
Copenhagen, Denmark
Friday 28th July, 2006

Student ID: s991237

Contents

1

Introduction

This chapter contains the formal introduction to the thesis. The objectives of the thesis is stated followed by an outline of the structure of the report.

1.1 Objectives

The objective of this thesis is to locate mechanisms that enables species coexistence in a size-structured model of marine ecosystems. The ecosystem model should be based on the model formulation by Andersen (2005) where coexistence has not been demonstrated.

1.2 Thesis Outline

Chapter 2 is the scientific introduction to this thesis. Inhere an introduction to size-structured models is given along with an introduction to why such models encapsulates much more ecological realism than their unstructured counterparts in aquatic environments. In size-structured models the population of a species is described by a density spectrum that describes the composition of the different sized individuals in the species population. In the chapter the Partial Differential Equation (PDE) that links individual-level processes of growth, mortality, and reproduction to the populations dynamics is derived. One of the advantages of the size-structured models is that the population dynamics emerge from the individual-level processes why the parameters in the model are naturally assessed since assessment of individual-level processes is more easy than assessment of population-level processes. The concept of the community spectrum is also introduced, which is the spectrum consisting of all individuals across all species.

The simple size-structured model that is later used to study coexistence is derived in chapter 3. This model is based on the formulation by Andersen (2005), but all parts of the model are more elaborately derived and some parts are modified. The derived model is denoted *simple* since only one trait, the ultimate body weight w_∞, is used to characterise a species. A bioenergetic growth model is derived that allocates the acquired energy from food intake into somatic growth, maintenance, and reproduction. The growth model is the key component of the ecosystem model since it determines the growth trajectory of the individuals. Mortality is

implemented as predation mortality from size-dependent food intake, starvation mortality if acquired energy is insufficient, and a background mortality that covers other sources of mortality and makes sure that the largest individuals are exposed to a mortality rate. The egg-stage is not modelled explicitly, but egg mortality is included when the reproduction effort of the matured individuals is routed into production of new recruits. Size-dependent food intake are realised with a size-selection function that enables a predator to eat of primarily smaller individuals with some selection width. Due to the size-dependent intake suitable food items are needed for the smallest individuals, and to solve this problem a background spectrum is included. The background spectrum represents the lower half of the community spectrum as i.e. (zoo)plankton, and the spectra of the species represent the upper half of the community spectrum. The details of how the resources are modelled are also treated in the chapter. The environment that an individual experiences is completely determined by all species spectra and the background spectrum from which the food intake is found, which then returns the experienced mortality and the reproduction of all matured individuals.

Chapter 4 treats the numerical setup that is needed to solve a PDE for each species along with a series of ODEs that describe the dynamics of the background resources. In the chapter convergence tests are carried out to find the number of required grid points in the species spectrum resolution along with the minimum required step size in the time dimension.

In chapter 5 the model from chapter 3 is examined using just a single species. First an analytical solution is found for the species spectrum in a reduced steady-state version of the full model. The distribution of different w_∞ species in the community spectrum is also found. This is followed by a numerical investigation using just a single species in the complete model. This is done to gain an understanding of the dynamics present in the model before advancing to multi-species studies.

A first mechanism for multi-species coexistence is located in chapter 6. Larger species need smaller species to acquire enough energy in the larger size stages to reach the size of maturation. Thus the mechanism enables coexistence since larger species need smaller species as a *trophic ladder*. This mechanism allows species coexistence in a completely mixed environment setting where everybody is capable of eating everybody if they are of a suitable size.

The structure of a food web configuration naturally also plays a role for species coexistence, and in chapter 7 the model from chapter 3 is generalised to be used as a framework for size-structured food webs. The framework allows preferences in $[0; 1]$ to both other species and the background resources. The preferences are different from interactions strengths in classical food web theory since the interaction strength in the size-structured framework is the preference times the size-selection function that is a function of prey and predator sizes. In the chapter it is shown that both the *structure* and the *preference strengths* are important for coexistence.

Chapter 8 provides the discussion of the main results along with suggestions for future research. Chapter 9 contains the conclusion, which rounds off the thesis.

1.3 Errata

Before print an error was discovered. Many figures print the unit of κ to be $[\mathrm{g/m^3}]$ instead of the correct unit of $[\mathrm{g}^{1+\lambda}/\mathrm{m^3}]$.

2

Structured Population Models

Why should we use the more complex structured population models instead of the simpler unstructured counterparts? This question is answered in this chapter to motivate the need for the model presented in chapter 3. A discussion on the outline of the structured models is also given. Following this the conservation equation for the structured systems is derived. Finally a brief introduction to the concept of a community spectrum is given. This concept is needed in chapter 3 when resources are introduced to the model.

2.1 Motivation for Structured Population Models

In unstructured population models such as i.e. Lotka-Volterra models (Lotka (1925) and Volterra (1926)) the populations are modelled as numbers, concentrations or biomasses. When species in such models are coupled in i.e. consumer-resource relationships then intake by the consumer of the resource immediately appear as an extra abundance or biomass of the consumer, and since intake are proportional to the abundance or biomass then this has the effect that the consumer population has instantaneously increased its population. Thus intake is immediately transformed into a larger population in unstructured models. In real life this is definitely not the case since reproduction is not an instantaneous process.

However, on a larger time-scale this might not be a problem in a modelling approach if the offspring will have diets comparable to the parents. Lion offspring are i.e. fed by the adults. However, in e.g. aquatic communities fish offspring must first go through an egg-stage where they suffer from a high mortality. Then they start their life with a diet very different from their parents and continue to change diet composition till they reach the adult stage where they will finally have the same diet as its parents. The diet composition is mainly determined through a size-dependent consumer-resource interaction. Thus for i.e. fish it is a bad approximation that the intake can be directly transformed into an increase of the population since there is a time-delay from the time of intake by the adult fish till it effectively causes an increase in the adult fish population. This process might take several seasons whereas the lion cub will have the same net effect on predation through its parents close to its birth.

The time-delay is not the most important difference between the two cases. More

notable is the very different life-histories. The lion cub is born and is being fed and protected by the parents, which clearly means that the age of the lion has a smaller effect on its mortality and diet composition. For fish this is very different. First they suffer from a high egg mortality, secondly they hatch at a very small size where they are vulnerably to both predation and other death causes. Thirdly they grow in size, and change their diet and potential enemies. They actually grow to become their own enemy. Fish may grow from the mg regime to the kg regime, which is six orders of magnitude! Notable is also that a female fish may produce several millions of eggs throughout its life, but that only two have to survive to sustain the population.

The size of individuals has implications beyond determining the trophic position, since it plays a large role in determining the type and strength of ecological processes that occur within a community. Most life-history processes such as food selection, foraging rates, growth, maturation, reproduction and mortality are functions of body weight. Peters (1983), Calder III (1984), Schmidt-Nielsen (1984), and McMahon & Bonner (1983) give details on allometric scaling relations and Werner & Gilliam (1984), Sebens (1987), and Ebenman & Persson (1988) provides theory on size dependent growth and interactions. The metabolic theory (Brown et al. (2004)*) and Dynamical Energy Budgets (DEB) frameworks are new approaches that provide theoretical frameworks for allometric scaling relations.

Complex life-histories as the one outlined for fish clearly requires a more elaborate modelling framework to incorporate realism – or at least to check that the unstructured modelling approach is sufficient.

The immediate solution to this problem is to introduce stage-structured models and model the discrete jumps between states (i.e. juveniles and adults). In the continuous model regime, which is the model regime considered in this thesis, the most simple method would be to employ Delay Differential Equation (DDE) models which can take into account i.e. the time required for maturation. An introduction to both of these methods may be found in Tuljaparker & Caswell (1996).

Instead of modelling the population dynamics directly we may take another approach where we start out by modelling the life-history of the individuals. Figure 2.1 shows a class of identical individuals (super-individuals) that are born at time step t_0 with size w_0. As time elapses they grow in size and decrease in numbers due to mortality. At some size they reach maturity and may start producing new recruits – and finally they have all disappeared because of mortality near some maximum size w_∞, which is the maximum size the individual can obtain. This discrete problem may easily be made continuous by making infinitesimal time steps and including a continuous range of super-individuals. With this approach we may include size-dependent processes in addition to the inclusion of the time-delay.

This approach is more intuitive than e.g. the DDE approach since we do not have to know how to model the population dynamics explicitly. Instead we can make models based on the individuals' physiology and life-history parameters, which are also easier to measure. This along with their size-structured interactions will then return the population dynamics. This kind of models are known as Physiologically Structured Population (PSP) models or merely size-structured models and they are the basis of the thesis at hand.

Figure 2.2 illustrates how we move from examining a class of super-individuals

*Marquet et al. (2005) provides a nice review including a show-case for the importance of size in especially aquatic environments.

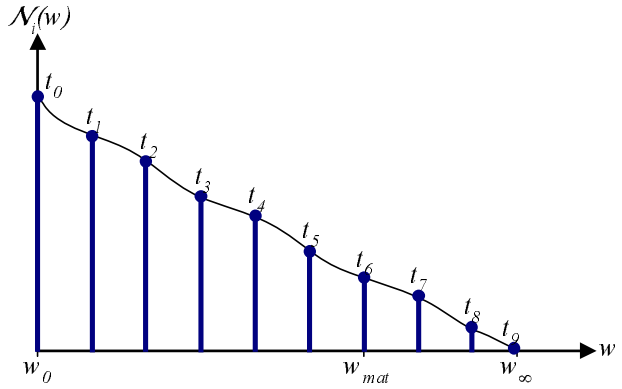

Figure 2.1: A class of identical individuals (super-individuals) at different time steps. Along the x-axis we have body size (i.e. weight) and the y-axis shows abundances (numbers/volume). Individuals enter the spectrum at size w_0, become reproductive (mature) at w_{mat}, and may obtain the asymptotic maximum size w_∞. Note that the time-steps should not necessarily be interpreted as being equally sampled since we do not expect a constant growth rate throughout the life of the individuals.

to a more general class consisting of all individuals within a species. Each species i is modelled with a continuous *density spectrum* $n_i(w,t)$ which contains the density (numbers per size per volume) of the species composition at time t in regards to body size w – that is: the density spectrum is a size-distribution consisting of infinitely many super-individuals. The dynamics within this spectrum is controlled by growth and mortality functions which again are dependent of interactions with other species. So, the super-individuals are described with individual-level functions and the population dynamics emerges from this. This means that the model is parameterised with individual-level parameters which are assessable. Thus we are moving away from the abstraction of unstructured models that are difficult to parameterise, to more concrete models where the parameters are more easily assessed.

So, super-individuals may grow in size, die off and have the option of reproducing if they have matured and have enough energy. Hatching mortality may be included by inferring a mortality on the transfer of the reproduction into w_0 sized recruits in the left-hand side of the spectrum. The figure furthermore shows that the species is cannibalistic with some size selection, which could as well be some size-dependent interaction with another species. This clearly illustrates that size-structured models encapsulates a lot of realism when time-delays and size-dependent processes are important. In nature super-individuals naturally do not exist, but should merely be considered as the average of the individual diversity.

The size w of the super-individuals may be length, volume, mass, age etc. However age is not very appropriate in an aquatic system since the physical size more or less determines the trophic position; so *age* is not a good variable for describing the *physiological state*. In the models considered in this thesis weight is selected as the physiological variable since i.e. metabolic requirements are easily measured in terms of weight. However, length could also be used since it is possible to define functions within a species that create a one-to-one map between weight and length. The symbol w is used for weight instead of m for mass since there is tradition for this in the literature of theoretical biology and fisheries research.

The articles de Roos & Persson (2001) and de Roos et al. (2003a) give a more

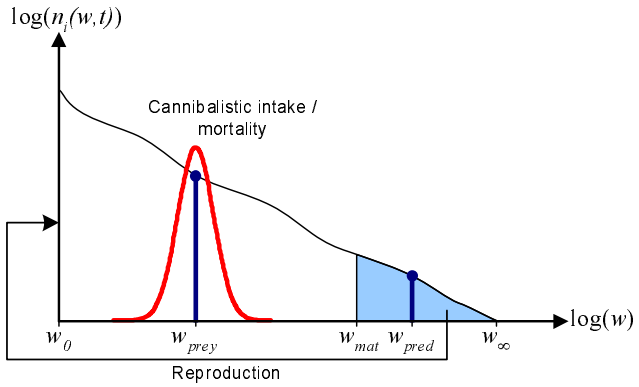

Figure 2.2: Spectrum (numbers/weight per volume) of one species with two outlined super-individuals – a prey and a predator of weights w_{prey} and w_{pred}, These act in a predator-prey relationship, where the predator has a food selection function (red curve). In this case the species feeds upon itself (cannibalism), but it is easy to imagine how this predation could be inflicted on another species' spectrum. A reproductional flux of new individuals (recruits) of size w_0 is produced by individuals that has passed the size of maturation w_{mat}. The axes are in logarithmic scale, which proves more illustrative when plotting natural size spectra.

in-depth introduction to why size-structured models are important along with more detailed references to experimental results. However, this introduction should have underlined the most important reasons for employing a more detailed modelling framework in aquatic systems: size matters for species that grow six orders in magnitude throughout their life since their enemies and feeding items are determined primarily by their size. We model individual-level processes and obtain population-level dynamics. An analogy may be drawn to statistical physics where atom level processes are described and thermodynamical descriptions emerge.

2.2 Outline of Structured Population Models

The first age-structured model by McKendrick (1926) was published almost at the same time as the unstructured counterparts by Lotka (1925) and Volterra (1926). McKendrick (1926) introduced the explicit Partial Differential Equation (PDE) continuous age-structured model in an example of epidemics, and von Foerster (1959) rediscovered the same PDE when describing the age-structure of a cellular population. These works are generalised by Sinko & Streifer (1967), which present a one-species model that can be used to model both the size- and age-structure of a population.

These models do not explicitly consider the individuals' interactions with resources and predators. Most probably since they were limited to consider analytical solutions of highly simplified – and somewhat biologically uninteresting – one-species versions. As indicated in the discussion of size-dependent life-history attributes in the last section these interactions are clearly important, and studies of them have been enabled with the introduction of computers and numerical techniques. The Physiologically Structured Population (PSP) models by Metz & Diekmann (1986) (compilation of lecture notes on PSP models) and de Roos et al. (1992) were apparently the first to include the size-dependent interactions in the continuous regime

with the aid of the Escalator Boxcar Train (EBT) numerical technique (de Roos (1988)) for solving the required PDE. A nice text-book examination can be found in de Roos (1996). In the PSP modelling notation there is a distinction between *the old* size-structured models and the new PSP models, and the former are called a subclass of PSP (e.g. de Roos et al. (2003a)). In this thesis I will however not distinguish between the notions size-structured and PSP since the models are structurally equivalent.

As indicated in the previous section and by considering figure 2.1 and 2.2 the dynamics of the size spectrum is definitely influenced by each individual's growth, mortality, and reproduction. This is essentially the functions needed to describe the evolution of each individual's state – or i-state to use the terminology set forward in Metz & Diekmann (1986) and de Roos (1996). In the models examined in this thesis it is assumed that only one state variable, namely the weight, is needed to distinguish super-individuals from each other within each species. In the model all individuals with the same size (super-individuals) are assumed to have identical behaviour.

At present unstructured population models are used in dynamic food webs; however inclusion of some size-specific parameters can be included by using the formulation by Yodzis & Innes (1992) where the parameters are more easily linked to real species parameters. The studies by the de Roos and Persson groups only consider one species size-structured and describes i.e. resources with unstructured models. This thesis will extend the pioneering work of de Roos and Persson and model more interacting species using a size-structured model (chapter 3), which is used to formulate size-structured food webs (cf. chapter 7).

Together with the i-states the *environment* (E-state) naturally plays an important role for the population dynamics. The E-state captures quantities that influence the behaviour of each individual. For instance the available food density, predator density, temperature, salinity etc. So it is important to point out that the E-state can be a function of may variables; $E(\phi(w), p_i(t), T, S, \ldots)$.

The i- and E-states give the resulting population dynamics via their interactions. The population state (p-state) can in size-structured models easily be described by the density function $n_i(w,t)$ over the i-state space. In the considered model the density function is a function of time and weight. Before proceeding with the description of the dynamics we will dwell on the basics of the density function for a while.

Figure 2.3 shows the size spectrum of a general species i^*. The distribution of individuals at different weights w at time t are described by the density function $n_i(w,t)$, which has dimensions number of individuals per mass per volume†. The number of individuals per volume in the size range $[w_1;\, w_2]$ is thus:

$$\aleph_{i,[w_1;\,w_2]}(t) = \int_{w_1}^{w_2} n_i(w,t)\,\mathrm{d}w \tag{2.1}$$

One of the most important relationships is of course the relation to species biomass. Unstructured models typically use abundance or biomass as the currency

*It should be noted that i subscripts used in this thesis indicate i^{th} specie, and *not* the individual i-state.

†Readers with a physical background may be well suited in density formulations from quantum mechanics, where electron densities are the key to all system property calculations in Density Functional Theory (Kohn (1999)).

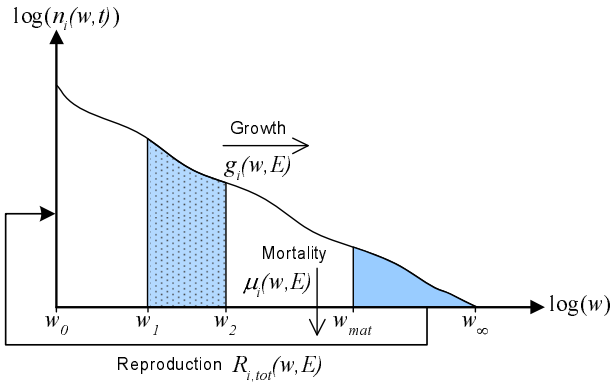

Figure 2.3: The density function of specie i over the individual state variable w. Individuals move up in the size hierarchy via growth, may leave the density spectrum due to mortality, and reproduce after having matured at a given size.

for population modelling. The total biomass per volume of species i in size range $[w_1; w_2]$ at time t is calculated as:

$$B_i(t) = \int_{w_1}^{w_2} n_i(w,t) w \, \mathrm{d}w \tag{2.2}$$

The i-state of each individual is controlled by its growth rate $g_i(w,E)$ and its mortality rate $\mu_i(w,E)$. Production of recruits is a function of each individual's reproduction rate per individual per volume, $\tilde{R}_i(w,E)$. All three functions are naturally dependent on both the i-state variable w and the current E-state. Working with density functions is quite common in engineering and physics, and it may be used to obtain total properties for the species as for example the total reproduction rate (number of recruits per volume per time):

$$R_{i,tot}(t) = \int_{w_0}^{w_\infty} \tilde{R}_i(w,E) n_i(w,t) \, \mathrm{d}w = \int_{w_{mat}}^{w_\infty} \tilde{R}_i(w,E) n_i(w,t) \, \mathrm{d}w \tag{2.3}$$

Recruits are being produced at a minimum species size w_0* and if they do not die they will grow asymptotically towards the size w_∞ ($w \in [w_0; w_\infty[$). Individuals mature at size w_{mat}, and may contribute to the total spawning till their death; the possibility of shrinking in size is treated in section 3.2.3. The point of maturation w_{mat} does not have to be a step function, but can be a smooth function over an interval (only the first integral in (2.3) is then valid). It should be noted that the model does not exclude the possibility of modelling species with determinate growth (that is no body growth after maturation) since these may included by making the $[w_{mat}; w_\infty[$ region very small by making the growth rate go to zero after maturation.

With this short introduction enough notions should be available to derive the equation describing the dynamics of the p-states in the next section.

2.3 Derivation of the Spectrum Dynamics PDE

To model the dynamics of the size spectrum (the p-state) considered in the previous section we need a differential equation describing the dynamics. This must be a PDE

*i subscripts on w_b, w_{mat}, and w_∞ are omitted for notational simplicity.

since we want to examine the evolution in both time t and individual body size w.

Figure 2.4 shows the density spectrum of a species i, and the inset is used to derive the PDE. The environmental state may e.g. in a simple case be thought of as the total spectrum of species for consumption (including cannibalism) and predators that will predate on species i. That the environment is a function of time naturally has the effect that the growth, mortality, and reproduction become time dependent. More info on the E-state in the model of this thesis is given in section 3.1.

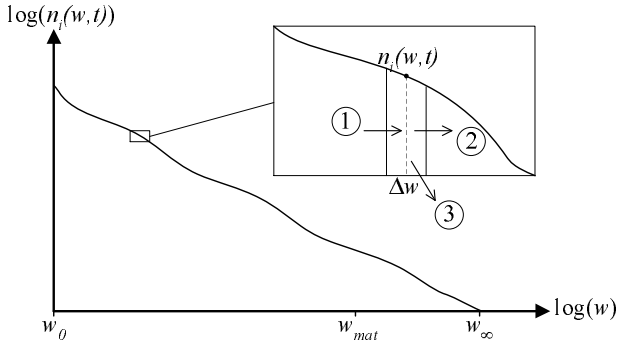

Figure 2.4: Density spectrum with inset that shows a small interval of Δw that is used to derive the PDE describing the dynamics of the p-state.

When looking at a small interval of Δw in the density spectrum, as shown in figure 2.4, the density may be changed in three ways: (1) by individuals growing into the interval, (2) by individuals growing out of the interval, and (3) by individuals dying and hence leaving the density spectrum. This naturally requires that $g_i(w, E)\Delta t \ll \Delta w$ since the argument fails if individuals can pass the selected interval without residing in it at any time step. Fulfilling this requirement is not problematic since Δt and Δw always can be selected to do so. The flux of individuals in and out of the selected region in a time step Δt is:

$$(1) \quad g_i(w - \frac{1}{2}\Delta w, E)n_i(w - \frac{1}{2}\Delta w, t) \tag{2.4a}$$

$$(2) \quad - g_i(w + \frac{1}{2}\Delta w, E)n_i(w + \frac{1}{2}\Delta w, t) \tag{2.4b}$$

$$(3) \quad - \mu_i(w, E)n_i(w, t)\Delta w \tag{2.4c}$$

For the last contribution we have used that Δw is very small and that $n_i(w, t)\Delta w$ gives the total number of individuals per volume within Δw at time t. If we use this principle again we may find the number of individuals in Δw at a later time $t + \Delta t$ as $n_i(w, t + \Delta t)\Delta w$. By assuming that the fluxes in (2.4) are constant during a small time step Δt and setting the fluxes multiplied with Δt up as a conservation equation we get:

$$\begin{aligned} n_i(w, t + \Delta t)\Delta w - n_i(w, t)\Delta w = {} & g_i(w - \frac{1}{2}\Delta w, E)n_i(w - \frac{1}{2}\Delta w, t)\Delta t \\ & - g_i(w + \frac{1}{2}\Delta w, E)n_i(w + \frac{1}{2}\Delta w, t)\Delta t \\ & - \mu_i(w, E)n_i(w, t)\Delta w\Delta t \qquad \Leftrightarrow \end{aligned}$$

$$\frac{n_i(w,t+\Delta t)-n_i(w,t)}{\Delta t} = -\mu_i(w,E)n_i(w,t) + \frac{g_i(w-\frac{1}{2}\Delta w,E)n_i(w-\frac{1}{2}\Delta w,t) - g_i(w+\frac{1}{2}\Delta w,E)n_i(w+\frac{1}{2}\Delta w,t)}{\Delta w}$$

By remembering the definitions for derivatives and letting $\Delta t \to 0$ and $\Delta w \to 0$ while fulfilling $g_i(w,E)\Delta t \ll \Delta w$ we get the PDE describing the dynamics of the p-state:

$$\frac{\partial}{\partial t}n_i(w,t) + \frac{\partial}{\partial w}\Big(g_i(w,E)n_i(w,t)\Big) = -\mu_i(w,E)n_i(w,t) \tag{2.5}$$

where the first term describes time evolution of the density spectrum $n_i(w,t)$ and the second term the advancement in the spectrum of the super individuals via the growth function $g_i(w,E)$. The term on the right-hand side is a sink term, which takes into account that parts of the super-individuals may leave the spectrum due to mortality $\mu_i(w,E)$.

2.3.1 General Comments on the PDE

Equation (2.5) describes the dynamics of the p-state. The equation is known as the McKendrick-von Foerster equation in mathematical biology because of the apparently independent discoveries by McKendrick (1926) and von Foerster (1959). Both these papers present an age-structured equivalent of (2.5) (cf. their equations (49) and (24), respectively).

As previously stated we need functions for the growth, mortality, and reproduction to describe all i-states. The first two are explicitly stated in (2.5), and the reproduction should be included as a boundary condition:

$$R_{i,tot}(t) = g_i(w_0,E)n_i(w_0,t) = \int_{w_0}^{w_\infty} \tilde{R}_i(w,E)n_i(w,t)\,\mathrm{d}w \tag{2.6}$$

where the boundary condition $g_i(w_0,E)n_i(w_0,t)$ (numbers per volume per time) naturally should be the number of recruits per volume per time as indicated in figure 2.3.

To study the effect of having individuals with differing growth trajectories instead of super-individuals a higher order term could be added to the left-hand side of (2.5). Such an investigation will however not be carried out in this thesis.

2.4 The Community Spectrum

In this section we will change focus. Instead of looking at the size distribution of individuals within a species we will now look at the summation of all species' size spectra. This we will denote the *community spectrum*, and in the following we will discuss that it obeys the relation:

$$N_c(w) = \kappa w^{-\lambda} \tag{2.7}$$

where κ is the magnitude of the spectrum and λ the slope of the spectrum in a loglog plot (cf. figure 2.5).

The concept of a size spectrum was introduced by Sheldon & Parsons (1967) to represent the particular matter composition in the sea. Sheldon et al. (1972)

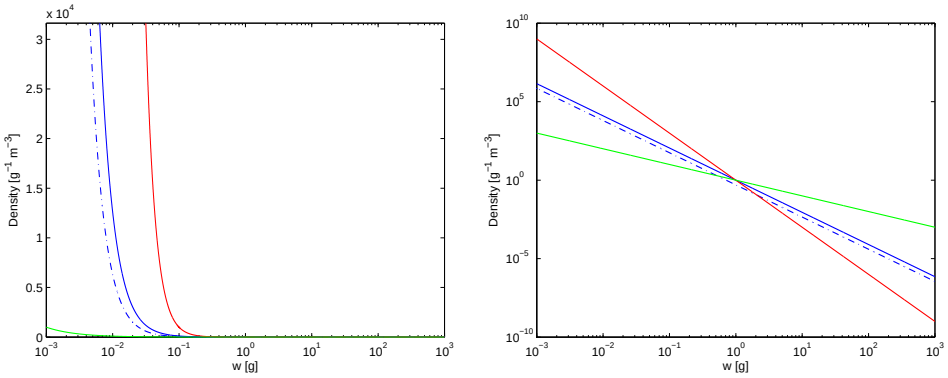

(a) (b)

Figure 2.5: Examples of the the community spectrum given by (2.7) in *(a)* normal plot, and *(b)* logarithmic plot. Green: $\lambda = 1$, blue: $\lambda = 2.05$, red: $\lambda = 3$, $\kappa = 1$ for all except the dashed where $\kappa = 0.5$. From these plots it cannot be seen that values of $\lambda < 2$ is not realistic as argued in the text.

conjectured that the total mass within logarithmically equally sized groups – as the presented density function – are constant over the size range from bacteria to whales. Silvert & Platt (1980) attributed this to the biological interpretation that the mass of the predators equals the mass of its prey.

By applying (2.2) we find that the biomass per volume within logarithmically equally sized groups at a given size w in the community spectrum is:

$$B_{cs}(w) = \int_w^{aw} N_c(w) w \, \mathrm{d}w = \int_w^{aw} \kappa w^{1-\lambda} \, \mathrm{d}w \propto \kappa w^{2-\lambda} \tag{2.8}$$

From this we may argue that $\lambda = 2$ to ensure $B_{cs}(w) = \text{const}$ which was conjectured by Sheldon et al. (1972). We may relax the interpretation of Silvert & Platt (1980) to *predator population biomass may not grow larger than their prey population biomass*, which gives $\lambda \geq 2$ as the plausible range for the slope.

Kerr (1974) used a discrete model of predator-prey interactions between size groups and derived $\lambda = 2.2$. A continuous study by Platt & Denman (1977) yielded $\lambda = 2.22$. This study did however ignore losses due to mortality, but in Silvert & Platt (1980) this was included in a McKendrick-von Foerster formulation and simplifications led them to $\lambda \in [1.97; 2.01]$. Camacho & Solé (2001) also used a McKendrick-von Foerster approach and arrived at $\lambda \approx 2$ mainly due to predation. The metabolic theory of ecology approach (Brown et al. (2004)) has also been applied to give $\lambda = 2$* (Brown & Gillooly (2003)). Finally Andersen & Beyer (2006) considers a simplified steady-state version of the dynamic model in this thesis and arrives at $\lambda = 2.05$. That the biomass abundance should be slightly declining as a function of weight w is also supported by Jennings & Mackinson (2003). Unlike oceanic systems the community spectrum of lakes have lumps and gaps (Havlicek & Carpenter (2001)). The reader is referred to Kerr & Dickie (2001) for in-depth treatment of the biomass spectrum in aquatic environments.

In the model of this thesis the concept of the community spectrum will be used to employ *background resources* in the model. From the discussions in the previous

*Remember that an abundance spectrum should be transferred into a density spectrum by division of $\mathrm{d}w$. Hence their value of $\propto w^{-1}$ becomes $\propto w^{-2}$.

section we know that species are modelled from a given recruit size w_0, but we have also discussed that feeding is a size-dependent process and clearly the preferred food items will be smaller than the recruits. To give the smaller individuals suitable food items resources will be added as in any modelling approach. In a model of everything the resources will be the primary production (light and nutrients). However, we will use the lower part of the community spectrum as background resources. Section 3.5 goes into the details of this modelling approach.

3

A Simple Size-Structured Population Model

In this chapter we will derive the size-structured model that is later used to study coexistence in. We denote this model a *simple* size-structured population model since we will only use *one* parameter to characterise a species. The parameter that characterises a species will be the ultimate weight w_∞ a species may obtain. In nature several species may obtain identical w_∞, which means that all such species are lumped into just one species.

In the chapter we will first simplify the environment of the individuals to be completely determined by the background resources and the spectra of all the species. From this we retrieve a Partial Differential Equation (PDE) for the population dynamics which requires functions for the growth, reproduction, and mortality of the individuals. These three functions are thus derived in the three succeeding sections.

After sections 3.1–3.4 we have determined the functions required for the individuals and the PDE to describe the dynamics of the species. In section 3.5 we turn the attention to the resources in the background spectrum and describe how these are modelled.

In the chapter typical values for all parameters in the model are determined. These are either assumed equal for all species or derived as being functions of the ultimate size w_∞. Thus we end up with the required simple model of an aquatic ecosystem where only w_∞ is used to separate the species. However, the model may easily be extended so that multiple traits are used to describe a species.

The chapter is rounded off with tables 3.2–3.5 which summarises the most important equations along with typical parameter values. In chapter 7 the model from this chapter will be extended to be used in a size-structured food web framework.

3.1 Outline of the Model

In the following we will apply Ockham's razor to reduce the complexity of the conservation equation (2.5) that describes the dynamics of the species' density functions. By doing so we end up with a PDE for the p-state in the model where the environment is completely determined by the spectra of the background resources and the individual species.

The environmental state, the E-state, gives a description of the environment that the super-individuals are located in. In natural systems the E-state is naturally a many-variable function dependent on the available food $\phi(w)$, density of predators $p_i(t)$, temperature T, and salinity S: $E(\phi(w), p_i(t), T, S, \ldots)$. In the model used in this thesis we model the environment as being the other species and the background resources: $E(\phi(w), p_i(t), T, S, \ldots) = E(n_b(w,t), n_i(w,t))$, where $n_b(w,t)$ is the density spectrum of the background resources (more details in section 3.5.1) and $n_i(w,t)$ the spectra of the different species spectra. From all species' individuals and the background resources the available food and the predators for any super-individual are obtained. This means that the environment consists of all living organisms in the model whereas no external factors are explicitly modelled – these may however be implicitly modelled in parts in other functions of the model.

The *total spectrum*, the E-state in the model, is the density spectrum of all species and the background spectrum:

$$E(\cdot) \equiv N(w,t) = n_b(w,t) + \sum_i n_i(w,t) \tag{3.1}$$

The background spectrum will not be introduced until section 3.5, but it represent the resources of the model. The modelled species are the higher trophic species, and the background represents species such as (zoo)plankton. The *total spectrum* should of course be the same as the *community spectrum* (section 2.4). Hence the modelled species represent the upper half of the community and the background spectrum the lower half.

The size w in the model will be in units of weight: $[w]$ =g. In the thesis we will use the intuitive, but mathematically incorrect, notion of $E(n_b(w,t), n_i(w,t)) = N(w,t)$ to obtain notational simplifications. It seems intuitive that the E-state is somehow given by the total spectrum, but of course incorrect in a strict mathematical sense since some super-individuals may be independent of each other. With the new notion for the E-state the conservation equation (2.5) that describes the dynamical behaviour becomes:

$$\frac{\partial}{\partial t} n_i(w,t) + \frac{\partial}{\partial w}\Big(g_i(w,N) n_i(w,t)\Big) = -\mu_i(w,N) n_i(w,t) \tag{3.2}$$

From the previous chapter we recall that the reproduction is used as a boundary condition: $R_{i,tot}(t) = g_i(w_0, N) n(w_0, t)$. Note that since $N(w,t)$ is a function of time then growth $g_i(w,N)$ and mortality $\mu_i(w,N)$ in (3.2) are also functions of time t. Since they are only implicitly functions of time via the population densities $n_i(w,t)$ we do not include time t in the arguments. From (3.2) we thus see that we need to determine functions for the growth, reproduction, and mortality of the individuals. This is the topic of the three following sections.

3.2 Individual Growth from a Bioenergetic Model

The main purpose of this section is to derive a bioenergetic model in the form of a growth function that describes the super-individuals advancement in the size spectrum. However, before deriving the growth function we need to know two important properties in the system:

1. How much food is available for the individual? A species may obtain its diet from the background resources and other species. A model based on size-dependent selection of food items and a search volume that scales with body size is derived to obtain the amount of food an individual encounters in a given environment.

2. How satiated is the individual? The intake of an individual will not continue to increase with an increasing amount of available food. The concept of a feeding level is employed to obtain a measure on the degree of satiation of the individual.

After having derived models for these properties a bioenergetic model for the growth of the individual is derived. We end up with a model that determines how much energy that should be put into maintenance of basal metabolic requirements, body growth, and reproduction. The allocation to these three energetic requirements is naturally a function of the actual food intake and satiation of the individual.

The reproduction is thus tightly connected to the structure of the derived bioenergetic model, and in section 3.3 the implementation of reproduction is discussed in detail.

3.2.1 Encountered Suitable Food by an Individual

The individuals have metabolic requirements and must grow from recruits into adults that can reproduce. Hence they must have a food consumption from the surrounding environment, which is the total spectrum $N(w,t)$ as previously discussed. In this chapter we assume a completely mixed environment setting meaning that an individual encounters all species and background resources simultaneously. In chapter 7 we will go into the details of handling different preferences towards different species.

In this section we will determine the amount of suitable food an individual of size w_p encounters per unit time as the product of its search volume $v_i(w_p)$ (volume per time) and the available concentration of suitable food items $\phi_i(w_p, N)$:

$$F(w_p, N) = v_i(w_p)\phi_i(w_p, N) \tag{3.3}$$

To calculate the encountered food per time the available concentration of suitable food will be found in the next section. The problem of the search volume is treated subsequently.

Food Selection and Available Food from Foraging

The individuals naturally cannot eat everything in the environment, so we introduce a selection function that gives a percentage of how likely a predator of weight w_p consumes a prey of size w:

$$s_i(w, w_p) = \exp\left[-\ln^2\left(\frac{w}{\beta_i w_p}\right)/(2\sigma_i^2)\right] \tag{3.4}$$

This log-normal function is adopted from the North Sea model by Andersen & Ursin (1977) and is based on investigations of cod and dab (Ursin (1973)) and copepods (Ursin (1974)).

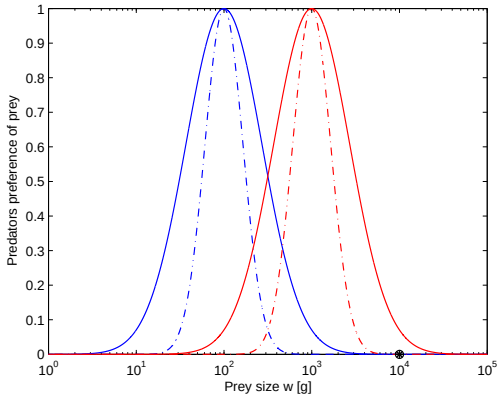

Figure 3.1: Examples of the prey selection function for a predator $w_p = 10^4$. Blue curves $\beta = 0.01$, red $\beta = 0.1$. Solid curves $\sigma = 1$, dashed curves $\sigma = 0.5$.

The preferred size of prey is $\beta_i w_p$ (β_i: prey-predator ratio), and σ_i is a measure of the width of the selection function. The size selection function is illustrated in figure 3.1. σ_i is probably the most important species dependent parameter in (3.4) since the smaller a σ_i the more specialised is the species. The typical values that will be used are $\beta = 0.01$ and $\sigma = 1$ which seems to be okay for at least cod and dab. Jennings et al. (2002) goes beyond diet analyses and find a mean prey-predator ratio of $\beta = 0.0092$ using stable isotope analyses.

In a completely mixed environment where all individuals in $N(w,t)$ are vulnerable to predation, the total concentration of available and suitable food items (mass per volume) to a predator of size w_p is:

$$\phi_i(w_p, N) = \int N(w,t) w s_i(w, w_p)\, \mathrm{d}w \tag{3.5}$$

To include spatial heterogeneity and different preferences towards different species for the diet of an individual this function naturally has to be generalised. However, to avoid too many technicalities in this chapter this is postponed to chapter 7 where the model from the current chapter is applied to a size-structured food web description.

The role of specialisation vs. generalisation (thin vs. wide σ_i) will not be treated in this thesis. Simple studies may however easily be made by requiring a fixed value of the integral of $s_i(w, w_p)$, so that i.e. generalists will have a wide selection function with low magnitude and specialists a thin selection function with a high magnitude.

Search Volume

We will now derive a model for the search volume per time for a cruising predator. Naturally, a predator does not forage continuously, but in the following we will parameterise the encounter process to obtain a simple allometric scaling relation of body weight for the search volume.

As illustrated in figure 3.2 the search volume per time is the product of the foraging speed $\nu_i(w)$ and the cross sectional area of the reactive field of the fish. We will assume a circular reactive field with radius $r_i(w)$, which gives us the search volume per time:

$$v_i(w) = \pi r_i^2(w) \nu_i(w) \tag{3.6}$$

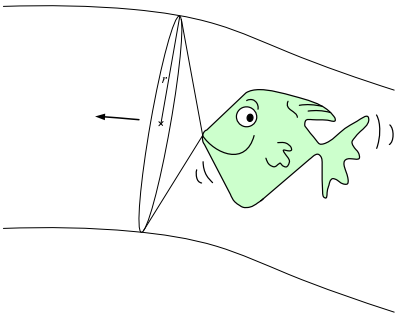

Figure 3.2: The search volume of a fish is the product of its velocity and and the cross sectional area of its reactive field. The reactive field is assumed circular with radius r.

Table 3.1: Collection of search volume parameters for five different sizes of fish. Table values derived using $\xi = 0.2$.

w_∞	*Length*	*Cross sec. area*	*Cross sec. radii*	*Avg. speed*	*Search vol.*
0.01 g	1.10 cm	1.22 cm^2	0.62 cm	5.91 cm/s	7.21 cm^3/s
0.1 g	2.26 cm	5.98 cm^2	1.38 cm	7.98 cm/s	47.7 cm^3/s
1 g	4.64 cm	29.3 cm^2	3.05 cm	10.8 cm/s	314.9 cm^3/s
1 kg	40.2 cm	0.344 m^2	33.1 cm	26.4 cm/s	0.0908 m^3/s
15 kg	93.7 cm	2.23 m^2	84.2 cm	37.6 cm/s	0.837 m^3/s

We will find that $r_i(w)$ and $\nu(w)$ can be expressed as allometric scaling relations of body weight w. Thus the search volume for an individual of weight w can be expressed as:

$$v_i(w) = \gamma_i w^{q_i} \tag{3.7}$$

We expect that the reactive field is related to the square of the body length l, and the velocity to be described by an allometric function of body weight w. Ware (1978) calculates that the reactive field area scales with $l^{2.2}$, and from a typical energy budget he finds the optimal cruising speed to be $15.1w^{0.136}$ cm/s and optimal foraging speed $20.3w^{0.132}$ cm/s (w in units of g). It is noted that most fish do not grow isometrically throughout their life ($w \neq \varpi l^3$), but with $w \propto l^\xi l^3$, where ξ typically is $0.1 - 0.4$. In this thesis the typical value $\xi = 0.2$ is used, which means that the reactive field scales with $w^{0.69}$. By combining the results we find that a typical value for q_i is $q = 0.82$.

In the body length domain $A(l) = l^{2.2}\,\mathrm{cm}^2$ gives reasonable cross-sectional radii of 3.05 cm for 4.64 cm (1 g) fish and 33.1 cm for 40.2 cm (1 kg) fish. We know that the cross-sectional area is given by $A(w) = a_c w^{0.69}\,\mathrm{cm}^2$, and from Peters (1983) we get $l = 4.64w^{1/(3+\xi)}$ (cm), which yields $a_c = 4.64^{2.2}\,\mathrm{cm}^2\ \mathrm{g}^{-0.69}$.

The prefactor γ_i for the search volume thus becomes $20.3 \cdot 4.64^{2.2}\,\mathrm{cm}^3/\mathrm{s} = 1.9 \cdot 10^4\,\mathrm{m}^3$/year. However, predators naturally do not forage continuously, so selecting for the typical parameters of $\gamma = 10^4\,\mathrm{m}^3\mathrm{g}^{-q}/\,\mathrm{year}$ and $q = 0.82$ seems acceptable. These values give the search volume parameters listed in table 3.1.

Ware (1978) states that the optimal foraging speed is 0.4–1.0 times the maximum sustainable swimming speed. Videler & Wardle (1991) find that the maximum sustainable swimming speed is given by $\nu_{ms}(L) = 0.15 + 2.4L$ m/s where L is in units of metres. Remembering that we reduced γ with 1/1.9 we find that the swimming speeds from table 3.1 corresponds to 0.3–0.6 times ν_{ms}. Thus comparison with

the data in Videler & Wardle (1991) gives confidence that we have estimated the parameters to the correct order of magnitude.

It is noted that the relation for the search volume in (3.7) may not be very good for smaller species (below 10 cm) according to Ware (1978). However the smallest individuals considered in the species spectrum has a weight of 0.01 g (1.10 cm) and thus a search volume of 7.21 cm^3/s, which does not seem an extremely large search volume for this individual compared to its reactive radius of 0.62 cm.

We derived this model for a cruising predator, and it is quite intuitive as a first hand description for pelagic and demersal species that do actually search for food. However, the approach can also be used for i.e. benthic species who use a sit-and-wait ambush strategy, where we may regard the search volume of the predator as the amount of food that flows through its reaction field. It is likely that both the prefactor and the scaling will differ from the derived values. However, we would still expect q to be positive, which means that we also do capture some realism for sit-and-wait predators.

As will become evident in section 5.2 the scaling of the search volume is important for the dynamics of the model. This means that the model is sensitive in regards to the γ parameter.

In nature foraging speed may be a function of the environment $\nu_i(w, N)$ since an individual may i.e. have different speeds at different food concentrations (Ware (1978)). This would appear has an environmental dependence in the $\gamma(N)$ prefactor in (3.7).

Further studies of the model should link the bioenergetics of the growth model more tightly with the search volume concept to enable studies of tradeoffs when species have different feeding strategies. In this case a sit-and-wait predator can have a i.e. a lower γ, but then also the advantage of a lower metabolism. It might however also be so that different strategies have different functional responses so that different variants of the feeding level concepts have to be implemented. Lessons learned from the more general problem of optimal foraging theory could also be incorporated (see e.g. Mangel & Clark (1986)).

3.2.2 Feeding Level

When foraging there is an upper level of how much food a predator can process. This is due to satiation and/or handling limitations, and is normally incorporated with a functional response.

In this thesis a Holling type II functional response is used (Holling (1959a, 1959b)). The total effect of satiation and limitation is denoted satiation, and the degree of satiation is the feeding level:

$$f_i(w_p, N) = \frac{F(w_p, N)}{F(w_p, N) + I_{i,max}(w_p)} = \frac{v_i(w_p)\phi_i(w_p, N)}{v_i(w_p)\phi_i(w_p, N) + I_{i,max}(w_p)} \tag{3.8}$$

which varies between 0 and 1. $I_{i,max}$ is the upper level of food that can be ingested per unit of time. By multiplying $f_i(w_p)$ with $I_{i,max}$ it is recognised that we get a Holling type II functional response. The maximum intake per time is given by:

$$I_{i,max}(w) = h_i w^{k_i} \tag{3.9}$$

An argument for this scaling of the maximum intake is given in the next section when discussing the metabolic requirements of an organism.

Diet of an Individual

To study the actual diet of individuals in a model run we may calculate e.g. the food intake per unit time from the background:

$$\varphi_{b,i}(w_p) = f_i(w_p, N) I_{max}(w_p) \frac{\phi_{b,i}(w_p, N)}{\phi_i(w_p, N)} \tag{3.10}$$

which is simply the amount of eaten food per time, $f_i(w_p)I_{max}$, multiplied with the ratio of the food available from the background and the total amount of available food.

3.2.3 Growth Function

In this section we will consider how the i-state is actually modelled. An individual can grow up in the spectrum by a growth function, which is the topic of this section, and it may leave the spectrum due to mortality, which is treated in section 3.4. As mentioned earlier one of the most important advantages of the size-structured models compared with the unstructured counterparts is that they are constructed upon a description of individual behaviour. Instead of setting constraints on the population behaviour from the top the bottom-up behaviour determines the upper level population dynamics. This is an advantage because individual level parameters are more easily assessed. The most important function for the individual behaviour is the growth function, which is derived in this section.

In general fish cannot shrink in body size, but the lipid and gametes mass may vary. This would of course decrease the weight w, so that the fish would have to move backwards in the density spectrum. Numerically this is not very convenient (cf. section 4.1), and not necessary since it may be avoided while keeping realism by organising the model in a smart way. Loss of lipid masses will occur when the fish is starving, which means that the lack of food can be converted into a corresponding mortality rate as argued in section 3.4.2. Loss of mass due to reproduction may be treated by not including gamete mass in the weight w that is used for the i-state variable – this is partly the topic of this section, but treated more thoroughly in section 3.3. This means that the weight w used as the i-state represents the *irreversible* mass or somatic mass ($\sim$the structural biomass) of the super-individuals.

The reader may be interested in going through Ursin (1967), which contains many theoretical and empirical considerations for fish growth models. Likewise Beyer (1989) may be a good starting point for theory on recruitment.

This section is divided into three subsections. In the first a general growth model is derived from first principles. In the second we dwell on the role of activity, which is important for fish since a substantial part of their energy budget is allocated to activity. In the third and final subsection we adopt the derived general growth model to the modelling framework of this thesis and determine typical values for the parameters in the model so that it can be expressed with just w_∞ as the species dependent parameter.

Derivation of a General Growth Model

Pütter (1920) was the first to introduce a mathematical framework to describe the growth of animals in terms that are very similar to the growth models used today. In the 1920 paper a model is proposed where the growth is the difference between

what comes in and what goes out. The intake is related to a surface process, and the decomposition of existing mass is dependent on body weight. In the more detailed and modern derivation of this section we will end up at a result very similar to the early result of Pütter (1920).

The following derivation of a growth model is a generalised version inspired by the work of West et al. (2001) and includes solutions to the critique put forward by e.g. Makarieva et al. (2004)*; excluding the temperature dependence introduced in Gillooly et al. (2002), which we are not interested in. Another theoretical framework that may be used for derivation of a growth model is Dynamical Energy Budgets (DEB) (Nisbet et al. (2000) and Kooijman (2000)).

Definitions of *metabolic rate* differs and are often very vague (cf. e.g. Schmidt-Nielsen (1983) and Kooijman (2000)). The metabolic rate is the energy flux required to fire all chemical reactions in an organism. Since this is difficult to operate with in practice the metabolic rate is often defined to be proportional or equivalent to respiration rate, which again is proportional to O_2 uptake or CO_2 uptake for plants (Zeuthen (1953)). Metabolism is proportional to respiration since combustion of food (proteins, carbon hydrates, and lipids) release almost the same energy per O_2 molecule (cf. Schmidt-Nielsen (1983)). This bookkeeping is however more complicated since all excess assimilated food is stored as lipids regardless of its type, which requires energy and hence more O_2. However, on longer time scales of the individuals the metabolic rate can be taken to be proportional to the respiration rate (West et al. (2004)).

Respiration of glucose: $C_6H_{12}O_6 + 6O_2 \rightarrow 6CO_2 + 6H_2O + E$

The assimilated food intake must also be proportional to the respiration, since the assimilated food contains the material part for the respiration process to take place. Hence we have the following useful relation:

$$\text{Metabolic rate} \propto \text{Resp. rate} \propto \text{Assim. food rate} \propto O_2 \text{ uptake rate} \tag{3.11}$$

The total metabolic rate B for an organism must then clearly be the sum of all O_2 demanding processes, which allow us to set up the following energy balance equation:

$$B = B_{main} + B_{growth} + B_{repro} + B_{heat} + B_{osmosis} + B_{activity} \tag{3.12}$$

The maintenance term B_{main} contains all energy requirements needed to sustain life in the body as i.e. continuous cell replacement. B_{growth} is the energy allocated for growth, and B_{repro} is the energy allocated to reproduction. Since fish are poikilothermic organisms (their internal temperature follows the environment) we have $B_{heat} = 0$. The energy required to sustain a body salinity lower than the surroundings can also be neglected ($B_{osmosis} = 0$) since this contribution of no more than 5-10% of B often is difficult to measure separately and can be included in B_{main} as a maintenance requirement (Andersen (2006)). However, euryhaline species (species living in waters with high variation in salinity) may spend up to $\sim 30\%$ of B on osmosis (Kooijman (2000)), which means that further considerations should be carried out for these species. The activity term $B_{activity}$ is important for fish since their metabolism varies a lot depending on its activity level. However to

*Makarieva et al. (2004) also claim another energy balance equation, which is not consistent with (3.12) (and hence incorrect). Many growth models are based on this incorrect energy balance equation, which origin cannot be tracked to a common source, but is still found in the literature. The problem with the balance equation is that it does not recognise that it takes O_2 to construct new biomass.

avoid complexity we will comment on the role of $B_{activity}$ later in this section and for now just accept that it is included in B_{main}. This yields a condensed balance equation consisting of just the maintenance, growth, and reproduction term, which can be expressed in a more detailed form:

$$\begin{aligned} B &\simeq B_{main} + B_{growth} + B_{repro} \\ &\simeq N_c B_m + \varepsilon E_c \frac{\mathrm{d}N_c}{\mathrm{d}t} + \psi(\cdot)\varepsilon E_g \frac{\mathrm{d}N_g}{\mathrm{d}t} \end{aligned} \tag{3.13}$$

where it is assumed that maintenance, $B_{main} \simeq N_c B_m$, is proportional to the numbers of cells N_c in the body.* The growth term is described as the change in number of cell times the energy εE_c needed to create a cell; the ε pre-factor is needed since the energy required to build a cell depends on the quality of the food. Lastly the reproduction term is included exactly as the growth term with the exception that the index g now refers to gametes† and the $\psi(\cdot)$ function is a Heaviside selection function that changes from 0 to 1 when the individual has matured; more details on this ontogenetic shift is found later in this section. In the condensed balance equation we treat all cells as average cells to avoid dealing with different kinds of tissue in the body.

Equation (3.13) can be expressed in terms of body weight w by recognising that $N_c = w/w_c$ where w_c is the weight of a single cell, and that the weight of produced gametes $w_g \Delta N_g$ in a given season Δt is proportional to the body weight $w_g \Delta N_g = \rho' w$ (Blueweiss et al. (1978)) – or equivalently mass investment in gametes per season $w_g \Delta N_g / \Delta t = \rho w$. Since we are already considering average cells we may assume $w_g = \eta w_c$ and $E_g = \eta / a E_c$, where a is some efficiency factor, which take into account that gametes primarily are formed from stored lipid reserves. These variable transformations leads to a general growth equation:

$$\begin{aligned} B &= \frac{B_m}{w_c} w + \frac{\varepsilon E_c}{w_c} \frac{\mathrm{d}w}{\mathrm{d}t} + \psi(\cdot) \frac{\varepsilon E_c \rho}{a w_c} w \\ &= \left(\frac{B_m}{w_c} + \psi(\cdot) \frac{\varepsilon E_c \rho}{a w_c} \right) w + \frac{\varepsilon E_c}{w_c} \frac{\mathrm{d}w}{\mathrm{d}t} \qquad \Leftrightarrow \end{aligned} \tag{3.14}$$

$$\frac{\mathrm{d}w}{\mathrm{d}t} = \frac{w_c}{\varepsilon E_c} B - \left(\frac{B_m}{\varepsilon E_c} + \psi(\cdot) \frac{\rho}{a} \right) w \tag{3.15}$$

Empirical data (cf. e.g. Peters (1983), Calder III (1984), Schmidt-Nielsen (1984), and McMahon & Bonner (1983)) agree that the metabolic rate can be described by the allometric power law $B = B_0 w^k$, where the exponent k typically is approximately 0.75 (known as Kleiber's law due to Kleiber (1947)) and the B_0 (energy $\times$ mass^{-k}/time) constant for each taxon ($\sim$ group of similar animals). For fish the exponent is more difficult to determine, and a wider range of exponents around this value have been measured (Schmidt-Nielsen (1984)). Theoretical derivations of the scaling exponent k have been carried out. Apparently the first derivation was by

*I will not go further into this assumption. Later we will see that the derivation leads to a von Bertalanffy growth equation which have been shown to describe measured growth curves to a high enough precision. See e.g. the fits in West et al. (2001).

†In the model we do not distinguish between males and females even though a larger amount of energy is put into reproduction by females. Males often also have extra energy expenses upon maturation by making themselves attractive to females, performing parental care and by being territorial (Roff (1983)). In this thesis I will not initiate construction of the still missing models that take into account sexual difference, but instead model the two sexes as average individuals.

McMahon (1973) who derived that the maximal power from a contracting muscle is proportional to $w^{3/4}$. West et al. (1997) derived the 3/4 power by looking at how the energy may be delivered to the body through a fractal network of branching tubes; later in West et al. (1999) they argue that evolution has optimised the body to this most efficient scaling of the metabolic rate. Banavar et al. (1999) and Banavar et al. (2002a) generalise this work and argues that deviations from the optimal 3/4 power is due to inefficiency or compensating physiological mechanisms in the organism. Darveau et al. (2002) points out that the 3/4 value only applies for the basal and not the maximal metabolic rate, which has a higher scaling power, and tries to explain it with a multiple-cause model which adds on to the theory of the limiting factor in the transport network that supply the cells with energy. This study is not very strong in a theoretical sense, and is also later criticised by the groups of West and Banavar, but it does however point out the need for a better understanding of the metabolic rate under different conditions. There is a long tradition to apply scaling laws in biology and it may just be so that the different scalings of the metabolic rate at different activity levels cannot be described by a power law. However, the power law do capture enough realism to be used in the general growth model in this thesis, and we may thus write (3.15) as:

$$\frac{\mathrm{d}w}{\mathrm{d}t} = \frac{w_c B_0}{\varepsilon E_c} w^k - \left(\frac{B_m}{\varepsilon E_c} + \psi(\cdot) \frac{\rho}{a} \right) w \tag{3.16}$$

Without reproduction ($\psi(\cdot) = 0$) we see that for $w \to w^r$ we have obtained the form of the general von Bertalanffy growth equation which was initially employed as a fitting function to empirical growth curves (von Bertalanffy (1934)). In fisheries research the von Bertalanffy growth equation has been successfully employed with $k = 2/3$ and $r = 1$ (von Bertalanffy (1957)). Von Bertalanffy saw the first term as energy intake, which he argued should be a surface process ($w^{2/3}$), and the second term as a maintenance term that should scale with the volume (w). As illustrated by Banavar et al. (2002b) the actual value of k for data fits is not very critical.

Some models state that $k \approx r$ based on empirical investigations (i.e. Lester et al. (2004)), and this has the effect that the maximal size w_∞ an individual may obtain becomes poorly defined; found by setting $\frac{\mathrm{d}w}{\mathrm{d}t} = 0$ and solving for $w = w_\infty$. $k \approx r$ is not readily justified theoretically since individuals may grow indefinitely, which is obviously not true, and is most probably due to confusion in measured properties and the earlier mentioned problems with incorrect definitions of metabolism. Often only the two terms *intake* and *maintenance* from a traditional von Bertalanffy growth curve are used for a growth function. This has the disadvantage that an individual will aim for a certain w_∞ throughout its life which is not in agreement with empirics, which find that growth is slowed down upon maturation (i.e. Roff (1983)). This often turns into a general critique of using measures of w_∞, but as seen in later in figure 3.3 the model in this thesis changes growth curve (and hence resulting w_∞) upon maturation as desired.

The Activity Term

The activity term in (3.12) is important for fish since it may constitute up to 80% of the total metabolic rate (Andersen (2006)) depending on the individuals level of activity. The required energy rate for swimming may be approximated by the drag

force times the travelled distance per unit of time:

$$B_{activity} = F_D u = \frac{1}{2} C_D \varrho u^3 A \propto b C_D \varrho w^{3 \cdot 0.134} w^{2/3} \propto b C_D \varrho w^{1.07} \tag{3.17}$$

where C_D is the drag coefficient, ϱ the density of water, u swimming velocity, and A the realised projected area of the fish. As we have seen in section 3.2.1 the velocity may be assumed proportional to $w^{0.134}$. We may also write the area as $w^{2/3}$ and then introduce b to get the units right.

As (3.17) shows the activity term in (3.12) scales approximately with body weight w. Since we are not interested in explicit modelling of activity we will include activity as an average energy rate, which can be included in the maintenance term in (3.12) since both terms have the same scaling.

The model at hand may be advanced by linking the search volume in (3.7) explicitly to metabolic requirements. Higher search volume implies larger velocity that requires more energy, which then enables trade-off studies to be made.

Adopting the General Growth Model to this Thesis

To apply (3.16) as a growth model in the thesis at hand we use relation (3.11), which yields that $B_0 w^k$ (energy/time) is proportional with food intake $I_{i,max}(w) = h_i w^{k_i}$ (mass/time) and disregard that food may have differing quality ($\varepsilon = 1$). As argued in section 3.2.1 the actual food intake is the feeding level times the intake at abundant food conditions. By multiplying the food intake with some assimilation efficiency α_i we have $w_c B_0 / E_c w^k \sim \alpha_i f_i(w, N) h_i w^{k_i}$. Similarly we may write $B_m / E_c \sim \delta_i$, and $\rho = \varrho_i$. The efficiency factor a may be approximated with the assimilation efficiency α_i. These transformations give a somatic growth equation for species i:

$$\begin{aligned} g_i(w, N) &= g_{i,in}(w) - g_{i,main}(w) - g_{i,repro}(w) \\ &= \alpha_i f_i(w, N) h_i w^k - \delta_i w^r - \psi_i(w) \frac{\varrho_i}{\alpha_i} w \end{aligned} \tag{3.18}$$

where we have now specified that the reproduction selection function is dependent on the somatic weight w. For generality we have also allowed an allometric scaling of $\delta_i w$; however, we derived the model for $r = 1$ and will only carry out investigations with this value. α_i is assimilation efficiency (dimensionless), h_i maximum food intake scaling (mass^{1-k}/time), δ_i maintenance requirement (mass^{1-r}/time), and ϱ_i investment in reproduction (1/time). The first term represents energy from food intake, second term maintenance, and the third term is the requirements for producing gametes (all in mass/time units). $(1-\alpha_i) f_i(w, N) h_i w^k$ is the energy that is lost from i.e. body heat due to activity, and the energy that is excreted.

From table 1 in West et al. (2001) we find for a cod $h_i = 21\,\mathrm{g}^{1-k}$/year, but in this thesis a typical value of $h = 25\,\mathrm{g}^{1-k}$/year is used. West et al. (2001) also indirectly determines $\delta = 0.11\,\mathrm{g}^{1-r}$/year. In the literature assimilation efficiencies in the order of 0.70–0.95 are often found for fish. However, these often results from laboratory tests. Andersen & Riis-Vestergaard (2004) find food conversion efficiency for saithe in the wild to be 0.43–0.50 where lab measurements yield 0.51–0.76. Since the assimilation efficiency in this thesis dictates a mass conversion efficiency and not an energy efficiency a typical value of $\alpha = 0.3$ seems reasonable. In more realistic studies α could be a function of the actual food source since i.e. herbivores have a lower efficiency than carnivores because herbivores have to transfer organic material

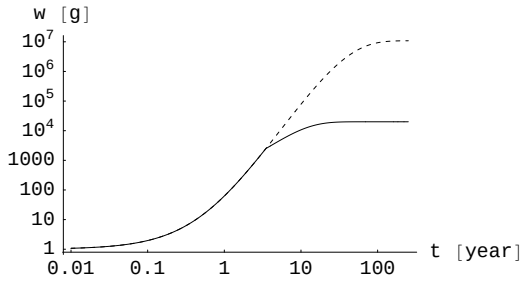

Figure 3.3: Growth pattern for an individual with $w_\infty = 20\,\mathrm{kg}$ (solid), and its genetically modified non-reproducing ($\psi_i(w) = 0$) counterpart (dashed). The non-reproducing individual grow faster, but at decreasing rate, compared to the reproducing individual after maturation. That the non-reproducing individual should continue to grow 1000 times larger is of course not realistic since some other mechanism will prohibit this.

into animal tissue. A typical value of $\varrho = 0.15\,/\mathrm{year}$ is compatible with the values of 0.1–0.2 that is often used (i.e. Andersen & Ursin (1977)). Estimating typical values for α_i, h_i, δ_i, and ϱ_i is difficult since the literature does not provide exhaustive amounts of data.

Figure 8.3 in Kooijman (2000) shows body temperature corrected Bertalanffy growth rates for many different animals. The figure basically states that the prefactor αh is constant for a given temperature, and at 25° C it is $\alpha h \approx 10\,\mathrm{g}^{1-k}/\mathrm{year}$. From the estimated parameters the value $\alpha h = 0.3 \cdot 25\,\mathrm{g}^{1-k}/\mathrm{year} = 7.5\,\mathrm{g}^{1-k}/\mathrm{year}$ seems okay since a typical marine environment definitely holds individuals at a lower body temperature.

For the r scaling employed on the maintenance term we may argue that $k \neq r$ since we then otherwise would expect individuals that was genetically modified not to reproduce to grow indefinitely at a constant rate. Such experiments causes individuals to change growth patterns and grow faster to a larger size (Andersen (2006)). Such a pattern is also seen in the growth model at hand ($r = 1$) as indicated in figure 3.3 where we see that an individual changes its growth curve after maturation. The new curve has a slower growth compared to the case where the fish has been genetically modified not to reproduce. In contrary to the $k = r$ case we see that the growth rate do decay for large w_∞ in the case of no reproduction, which seems intuitively correct.

We note that the growth function may become negative if the intake is smaller than the expenses for maintenance and reproduction. As it will be made clear in the next section energy will only be spent on reproduction if intake minus maintenance is positive, and if intake is lower than maintenance requirements (i.e. for low feeding level) a starvation mortality is employed as described in section 3.4.2.

The maximal size an individual may obtain at abundant food conditions ($\forall w : f(w) = 1$) is given by:

$$g_i(w_\infty) = 0 = \alpha_i h_i w_\infty^k - \delta_i w_\infty^r - \psi_i(w_\infty)\frac{\varrho_i}{\alpha_i} w_\infty \tag{3.19}$$

$$w_\infty = \left(\frac{\alpha_i h_i}{\delta_i + \varrho_i/\alpha_i}\right)^{\frac{1}{1-k}} \quad \text{for } r = 1 \tag{3.20}$$

From this we see that we cannot use all of the above mentioned typical values for α_i, h_i, δ_i, and ϱ_i since we then cannot get differing w_∞ for different species. Due to

Kleiber's law (cf. the discussion above) we may assume $h_i = h$ species independent. Assimilation efficiency is also assumed species independent $\alpha_i = \alpha$. At a first glance it might also seems alright to assume that all species spend the same percentage of their body mass on reproduction; $\varrho_i = \varrho$. The last parameter δ_i may then be determined by rearranging (3.19) to obtain:

$$g_i(w,N) = \alpha_i f_i(w,N) h_i w^k - \left(\alpha_i h_i w_\infty^{k-r} - \frac{\varrho_i}{\alpha_i} w_\infty^{1-r}\right) w^r - \psi_i(w)\frac{\varrho_i}{\alpha_i} w \quad (3.21)$$

where we note that $\delta_i = \alpha_i h_i w_\infty^{k-r} - \frac{\varrho_i}{\alpha_i} w_\infty^{1-r}$ becomes negative for large w_∞. Actually this happens at $w_\infty = w_{\delta,++} = (\varrho_i/(\alpha_i^2 h_i))^{\frac{1}{k-1}}$, which then will represent an upper size on viable values of w_∞.

If we alternatively assume $\delta_i = \delta$ species independent we may write the growth function as:

$$g_i(w,N) = \alpha_i f_i(w,N) h_i w^k - \delta_i w^r - \psi_i(w)\left(\alpha_i h_i w_\infty^{k-1} - \delta_i w_\infty^{r-1}\right) w \quad (3.22)$$

which also imposes an upper value: $w_\infty = w_{\varrho,++} = (\delta_i/(\alpha_i h_i))^{\frac{1}{k-r}}$.

How do these formulations differ? The $\delta(w_\infty)$ (3.21) formulation postulates that all species use the same percentage of body mass for reproduction and that increasing efficiency of maintenance is what allows larger species to obtain a larger w_∞. Alternatively the $\varrho(w_\infty)$ (3.22) formulation assumes that all species use the same body mass percentage for maintenance and that larger species are obtained by lowering the reproduction effort.

The $\delta(w_\infty)$ assumption seems rather weak since both growing to a larger size (avoiding predation) and having lower maintenance requirements are positive effects; i.e. there is no trade-off. Now, the trade-off do exist in the $\varrho(w_\infty)$ formulation since species will have to pay the cost of lower reproduction to obtain a larger size. Figure 3.4 shows the required $\delta(w_\infty)$ and $\varrho(w_\infty)$ values in the two formulations. We immediately see that the $\varrho(w_\infty)$ formulation allows studies of species over a larger w_∞ range, but also the weakness of this formulation. As w_∞ becomes smaller $\varrho(w_\infty)$ exceeds 1, which is only possible if the species spawn more than its own mass in a season, which again only seems possible if it spawns several times in each season.

This discussion clearly shows that more research should be put into a general growth equation. Maybe all parameters (α_i, h_i, δ_i, and ϱ_i) should somehow be related to w_∞. Larger fish like tuna may i.e. have a higher h_i value since their large body size and activity give them higher internal temperatures which might mean

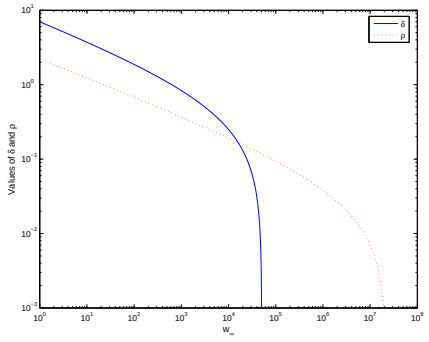

Figure 3.4: Plot of $\delta(w_\infty)$ and $\varrho(w_\infty)$ in (3.21) and (3.22) using the typical values of $\alpha = 0.3$, $h = 25\,\mathrm{g}^{1-k}/\mathrm{year}$, $\delta = 0.11\,\mathrm{g}^{1-r}/\mathrm{year}$, and $\varrho = 0.15\,/\mathrm{year}$. The $\varrho(w_\infty)$ formulation allows studies of larger w_∞ species, but the ϱ value goes above 1 for small w_∞ which is only possible for species that spawn several times in one season.

that their metabolic capability becomes higher like endotherms ($\sim$ mammals). One might also put an upper limit to how much a species can reproduce, but then a sink term has to be introduced to the growth equation.

The weaknesses of the growth function pointed out in the above discussion imply that caution should taken in interpretations of the upper limits w_{++} that is imposed on maximal w_∞ values. However, when the w_{++} values are approached the model breaks down and this may correspond to a shift in life strategy as when e.g. moving from fish to sharks; instead of i.e. aiming at many small eggs it becomes favourable to go for fewer larger offspring, which can be protected and are more capable of avoiding predation.

In this thesis the $\varrho(w_\infty)$ formulation (3.22) of the growth function is selected for the modelling studies. This formulation is from the discussion clearly more realistic than the $\delta(w_\infty)$ (3.21) formulation, which requires reduction of maintenance requirement to allow species with larger w_∞.

3.3 Reproduction using the Bioenergetic Model

In this section we will use the bioenergetic model for the growth of the individuals from section 3.2.3 to obtain an explicit function for reproduction, which is used as the boundary condition in the PDE (3.2) describing the spectrum dynamics.

By using the method outlined in section 3.2.3 we do not have to add gametes to the body weight w since we may use the mass rate $\frac{\varrho_i}{\alpha_i} w$ directly to calculate the reproduction needed in the flux boundary condition as outlined in (2.6):

$$R_{i,tot}(t) = g_i(w_0) n_i(w_0, t) = \frac{e_i \alpha_i}{w_0} \int g_{i,repro,eff}(w') n_i(w') \, \mathrm{d}w' \tag{3.23}$$

where e_i is the recruiting efficiency constant that sets the probability that recruits survive up to size w_0. Assimilation efficiency α_i is also a prefactor since the reproductive investment compared to body weight should be $\varrho_i w$ (Blueweiss et al. (1978)). The integral gives the invested mass/volume/time in gametes, and by dividing this with w_0 we get the number of recruits/volume/time that should be used as the boundary condition. Wootton (1979) indicates that we may employ an approximation where we use the same w_0 for all species since the number of produced eggs has a tendency towards linear scaling with body weight. Stochasticity in the reproduction may be obtained by putting a stochastic variance on the reproductive efficiency constant e_i. We postpone determination of typical values for w_0 and e_i to the proceeding section of the following treatment of reproduction.

The subscript *eff* is added to the growth function in (3.23) to indicate that the *effective* reproductive growth function may differ from the ideal defined in (3.18) since excess energy may not be available to allow ideal reproduction. The effective reproductive growth-rate is defined by:

$$\begin{aligned} g_{i,repro,eff}(w) &= g_{i,repro}(w) - g_{i,repro,miss}(w) \qquad (3.24) \\ g_{i,repro,miss}(w) &= \max\Big(0\,,\, g_{i,repro}(w) - g_{i,repro,avail}(w) \Big) \\ &= \max\Big(0\,,\, g_{i,repro}(w) - \max\big(0\,,\, g_{i,in}(w) - g_{i,main}(w) \big) \Big) \end{aligned}$$

This means that in shortage of energy ($g_{i,repro}(w) > g_{i,in}(w) - g_{i,main}(w)$) the available energy $g_{i,repro,eff}(w)$ is spend on reproduction. In shortage of energy the

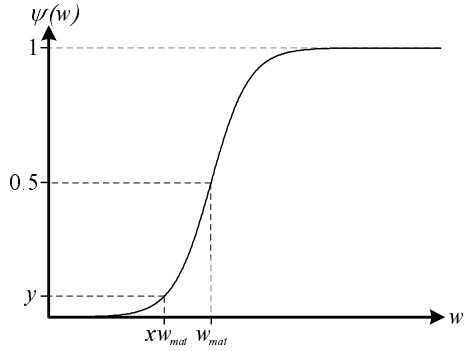

Figure 3.5: The reproductive selection function $\psi_i(w)$ is defined with a Fermi-Dirac distribution. The width of the passage is given by a constant χ_i which is a function of x and y.

available energy is spent on reproduction, and nothing on growth. Maybe a trade-off should be made in a later version of this model so that some energy is still routed to growth.

In the simplest case the reproduction selection function $\psi_i(w)$ is a Heaviside step function that gives 1 for $w \geq w_{mat}$, but it may more realistically (and nice in a numerical sense) be a probability function stating the probability that an individual at size w has matured since the total biomass of a size-class will not enter the Spawning Stock Biomass (SSB) simultaneously. The Fermi-Dirac probability function gives the probability that a quantum state at energy level E is occupied at a given temperature T. The Fermi energy E_F is defined as the energy where the probability is 1/2:

$$f_F(E) = \frac{1}{1 + \exp\left(\frac{E - E_F}{k_B T}\right)}$$

To represent $\psi_i(w)$ we are interested in $1 - f_F(E)$, which gives:

$$\psi_i(w) = \frac{1}{1 + \exp\left(\frac{w_{mat} - w}{\chi_i}\right)} \tag{3.25}$$

where χ_i is a constant that sets the width of the passage from a non-reproducing size to a fully reproducing size. It may be defined with the aid of the x and y parameters in figure 3.5, and is given by:

$$\chi_i = \frac{1 - x}{\ln\left(\frac{1}{y} - 1\right)} w_{mat} \tag{3.26}$$

Selecting $x = 0.8$ and $y = 0.1$ means that 10% has matured at $0.8 w_{mat}$. This seems reasonable and corresponds to a typical χ value of $\chi = 0.091$.

To reduce the number of parameters in the model we link the size at maturation (now understood as the size where the maturation probability is 0.5) with the maximum size an individual may obtain:

$$w_{mat} = \eta_i w_\infty \tag{3.27}$$

Actually the size at maturation should be determined from optimal life-history theory (cf. i.e. Thygesen et al. (2005)), but this is out of the scope of this thesis. As a typical value we use $\eta = 1/8$ which seems viable with the assumption of (3.27).

The effective reproduction growth function $g_{i,repro,eff}(w)$ in (3.23) may also be stated as the ideal mass rate $\frac{\varrho_i}{\alpha_i}w$ times an effective reproduction selection function $\psi_{i,eff}(w)$ given by:

$$\psi_{i,eff}(w) = \psi_i(w) - \frac{\alpha_i}{\varrho_i w} g_{i,repro,miss}(w) \tag{3.28}$$

This function may be used to simplify interpretation of numerical simulations.

In the model we are considering only fish exposing indeterminate growth – that is fish that continue to grow after maturation. Determinate growth may however also be included for species like salmon by causing complete extinction after first reproduction.

Assessing Recruit Size w_0 and Efficiency e

Assessing the the constants in (3.23) is difficult. Selecting for a high w_0 is desirable for the numerical simulations since the $[w_0; w_\infty[$ span determines how many grid points that is needed in the simulations. Contrary a low w_0 is needed to include dynamics of the small individuals. The latter is most important to include realism, and hence the value $w_0 = 0.01\,\mathrm{g}$ is selected. Egg size varies from species to species, but a typical size of $w_{egg} \approx 0.5\,\mathrm{mg}$ may be assumed (Wootton (1979)). To determine a typical value for e_i we have to assess how many of the eggs that will become recruits at size w_0. If we had used $w_0 = w_{egg}$ the number of recruits (=eggs) in (3.23) would have been $w_0/w_{egg} = 20$ times higher, which means that we have some inclusion of mortality from the egg stage to the recruiting size w_0 in (3.23).

To ultimately determine e_i we will try and determine the fraction of individuals that survives from w_{egg} to w_0. From Andersen & Beyer (2006) (cf. section 5.1) we get that the density spectrum of a species scales with $n_i(w) \propto w_i^{-k-a}$, where $k = 3/4$ is the allometric scaling of metabolic requirements and a is a number characterising the predation strength. This gives the fraction of survival from w_{egg} to w_0: $n(w_0)/n(w_{egg}) = (w_0/w_{egg})^{-k-a}$. If the survival probability from egg to larvae stage is p then the typical value for e becomes:

$$e = p\frac{n(w_0)}{n(w_{egg})}\frac{w_0}{w_{egg}} = p\left(\frac{w_0}{w_{egg}}\right)^{1-k-a} \tag{3.29}$$

where we multiply with w_0/w_{egg} to account for the survival rate that is already included in (3.23). The eggs are exposed to a mortality rate μ, which makes us solve $\dot{n}(w_{egg}, t) = -\mu n(w_{egg}, t)$ to obtain $n(w_{egg}, t) = n(w_{egg}, 0)\exp(-\mu t)$. If the hatching time for the eggs is t_{hatch} then the survival probability will be $p = n(w_{egg}, t_{hatch})/n(w_{egg}, 0) = \exp(-\mu t_{hatch})$. From section 3.4 we know that predation mortality scales with $w^{-1/4}$, and from Andersen & Beyer (2006) we get the proportionality factor $\alpha h a$ (scaling of μ is 1/year). If we thus assume that size dependent predation mortality is the main mortality source for eggs we can specify (3.29) further:

$$e = \exp(-\alpha h a t_{hatch} w_{egg}^{-1/4})\left(\frac{w_0}{w_{egg}}\right)^{1-k-a} \tag{3.30}$$

where we immediately recognise a, t_{hatch}, and w_{egg} as the important and unknown parameters. The value of e is very sensitive to the value of a that characterises the

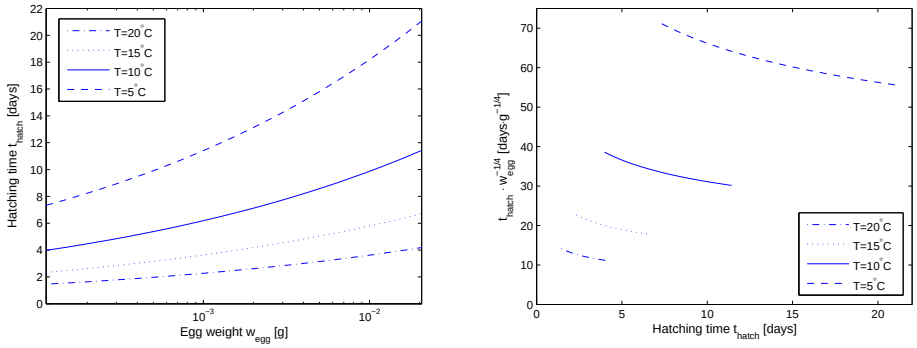

(a) (b)

Figure 3.6: *(a)* Hatching time as a function of egg weight. *(b)* Plot of $t_{hatch} w_{egg}^{-1/4}$ from (3.30) where it is seen that the actual selection of a (t_{hatch}, w_{egg}) pair plays a smaller role for the survival probability. Temperature is more important for the survival probability. Data obtained using a regression model from Pauly & Pullin (1988) that correlates egg diameter, temperature, and hatching time. Weights are obtained by assuming spherical shape and a density equivalent to water.

predation strength in the system. Larger values of a causes e to decline rapidly. The e value also depends strongly on both w_{egg} (positively) and t_{hatch} (negatively), but these parameters are easier to assess. Figure 3.6(a) shows the typical relationship between w_{egg} and t_{hatch}. Since w_{egg} and t_{hatch} have opposite effects on e we may expect that how we choose the actual (t_{hatch}, w_{egg}) pair plays a smaller role compared to the chosen value of a. This is indeed the case as shown in figure 3.6(b), which indicates that temperature on the other hand plays a key role.

To obtain a typical value of e we plot (3.30) in figure 3.7(a) for $w_{egg} = \{0.5, 5\}$ mg and overestimated hatching times of $t_{hatch} = \{2, 4\}$ weeks to include extra mortality that is not included in the survival property. Actual values of $a \in [0; 1.3]$ (Andersen & Beyer (2006)) are difficult to determine, but a typical value of $a \approx 0.6$ may be a good guess (Andersen (2006)). From these considerations we may thus select the typical value $e = 0.1$ for $w_0 = 0.01\,\mathrm{g}$ recruits from the plots in figure 3.7(a).

3.4 Mortality

In the previous section it was studied how individuals may grow to a larger size w in the size spectrum. In the following a mortality model will be derived that makes it possible for individuals to leave the spectrum.

An individual may die from size-dependent predation or from starvation when food abundance is sparse. Other causes of mortality, e.g. diseases, are more difficult to assess and are therefore included in a non-dominating constant *background mortality* term to ensure that mortality do occur for the largest individuals in the model. This means that the mortality rate for species i super-individuals of size w can be expressed as:

$$\mu_i(w, N) = \sum_j \mu_{p,j}(w, N) + \mu_{i,s}(w) + \mu_{i,0} \tag{3.31}$$

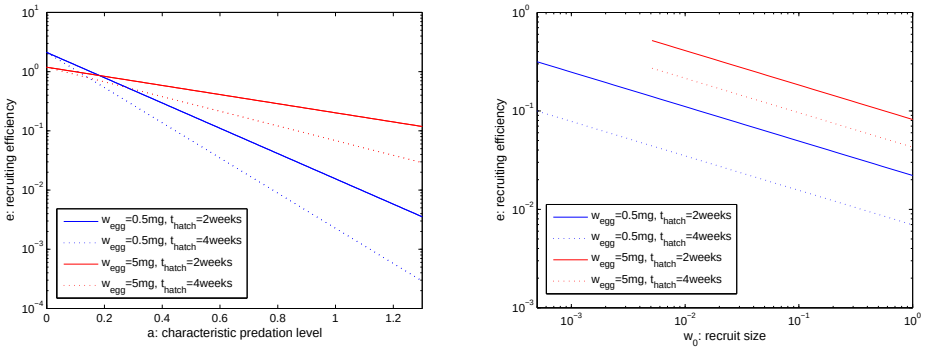

(a) (b)

Figure 3.7: *(a)* The recruiting efficiency e as a function of a using typical values from table 3.5. e is plotted for two different egg sizes: $w_{egg} = 0.5\,\mathrm{mg}$ (blue) and $w_{egg} = 5\,\mathrm{mg}$ (red). The solid plots show e for a hatching time of $t_{hatch} = 2\,\mathrm{weeks}$, and the dashed plots a value of $t_{hatch} = 4\,\mathrm{weeks}$. It is expected that natural systems have $a \approx 0.6$, which means that a value of $e = 0.1$ may be a typical value for recruiting efficiency to $w_0 = 0.01\,\mathrm{g}$ in (3.23). *(b)* Recruiting efficiency e as a function of recruiting size w_0 ($a = 0.6$).

where $\mu_{p,j}(w, N)$ is predation mortality from species j for an individual of size w, $\mu_{i,s}(w)$ a starvation mortality, and $\mu_{i,0}$ the background mortality. It is noted that cannibalism naturally is a special case of predation; $\mu_{p,i}(w, N) = 0$ if cannibalism is not included.

3.4.1 Predation Mortality

The size-dependent predation mortality rate from predator species j experienced by an individual with size w is the probability of being consumed at a given time-step by that species. This clearly means that the predation mortality is dependent on the density of predators ($\sim$ the environment $N(w, t)$).

Predation mortality rate may be calculated as the ratio of species j's total food intake of items with size w and the total amount of available food $\phi_j(w_p, N)$ for species j; cf. equation (3.5). The food intake of size w prey items by a predator of size w_p is the selection function times the feeding level times the optimally desired intake: $s_j(w, w_p) f_j(w_p, N) I_{j,max}(w_p)$. The total intake is then $s_j(w, w_p) f_j(w_p, N) I_{j,max}(w_p)$ multiplied with the predator density $n_j(w_p)$ integrated over w_p. The predation mortality from species j for an individual of size w thus becomes:

$$\mu_{p,j}(w, N) = \int \frac{s_j(w, w_p) f_j(w_p, N) I_{j,max}(w_p) n_j(w_p)}{\phi_j(w_p, N)} \, \mathrm{d}w_p \tag{3.32a}$$

We may express $I_{j,max}(w_p)$ in terms of $v_j(w_p)$, $\phi_j(w_p, N)$, and $f_j(w_p, N)$ via (3.8), which gives us the computationally simpler expression for the predation mortality:

$$\mu_{p,j}(w, N) = \int s_j(w, w_p) \left(1 - f_j(w_p, N)\right) v_j(w_p) n_j(w_p) \, \mathrm{d}w_p \tag{3.32b}$$

At a first glance this result might seem counterintuitive to the reader. Why is predation mortality zero when $f_j(w_p, N) = 1$ (full feeding) and large when $f_j(w_p, N) = 0$ (no feeding)? To understand this we take a look at the feeding

level $f_j(w_p, N)$ in (3.8). We note that the feeding level is an implementation of a functional response of type II. First we see that the two extremes of $f_j(w_p, N) = 0$ and $f_j(w_p, N) = 1$ only can be reached asymptotically. When feeding level goes to zero we effectively get a a type I functional response which means that the predation mortality should indeed be proportional to the swept search volume by the predator times the size-selective function: $\mu_{p,j}(w, N) = \int s_j(w, w_p) v_j(w_p) n_j(w_p)\, \mathrm{d}w_p$. On the other hand when feeding level goes towards one it means that the optimally desired intake $I_{j,max}(w_p)$ becomes very small compared to the available food ($v_j(w_p)\phi_j(w_p, N) \gg I_{j,max}(w_p)$), and thus the mortality rate should indeed go towards zero.

Peterson & Wroblewski (1984) found from theoretical justifications that the mortality in the pelagic ecosystem scales with w^{-x}, where $x \in [0.1; 0.4]$. One of the assumptions in Peterson & Wroblewski (1984) is that mortality due to predation is dominant, which is also consistent with the observed decrease of mortality for increasing body size. We may assume that the density of predators has the scaling of the community spectrum $w^{-\lambda}$. Thus in an equilibrium situation ($f_j(w_p, N) = const \neq 1$) it is easily seen that (3.32b) scales with $\mu_p \propto \int v(w) N_c(w)\, \mathrm{d}w \propto w^{q-\lambda+1}$. This yields $-x = q - \lambda + 1 \approx 0.83 - 2.05 + 1 = -0.22$, which is in agreement with Peterson & Wroblewski (1984). Typically size dependent predation mortality is assumed to scale with $w^{-1/4}$ if size dependent mortality is not modelled explicitly as in this thesis.

From (3.31) it seems that species i has no effect in itself on the mortality imposed by the predator species j. This is not true since it has an implicit effect on the predation mortality since individuals may aim for a high growth rate to escape mortality in a shorter time, and thus experience less mortality. In natural systems it would then be more vulnerable to starvation during periods of limited resources since it may spend less on building of lipid reserves, and it may also expose itself to a larger predation risk in the search for food items; see e.g. Biro et al. (2005) for inspiration. But by performing a trade off between risks there is an implicit effect from the individual itself on the predation mortality. Such optimal strategies will not be considered in this thesis, but can be incorporated in the model in a natural way. The predation mortality may also be reduced if there is low spatial connectivity between the prey and predator as illustrated in section 7.1 on network structure.

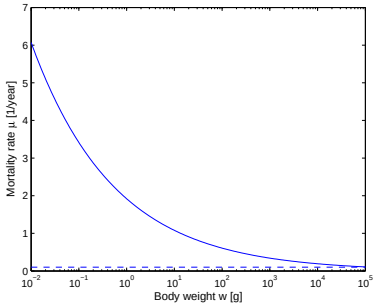

Figure 3.8: Plot of the typical size-dependent predation mortality $\mu_p(w) = 1.92 w^{-1/4}\,\mathrm{year}^{-1}$ (prefactor from Peterson & Wroblewski (1984)), and the constant background mortality $\mu_0 = 0.1\,\mathrm{year}^{-1}$. It is noted that the predation mortality in the model is explicit, so that the predation mortality is absent for the largest predators.

3.4.2 Starvation Mortality

Starvation mortality may occur when food abundance is sparse. Assessment of starvation mortality is difficult, and no data is available for validation of a model. However, an expression for starvation mortality is desired in the case that there is no food available for a given large predator. Otherwise, in simulations, we would have to wait for the background mortality to wipe out individuals that persist with no food and no enemies; and this can take up a lot of computational time.

Starvation occur if the maintenance requirements exceed the intake so that $e(w) = g_{i,main}(w) - g_{i,in}(w)$ is a positive quantity of the missing energy per time. We may assume that the time-scale before starvation death is inversely proportional to the missing energy, and proportional to the energy reserves (mostly lipids). The lipid masses (energy reserves) is a function of body weight, and as a first approximation it may be assumed proportional to body weight: ϵw. Thus the time-scale for starvation death is $\tau_s(w) = \epsilon w/e(w)$. The starvation rate can then be defined to be $\mu_s(w) = \tau_s(w)^{-1}$, which yields:

$$\mu_{s,i}(w) = \begin{cases} 0 & g_{i,in}(w) - g_{i,main}(w) \geq 0 \\ s_i \frac{g_{i,main}(w) - g_{i,in}(w)}{w} & g_{i,in}(w) - g_{i,main}(w) < 0 \end{cases} \tag{3.33}$$

where $s_i = 1/\epsilon$ is a dimensionless constant. An evaluation of the range of the prefactor s_i is easily made. A typical value for ϵ in the $0.05-0.2$ range seems reasonable, which again means that $s_i \in [5; 20]$. As discussed above starvation mortality should not play a significant role for the resulting total mortality in (3.31) so we select for a low typical value of $s = 5$.

In e.g. Persson et al. (1998) (and later models by Persson and de Roos) both the somatic and lipid mass of the individuals are modelled. When the lipid mass comes below a certain percentage of the somatic mass this is converted to a starvation mortality, which is inversely proportional to the lipid mass. An average effect of this is achieved by the starvation mortality in (3.33). In the Persson et al. (1998) model the starvation mortality goes to infinity when the lipid mass goes to zero. The net effect of starvation is not that pronounced in (3.33) but in the intermediate range the models are similar.

As mentioned earlier the starvation model is not validateable, and thus it cannot be used to study systems where the results depends heavily on the starvation mortality. States that have a strong dependence on starvation should hence be interpreted with caution. However, we do not see an important effect of (3.33) in simulations. Only if unrealistic initial conditions are used, where the simulation is started in a state where many individuals have access to too few suitable food items, then clearly the transient depends heavily on the starvation mortality. However, once the final state has been reached starvation will no longer play a key role since individuals in the continuous model clearly will not grow into a state where there is too little food. Such states will primarily occur if the system is disturbed. One can therefore say that the predation mortality actually incorporates an indirect effect of starvation mortality: if individuals cannot grow due to limited food then they will not able to escape predation mortality, and thus be more vulnerable to predation.

A more realistic starvation model may be obtained by taking into account that matured individuals has a higher proportion of lipid masses in form of gonads, which means that the denominator should be $w + \psi_i(w)\varrho_i w$. However, this would

require modifications of the resulting reproduction and since we are not interested in starvation dependent effects we avoid this complication.

3.4.3 Background Mortality

Causes of mortality different from predation and starvation is included in the background mortality. The background mortality is assumed constant and independent of size. Inclusion of a background mortality thus makes sure that mortality indeed do occur for the largest individuals in the model. A typical value of $\mu_0 = 0.1\,\text{year}^{-1}$ is used in the model (i.e. Andersen & Ursin (1977)).

3.5 Resource Supply from a Background Spectrum

This far we have described the individual growth, mortality, and reproduction. We envisage that the food intake for growth and reproduction comes from other species in the model, and that the species inflict predation mortality on each other. However, since we are modelling the species from a given recruit size w_0 and since the food selection (3.4) is a size-dependent process, then clearly suitable food items are missing for the smallest individuals in all species. To solve this we introduce the concept of a *background spectrum* to provide resources for small individuals. The first part of this section describes the concept of a background spectrum, and the second goes into the details of how the dynamics of the spectrum is modelled.

3.5.1 The Background Spectrum

In addition to the different species densities $n_i(w,t)$ we need a background spectrum to give the smaller individuals something to feed on as illustrated in figure 3.9. We aim at examining coexistence at the higher trophic levels, which means that we will not model the life-histories of small marine species/particles such as e.g. (zoo)plankton. The background will act as the limiting resource as for instance in the Rosenzweig-MacArthur model (Rosenzweig & MacArthur (1963)) – this means that the density dependence is food limitation. Engineers and physicists may think of the background spectrum as the energy input to the system, and loss of energy in non-ideal food intake and reproduction may be regarded as sinks.

In section 2.4 we introduced the concept of a *community spectrum* as the spectrum of everything in the sea. Naturally this is the sum of all the higher trophic species spectra modelled explicitly plus everything else as e.g. (zoo)plankton. The *total spectrum* (section 3.1) was introduced exactly as this summation, and from that discussion we know that the background spectrum represents the lower half of the community spectrum, and the modelled higher trophic species the upper half. We do not model the life histories of the species in the background spectrum since we are describing the higher trophic levels. And if we were to model the life histories the model would get very complicated since we then would have to model e.g. detritus and particles such as phosphorous. The steady-state or time average of the background spectrum should be a subset of the community spectrum (2.7):

$$n_{b,ss}(w) \equiv N_c(w)\big|_{w\le w_{cut}} = \kappa w^{-\lambda} \quad , \quad \text{for} \quad w \le w_{cut} \tag{3.34}$$

Thus the background spectrum is the lower half of the community spectrum up to a cut-off size w_{cut} as depicted in figure 3.9. The cut-off is located above $w_0 = 0.01\,\text{g}$

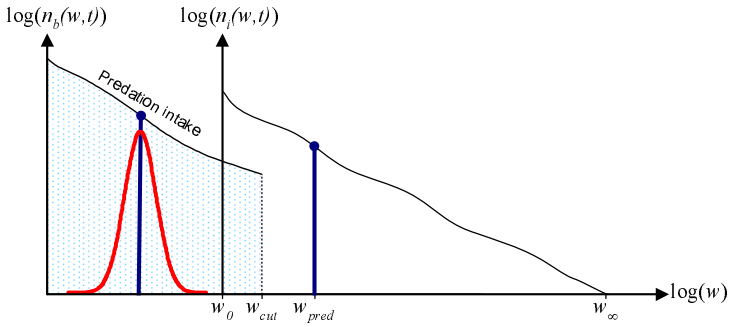

Figure 3.9: The modelled individuals enter the spectrum at weight w_0. A background spectrum $n_b(w,t)$ is introduced to give the smaller individuals items to feed on. The background spectrum is actually the lower half of the community spectrum (section 2.4) and the modelled species represent the upper half. Thus the background spectrum naturally should be cut-off at some weight w_{cut} since it should only provide resources to the system. The background spectrum is the primary production (∼energy input) in the system.

since resources are present at the size-scale of the recruits. Ideally the background spectrum should thus have a lower magnitude after w_0 (i.e. a bend downwards) to fulfill the concepts of the total- and the community spectrum. However, since we are also clearly missing out some higher trophic species (i.e. large octopuses) this is not important and will not change the qualitative results of the model.

As a default cut-off a value of $w_{cut} = 0.05\,\mathrm{g}$ is used in this thesis. Thus the background spectrum represents all resources with a weight up to $0.05\,\mathrm{g}$.

In the discussion in section 2.4 we discussed the value of λ. Andersen & Beyer (2006) considers a simplified steady-state version of the dynamic model in this thesis and arrives at $\lambda = 2.05$. This value of $\lambda = 2.05$ will be used as the slope for the background spectrum in the simulations of this thesis. The magnitude κ of the spectrum determines the resource abundance and thus the dynamic behaviour of the system as described in section 5.2.3. In section 3.5.2 a realistic value of κ is assessed.

The background spectrum is an elegant way of including multiple resources in the model, which is essential in any realistic model of a marine ecosystem. In aquatic environments the size-structured models have mainly been employed in freshwater systems where fewer resources most commonly are present (Havlicek & Carpenter (2001)). Here typically only one or two resources are modelled in a manner consistent to the approach in the Rosenzweig-MacArthur model – see i.e. de Roos et al. (1992), Claessen et al. (2000) and Persson et al. (2004). These models tend to get complicated at just two resources since they have to model the attack rate of the different resources independently (Persson et al. (2004)). This thesis aims for a lower level of detail and attacks the problem of an unlimited number of resources in a simple manner by employing the background spectrum.

In a simple case where the background is so abundant that the species cannot bring its density down at any size range the spectrum may be considered constant, and the total density of available food for a species i individual of size w_p can then be obtained analytically (cf. appendix A.2) if the background is extended throughout the species spectrum ($w_{cut} \to \infty$). This naturally corresponds to the total food

available from the community spectrum:

$$\begin{aligned}\phi_{i,c}(w_p) &= \int N_c(w) w s_i(w, w_p)\,\mathrm{d}w \\ &= \sqrt{2\pi}\kappa\sigma\beta_i^{2-\lambda}\exp\left[\frac{1}{2}\sigma_i^2(2-\lambda)^2\right] w_p^{2-\lambda}\end{aligned} \tag{3.35}$$

This result is used for steady-state considerations elsewhere in this thesis, and is stated here instead of in section 2.4 since the concept of the size selection function $s_i(w, w_p)$ had not been introduced at that stage. The case of a constant background density can also be used when examining the dynamics of the model without the influence of the background spectrum. Another density dependence (i.e. cannibalism) then naturally has to be included to avoid having the biomass going towards infinity. Such investigations are not carried out in this thesis.

3.5.2 Modelling the Background Spectrum

In this section we elaborate on how to model the background spectrum where it should be noted that each size in the background spectrum represents densities for different species, which means that the background spectrum is *not* modelled as the species spectra. Instead each size (in practice size ranges) is modelled with a population growth model.

The first step is naturally to employ the knowledge of the steady-state solution $n_{b,ss}(w)$ (3.34) in the construction of a time-dependent function of the background spectrum: $n_b(w,t)$. Since $n_{b,ss}(w)$ is the steady-state or the temporal average of $n_b(w,t)$ we may assume that $n_{b,ss}(w) = \kappa w^{-\lambda}$ is the carrying capacity $K_w = \kappa w^{-\lambda}$ in a density dependent growth equation (i.e. logistic growth). This employs food limitation which is the density dependence we are interested in.

The Ordinary Differential Equation (ODE) describing the dynamics of the background density spectrum at w is thus naturally given by the population growth rate $G(n_b, w)$ minus the experienced mortality $\mu_b(w, N)$:

$$\dot{n}_b(w,t) = n_b(w,t)\Big(G(n_b,w) - \mu_b(w,N)\Big) \tag{3.36}$$

where the mortality is given in the previous section by (3.31). We will only include predation mortality from the species spectra $n_i(w,t)$. Including background mortality would just be an effective re-scaling of regeneration rate and was only included on the species to make sure that the largest individuals are exposed to a mortality rate; this is clearly not needed on the density dependent resource. A starvation mortality does not make any sense for the background spectrum as we are not modelling its growth energetically.

In the following we will first elaborate on the form of the population growth function $G(n_b, w)$. Secondly analytical solutions to (3.36) will be provided. These are very useful since we have to solve (3.36) at many (+100) w grid points to obtain a continuous background spectrum. In the last two sections we will determine the parameters for regeneration rate and density magnitude for the background.

Details on Population Growth Rates: $G(n_b, w)$

In the following three different functions for the population growth $G(n_b, w)$ are presented. We will see that the functions have the same qualitative behaviour with

respect to studies of enrichment via the carrying capacity $K_w = \kappa w^{-\lambda}$. In the succeeding section we will discuss the three models further and select one of them for the studies in this thesis.

The most commonly used growth rate function is logistic growth (Verhulst (1838)) that once plugged into (3.36) constitutes the Rosenzweig-MacArthur model (3.37a) (Rosenzweig & MacArthur (1963)). The logistic growth does however not obey the relation $\partial_{n_b} G|_{n_b(w,t)=0} = 0$, which states that density dependency should go towards zero for a decreasing population. This is discussed by Getz (1998) who agitate for more complex functions. The problem may however be circumvented in a more simple manner by making a parabolic version of logistic growth as in (3.37b). As it will become evident in section 5.2.3 there is however not any practical difference between the two functions; see also figure 3.11(a). In explicit forms the growth functions appear as:

$$G_{RM}(n_b, w) = r_w \left(1 - \frac{n_b(w,t)}{K_w}\right) \tag{3.37a}$$

$$G_P(n_b, w) = r_w \left(1 - \frac{n_b(w,t)^2}{K_w^2}\right) \tag{3.37b}$$

$$G_{SC}(n_b, w) = r_w \frac{1}{n_b(w,t)} \Big(K_w - n_b(w,t)\Big) \tag{3.37c}$$

where r_w is a scaling of the population regeneration rate, and $K_w = n_{b,ss}(w) = \kappa w^{-\lambda}$ the carrying capacity for the background spectrum at w.

In the size-structured studies by the de Roos and Persson group a third growth rate function denoted semi-chemostatic growth (3.37c) is used. This growth model is fundamentally different and is supposed to represent resources that have a physical and/or size refuge as indicated in figure 3.10 (cf. e.g. Persson et al. (1998)). It also has a stabilising effect on the population dynamics compared to logistic growth (de Roos et al. (1990) and section 5.2). This can be understood by rewriting (3.37c):

$$G_{SC}(n_b, w) = r_w \frac{K_w}{n_b(w,t)} \left(1 - \frac{n_b(w,t)}{K_w}\right) \tag{3.38}$$

By comparison with (3.36) we see that semi-chemostatic growth is identical with logistic growth if the $n_b(w,t)$ pre-factor for $G(n_b, w)$ is changed to K_w. This gives a very rapid regeneration of resource depletion as illustrated in figure 3.11(a).

Semi-chemostatic growth is often argued to model abiotic resources and the logistic growth to model biotic resources. However, as argued above we may use it to represent a resource that i.e. has a refuge. Based on the idea from HilleRisLambers et al. (2006) we will now show that the three growth models considered in this thesis even have the same qualitative behaviour. The zero isoclines (equilibrium solutions)

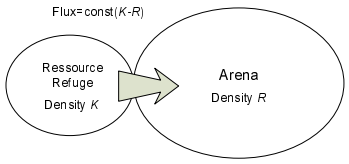

Figure 3.10: Semi-chemostatic population growth represents the scenario where the resource has a refuge that through a flux will try to keep the arena at the carrying capacity, which is equivalent to the refuge density.

for the growth models are found by solving (3.36) for $\dot{n}_b(w,t) = 0$:

$$G(n_b, w) = \mu_b(w, N) \tag{3.39}$$

The zero isoclines may now be explicitly written by solving this expression for $n_b(w,t)$ and inserting the three growth functions:

$$n_{b,RM}(w,t) = K_w \left(1 - \frac{\mu_b(w,N)}{r_w}\right) \qquad \vee \qquad n_{b,RM}(w,t) = 0 \tag{3.40}$$

$$n_{b,P}(w,t) = K_w \sqrt{1 - \frac{\mu_b(w,N)}{r_w}} \qquad \vee \qquad n_{b,RM}(w,t) = 0 \tag{3.41}$$

$$n_{b,SC}(w,t) = K_w \frac{r_w}{r_w + \mu_b(w,N)} \tag{3.42}$$

We thus see that the zero isoclines of the three growth models have the same proportionality in regards to the carrying capacity K_w. The zero isoclines separate the regions of phase space with effective negative and positive population growth rates; that is the regions of resource extinction and survival. In modelling studies the productivity or enrichment in form of the carrying capacity K_w is often the interesting parameter to vary; i.e. when examining the paradox of enrichment (Rosenzweig (1971)) and Intraguild Predation (IGP) (Holt & Polis (1997), Mylius et al. (2001)). This means that we will get the same qualitative response with either one of the three growth models. However, studies of the influence of regeneration rate r_w may differ as the regeneration times to identical mortality rates differ.

Analytical Solution of the Background ODE

Above three different growth functions were presented, and in the following we will provide analytical solutions to each of them. Furthermore we will provide arguments for selecting the semi-chemostatic model as the population growth model for the background resources.

By making the (very good) assumption that the mortality is constant from t to $t + \mathrm{d}t$ the three growth regimes inserted in (3.36) may be solved analytically as shown in appendix A.1. Analytical solutions for the ODEs describing the background spectrum allow a substantial reduction of computational time compared to the case where each ODE is solved numerically (cf. section 4.1.2).

Multiplying the solutions in appendix A.1 with $1/\Delta w$ give the solutions for the background density spectrum with the three different growth rate functions:

$$n_b(w,t)|_{RM} = \frac{K_w \left(1 - \frac{\mu_w}{r_w}\right) n_b(w,0)}{\left(K_w(1 - \frac{\mu_w}{r_w}) - n_b(w,0)\right) e^{-(r_w - \mu_w)t} + n_b(w,0)} \tag{3.43a}$$

$$n_b(w,t)|_P = K_w \sqrt{\frac{\frac{r_w - \mu_w}{r_w} n_b(w,0)^2}{(\frac{r_w - \mu_w}{r_w} K_w^2 - n_b(w,0)^2) e^{-2(r_w - \mu_w)t} + n_b(w,0)^2}} \tag{3.43b}$$

$$n_b(w,t)|_{SC} = \frac{r_w K_w}{r_w + \mu_w} - \left(\frac{r_w K_w}{r_w + \mu_w} - n_b(w,0)\right) e^{-(r_w + \mu_w)t} \tag{3.43c}$$

where $\mu_w = \mu_b(w,N)$ and $K_w = n_{b,ss}(w) = \kappa w^{-\lambda}$. The three resource responses are depicted in figure 3.11(a), and as seen in the figure and discussed in section 5.2.3 there is no practical difference between logistic and parabolic growth.

Logistic (and parabolic) regeneration times upon depletion depends heavily on the degree of depletion since the population is regenerated exponentially. Regeneration time in the semi-chemostatic model is only a very weak function of depletion level since the inflow flux dominates. This is depicted in figure 3.11(b).

In the numerical implementation we have to use a minimum level of $n_b(w, 0)$ to avoid that parts of the spectrum goes extinct in the transient of the simulation. If predator-prey dynamics are strong enough in the resulting cycle then the resources may be grazed to this minimum level. In this case simulations based on logistic and parabolic growth models will be dependent on the choice of the minimum level as depicted in figure 3.11(b). To avoid this we use the semi-chemostatic growth model in the simulations.

Furthermore, there is also a good physical reason for using semi-chemostatic growth: it is not likely that resources may be completely depleted, but that a flux of resources will occur from areas with higher resource abundances.

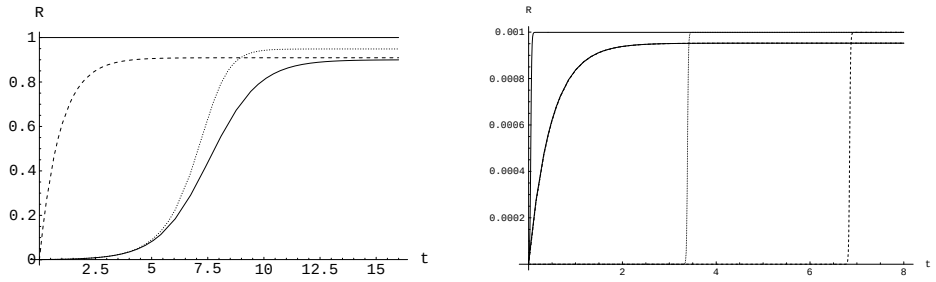

(a) (b)

Figure 3.11: *(a)* Comparison of logistic (solid), parabolic (dotted), and semi-chemostatic (dashed) growth. Parameters: $r_w = 1$, $K_w = 1$, $\mu_w = 0.1$, $R_{w,0} = 0.001$; cf. appendix A.1. *(b)* Comparison of regeneration time for logistic and semi-chemostatic growth for different initial conditions: $R_{w,0} = 10^{-5}$ (solid), $R_{w,0} = 10^{-150}$ (dotted), and $R_{w,0} = 10^{-300}$ (dashed). Initial condition plays a major role for logistic, but no role for semi-chemostatic growth (plots coincide). Parameters: $r_w = 100$ (logistic), $r_w = 2$ (semi-chemostatic), $K_w = 10^{-3}$, $\mu_w = 0.1$.

Determination of the Rate of Population Regeneration: r_w

In this section we will determine a biologically plausible value to be used as a typical value for the regeneration rate r_w in the semi-chemostatic population growth model. We will find regeneration rate to be an allometric function of resource size w, where we will determine both the prefactor and the scaling. In the succeeding section we will determine a typical value for the scaling of the carrying capacity κ.

r_w scales the rate of population regeneration. More technically r_w is the multiplicative inverse of the characteristic time τ for a population to recover, which must scale with the time it takes a recruit to reach maturation, which again scales with body size:

$$r_w = r_0 w^{-b} \tag{3.44}$$

The scaling of the characteristic life time for an individual with the maximum size w_∞ should principally be found by integration of the growth rate given in (3.18)

for the case of reproduction $\psi = 1$, and abundant food $f = 1$:

$$t(w_\infty) = \int_0^{w_\infty} \frac{1}{\alpha_i h_i w^k - \delta_i w^r - \psi_i(w)\frac{\varrho_i}{\alpha_i} w} \, \mathrm{d}w \tag{3.45}$$

However, since w_∞ is only reached asymptotically the integral is clearly divergent, which means that we cannot determine the size of the r_0 scaling in (3.44). We may however determine the b parameter by evaluating the integral to some size as i.e. the size at maturation w_{mat}:

$$\begin{aligned} t(w_\infty) \sim t(w_{mat}) &= \int_0^{w_{mat}} \frac{1}{\alpha_i h_i w^k - \delta_i w^r} \, \mathrm{d}w \\ &= \int_0^{w_{mat}} \frac{w^{-r}}{\alpha_i h_i w^{k-r} - \delta_i} \, \mathrm{d}w \\ &\approx \int_0^{w_{mat}} \frac{w^{-r}}{\alpha_i h_i w^{k-r}} \, \mathrm{d}w \propto w_{mat}^{1-k} \end{aligned} \tag{3.46}$$

where the approximation is carried out by using $\alpha_i h_i w^{k-r} \gg \delta_i$ (cf. section 3.6). We note that the scaling of the characteristic time to maturation (3.46) is independent of r. As discussed in section 3.3 the size at maturation w_{mat} is proportional to the maximum size w_∞, which means that we may determine b:

$$t(w_{mat}) \propto r_w^{-1} \quad \Leftrightarrow \quad r_w \propto w^{k-1} \quad \Rightarrow \quad b = 1 - k \tag{3.47}$$

To check that the assumptions used in this derivation actually holds (3.45) is integrated numerically and $t(0.9w_\infty)$ is plotted and fitted for various w_∞ in figure 3.12. We see that the obtained $b = 0.250$ is identical to the derived $b = 1-3/4 = 1/4$.

An emerging property of the growth model in this thesis is thus the general scaling of $r \propto w^{-1/4}$. Metabolic theory (Brown et al. (2004)) and DEB (Kooijman (2000)) set forward a theoretical framework to study and understand the mechanisms behind empirically observed scaling relationships. Both these frameworks yield the same scaling of $r \propto w^{-1/4}$.

Determining a realistic size range for r_0 is more difficult. For large r_0 the background spectrum in (3.36) becomes close to constant at the carrying capacity. For small values of r_0 the background will go to zero very easily in size ranges that

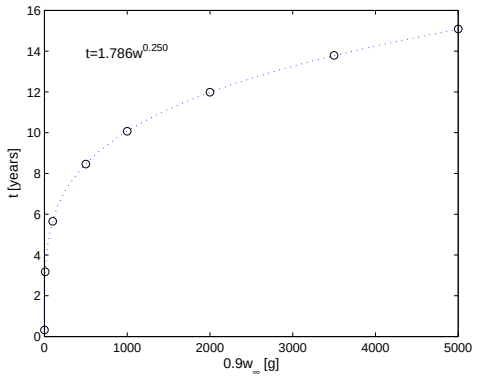

Figure 3.12: Result of numerical integration of $t(0.9w_\infty)$ in (3.45) and polynomial fit in logspace. The time to reach $0.9w_\infty$ is plotted on linear axes to emphasise the strong dependence of ultimate size w_∞. Parameters from table 3.5.

are exposed to predation. Large r_0 will alow species populations feeding on the background spectrum to reach higher biomasses.

We may not use the r_0 value of $r_0 = 1/1.786\,\mathrm{g^b/year}$ from figure 3.12 without caution since this value changes if we change the end-point of integration ($0.9w_\infty$) due to the flattening of the growth curve (cf. figure 3.3); w_∞ is only reached asymptotically.

From Savage et al. (2004) we can extract $r_0 \in [0.6;\, 19]\,\mathrm{g^b/year}$ for zooplankton in the $[3;\, 32]\,\mathrm{C^\circ}$ range ($r_0 \in [0.6;\, 4.2]\,\mathrm{g^b/year}$ in $[3;\, 17]\,\mathrm{C^\circ}$) and $r_0 \in [1.6;\, 4.2]\,\mathrm{g^b/year}$ for fish in the $[3;\, 17]\,\mathrm{C^\circ}$. They relate the regeneration rate to r in the exponential solution to $\dot{N} = rN$, which is equivalent to the regeneration rate in the logistic growth equation when the population density is far away from the carrying capacity. Yodzis & Innes (1992) calculated regeneration rates from the difference between maximum intake rate and maintenance and arrives at $r_0 = 37.1\,\mathrm{g^b/year}$ for vertebrate ectotherms*, which is a quite high value for regeneration rate that corresponds to the value for tropical waters in Savage et al. (2004).

Yodzis & Innes (1992) also states a regeneration rate of $2.17\,\mathrm{g^b/year}$ for phytoplankton in the $10^{-8} - 10^{-11}\,\mathrm{g}$ range, which again seems overestimated compared to the graph for algae in Savage et al. (2004). Also as stated above Savage et al. (2004) give larger regeneration rates for fish than zooplankton. The lower regeneration rates at lower trophic levels means that we may expect the lower levels to have a higher trophic transfer efficiency (efficiency of moving biomass between trophic levels) to allow constant biomass throughout the community spectrum. More research should however be put into this problem before making conclusions.

We have that $r_0 \in [0.6;\, 19]\,\mathrm{g^b/year}$, and as a typical value we may aim for using $r_0 \approx 1.6\,\mathrm{g^b/year}$ ($T = 10^\circ$). In the previous section we argued that the semi-chemostatic model will be used in the simulations of this thesis. The mechanism behind the semi-chemostatic model is inflow from a resource refuge, and to link values of r_0 in this model to the regeneration rate $r_w = r_0 w^{-b}$ in the logistic population model we plot the two models for three different resource sizes w in figure 3.13. From the plots we see that $r_0 = 1.0\,\mathrm{g^b/year}$ would be the corresponding value for the semi-chemostatic model. We note that we actually end up with a r_0 value close to value of $r_0 = 1/1.786\,\mathrm{g^b/year}$ from figure 3.12. In the fresh water studies of Persson et al. (2004) their influx rate in the semi-chemostatic resource corresponds to $r_0 = 1.7\,\mathrm{g^b/year}$ in the framework of this thesis. Section 5.2 investigates the role of r_0 in a one-species version of the model.

Determination of the Spectrum Magnitude: κ (and spectrum slope λ)

In the following a typical value for the magnitude κ of the background spectrum will be determined. The magnitude of the background spectrum sets the carrying capacity $K_w = \kappa w^{-\lambda}$ for the growth model of the background.

Determining a realistic size range of κ from the literature is very difficult due to low interest in the absolute magnitude of the spectrum and intense focus on the allometric exponent λ. κ sets the total biomass of the resource spectrum and may thus be quite different among ecosystems. In the following we will try to assess κ from three different approaches.

Approach 1) Rodriguez & Mullin (1986) presents data from the North Pacific Central Gyre from which we may calculate κ from the biomass density given by

*However, they do not state whether it is for fish or terrestrial species.

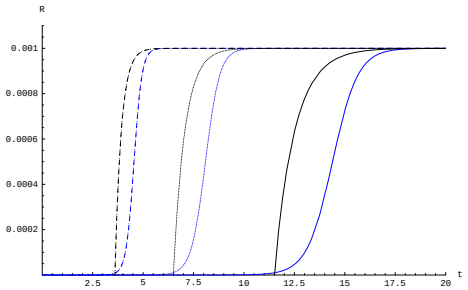

Figure 3.13: Comparison of population regeneration times for different sizes of resources: $w = 1\,\mathrm{g}$ (solid), $w = 0.1\,\mathrm{g}$ (dotted), and $w = 0.01\,\mathrm{g}$ (dashed). Blue curves show logistic growth using $r_w = 1.6w^{-1/4}\,\mathrm{year}^{-1}$, and black curves semi-chemostatic growth using $r_w = 1.0w^{-1/4}\,\mathrm{year}^{-1}$; the black curves are shifted to the right to allow comparison with the logistic regeneration times. We see that the actual time of active recover is equivalent for the two growth models with the used r_0. Parameters: $K_w = 10^{-3}\,\mathrm{gm}^{-3}$, $\mu_w = 0\,\mathrm{year}^{-1}$, $R_{w,0} = 10^{-10}\,\mathrm{gm}^{-3}$.

$b(w) = n_b(w)w = \kappa w^{1-\lambda}$ to be $\kappa = 10^{-3}\,\mathrm{g}^{1+\lambda}/\mathrm{m}^3$ (assuming $\lambda = 2$, and using conversion factors from Boudreau & Dickie (1992)).

Approach 2) According to Lewy (2006) ICES data indicate that the 10 most commercially important species in the North Sea have a biomass of $\sim 1.5 \cdot 10^{12}\mathrm{g}$ in the [5.8g; 11.3g] part of the community spectrum. If we thus assume that the total biomass in this range is $5 \cdot 10^{12}\mathrm{g}$ then we may find the biomass concentration by dividing with the volume of the North Sea ($94 \cdot 10^3\,\mathrm{km}^3$ from MUMM (2006)). Finally the biomass concentration $B = \int_{w_1}^{w_2} n_b(w)\,\mathrm{d}w = \kappa \ln(w_2/w_1)$ gives us $\kappa = 7.9 \cdot 10^{-2}\,\mathrm{g}^{1+\lambda}/\mathrm{m}^3$ (assuming $\lambda = 2$).

Approach 3) Andersen & Beyer (2006) examine steady-states in the community spectrum based on a model that is equivalent to parts of the model in this thesis (cf. section 5.1). From the idea set forward herein we may equate the required intake $f(w,N)I_{max}(w)$ (cf. (3.9)) with the encountered food from a constant community spectrum, which is given by $v(w)\phi_c(w)$ (cf. (3.35)). This can be used to find the minimum required κ to sustain the species (again we assume $\lambda \approx 2$):

$$\begin{aligned} f(w,N)I_{max}(w) &= f(w,N)hw^k = v(w)\phi_c(w) \\ &= \gamma w^q \sqrt{2\pi}\kappa\sigma\beta^{2-\lambda} \exp\left[\frac{1}{2}\sigma^2(2-\lambda)^2\right] w^{2-\lambda} \\ &\approx \gamma\sqrt{2\pi}\kappa\sigma w^{q+2-\lambda} \quad \Leftrightarrow \\ \lambda = 2+q-k \approx 2.08 \quad \wedge \quad \kappa &= \frac{hf(w,N)}{\sqrt{2\pi}\gamma\sigma} \approx 10^{-3}\,\mathrm{g}^{1+\lambda}/\mathrm{m}^3 \end{aligned} \tag{3.48}$$

The calculation was carried out using the default parameters in table 3.5 with a feeding level of 1. We see that the slope of the spectrum only depends on the allometric exponents for search volume and metabolic requirements. The slope is invariant of predator-prey ratio β and the width of the food selection function σ.

The magnitude of the background spectrum κ is a function of σ and more specialised species (small σ) require larger magnitudes. h and γ may be correlated such that a high search volume (high γ) requires a high metabolism (high h). It could be expected that κ should depend on the scaling of the primary production

(essentially light and nutrients). This is not the case in this derivation since the minimal required κ is calculated from a matching to species requirements. Furthermore no connection to primary production mechanisms that control the background spectrum are present in the model at hand. The background spectrum may be considered the primary production.

Instead of understanding (3.48) as a matching of κ to the species it might be more informative to understand it as an evolutionary fitting of the physiological requirements of the species to the available primary production. A study that examines actual values of κ, h, γ, and σ from different ecosystems (ie. deep sea vs. traditional pelagic/demarsal systems) could be interesting since this framework proposes a simple relation.

From the three different approaches we select $\kappa = 10^{-3}\,\mathrm{g}^{1+\lambda}/\mathrm{m}^3$ as a typical value for the magnitude of the background spectrum. This value is supported by the data from Rodriguez & Mullin (1986) and by theory from Andersen & Beyer (2006) in a model equivalent to the size-structured model of this thesis.

3.6 Model Summary and Default Parameters

In this chapter we have developed a simple size-structured population model for a marine ecosystem. The model is *simple* since only one parameter is used to characterise a species, namely the ultimate size w_∞. Thus real species are lumped into the species notion of this framework by considering their ultimate size.

Table 3.2 summarises the equations needed for modelling the p-state of the species, which are the PDE conservation equation and the reproduction that is the boundary equation in the PDE. The table also includes the equations needed for modelling the resources in the background spectrum. Table 3.4 lists the default parameters for the background spectrum. With these parameters the resources are employed in a biologically plausible region of parameter space.

After each equation the original equation number is shown in square brackets, and a new number is provided to make future references more easy. A reference to the section where each parameter was determined is given for all parameters.

The equations required for modelling the i-state are given in table 3.3. These include equations for growth, selection of reproducing individuals, food intake, and mortality.

The model naturally includes more species parameters than just w_∞. These are constant over all species, but in future studies one might try and make more parameters species-dependent. Maybe inter-species differences in more than one trait is important for coexistence (cf. chapter 8). Table 3.5 lists the default species parameters. These parameters are needed to scale the model into a biologically plausible region of the parameter space, which makes interpretation of model simulations easier.

When simulations are carried out the initial values of the spectra are: 1) a slope of -2 to ensure that larger individuals are under-estimated according to the results in section 5.1. 2) $K(w_\infty)$ magnitudes of the species spectra are selected according to (5.6) with a total magnitude below the background spectrum. The initial configuration is mainly important for the length of the transient, but if one wants to study states that are bistable one should of course select initial conditions more carefully.

Later in chapter 7 the model is extended to be used as a framework for size-structured food webs. With this addition actual food web configurations can be examined.

Table 3.2: Summary of p-state, E-state, and background spectrum equations.

Species PDE conservation equation:

$$\frac{\partial}{\partial t}n_i(w,t) + \frac{\partial}{\partial w}\Big(g_i(w,N)n_i(w,t)\Big) = -\mu_i(w,N)n_i(w,t) \qquad [3.2] \quad (3.49)$$

Reproduction (flux boundary condition, see details in sec. 3.3):

$$R_{i,tot}(t) = g_i(w_0)n_i(w_0,t) = \frac{e\alpha}{w_0}\int g_{i,repro,eff}(w')n_i(w')\,\mathrm{d}w' \qquad [3.23] \quad (3.50)$$

Total spectrum (the environment – E-state – for the species):

$$N(w,t) = n_b(w) + \textstyle\sum_i n_i(w,t) \qquad [3.1] \quad (3.51)$$

Background spectrum without exploitation (steady-state or time average):

$$n_{b,ss}(w) = \kappa w^{-\lambda} \qquad [3.34] \quad (3.52)$$

Background ODE conservation equation (details in sec. 3.5.2):

$$\dot{n}_b(w,t) = n_b(w,t)\Big(G(n_b,w) - \mu_b(w,N)\Big) \qquad [3.36] \quad (3.53)$$

Semi-chemostatic resource population growth rate function:

$$G(n_b,w) = r_w\frac{1}{n_b(w,t)}\Big(K_w - n_b(w,t)\Big) \qquad [3.37c] \quad (3.54)$$

Background regeneration rate for background resources of weight w:

$$r_w = r_0 w^{-b} \qquad [3.44] \quad (3.55)$$

Carrying capacity for size w resource (cf. section 3.5.2):

$$K_w = n_{b,ss}(w) \qquad (3.56)$$

Table 3.3: Summary of i-state and the most important supporting equations.

Growth function (see complications in sec. 3.2.3):

$$g_i(w,N) = \alpha f_i(w,N) h w^k - \delta w^r - \psi_i(w)\frac{\varrho}{\alpha} w \quad [3.18] \quad (3.57)$$

Growth function in the $\varrho(w_\infty)$ formulation:

$$g_i(w,N) = \alpha f_i(w,N) h w^k - \delta w^r - \psi_i(w)\left(\alpha h w_\infty^{k-1} - \delta w_\infty^{r-1}\right) w \quad [3.22] \quad (3.58)$$

Reproduction selection function:

$$\psi_i(w) = \frac{1}{1+\exp\left(\frac{w_{mat}-w}{\chi}\right)} \quad [3.25] \quad (3.59)$$

Relation between w_{mat} and w_∞:

$$w_{mat} = \eta w_{\infty,i} \quad [3.27] \quad (3.60)$$

Feeding level:

$$f_i(w_p,N) = \frac{v(w_p)\phi_i(w_p,N)}{v(w_p)\phi_i(w_p,N)+I_{max}(w_p)} \quad [3.8] \quad (3.61)$$

Search volume:

$$v(w) = \zeta\gamma w^q \quad [3.7] \quad (3.62)$$

Maximum food intake rate:

$$I_{max}(w) = h w^k \quad [3.9] \quad (3.63)$$

Available food:

$$\phi_i(w_p,N) = \int N(w,t) w s_i(w,w_p)\,\mathrm{d}w \quad [3.5] \quad (3.64)$$

Food selection function:

$$s(w,w_p) = \exp\left[-\ln^2\left(\frac{w}{\beta w_p}\right)/(2\sigma^2)\right] \quad [3.4] \quad (3.65)$$

Total mortality rate:

$$\mu_i(w,N) = \textstyle\sum_j \mu_{p,j}(w,N) + \mu_{i,s}(w) + \mu_{i,0} \quad [3.31] \quad (3.66)$$

Predation mortality from species j:

$$\mu_{p,j}(w,N) = \int s(w,w_p)\left(1 - f_j(w_p,N)\right) v(w_p) n_j(w_p)\,\mathrm{d}w_p \quad [3.32b] \quad (3.67)$$

Starvation mortality:

$$\mu_{s,i}(w) = \begin{cases} 0 & g_{i,in}(w) - g_{i,main}(w) \geq 0 \\ s\frac{g_{i,main}(w) - g_{i,in}(w)}{w} & g_{i,in}(w) - g_{i,main}(w) < 0 \end{cases} \quad [3.33] \quad (3.68)$$

Table 3.4: Default background parameters.

κ	10^{-3}	$\mathrm{g}^{1+\lambda}/\mathrm{m}^3$	Background spectrum magnitude (sec. 3.5.2).
λ	2.05	-	Slope of background spectrum (sec. 3.5.1).
r_0	1.0	g^b/year	Prefactor for resource regeneration rate (sec. 3.5.2).
b	1/4	-	Allometric scaling exponent for resource regeneration rate (sec. 3.5.2).
w_{cut}	0.05	g	Cut-off of the background spectrum (sec. 3.5.1).

Table 3.5: Default species parameters. Maximum size w_∞ is the only parameter used to characterise a specie.

w_0	0.01	g	Recruit size (sec. 3.3).
k	3/4	-	Allometric scaling of food intake (sec. 3.2.3).
r	1	-	Allometric scaling of maintenance (sec. 3.2.3).
α	0.3	-	Assimilation efficiency (sec. 3.2.3).
h	25	g^{1-k}/year	Prefactor for maximum food intake (sec. 3.2.3).
δ	0.11	g^{1-r}/year	Prefactor for maintenance (sec. 3.2.3).
ϱ	0.15	1/year	Mass percentage rate invested in reproduction (sec. 3.2.3). Not used in the $\varrho(w_\infty)$ (3.57) formulation.
e	0.1	-	Efficiency of turning spawning mass into recruits of size w_0 (sec. 3.3).
η	1/8	-	Fraction of ultimate size that determines maturation size in (3.60) (sec. 3.3).
χ	0.091	-	Scaling of the reproduction selection function width (corresponds to $x = 0.8$ and $y = 0.1$, sec. 3.3).
q	0.82	-	Allometric scaling of search volume (sec. 3.2.1).
γ	10^4	$\mathrm{m}^3\mathrm{g}^{-q}/\,\mathrm{year}$	Search volume prefactor (sec. 3.2.1).
β	0.01	-	Prey-predator mass ratio (sec. 3.2.1).
σ	1	-	Width of prey selection function (sec. 3.2.1).
μ_0	0.1	1/year	Background mortality rate (sec. 3.4).
s	5	-	Starvation mortality coefficient (sec. 3.4.2).

4

Numerical Setup

In this chapter a method for solving the Partial Differential Equation (PDE) describing the dynamics of the p-state in (3.49) is derived. After the derivation convergence tests is carried out to determine how many grid points and how small time steps that is needed in simulations. It is found that numerical diffusion plays a minor role in the numerical method. However, diffusion is concluded not to have a qualitative effect, and methods for removing diffusion are also discussed.

The treatment of the numerical method for solving the PDE is followed by a description of the setup of the non-linear grid and the numerical evaluation of integrals.

4.1 Numerical Solution of the p-state PDE

General formulations of the structure of analytical solutions to the PDE in (3.49) that describes the dynamics of the p-state can be found in e.g. de Roos (1996). However, it is not possible to extract explicit numerical solutions of the PDE, which means that we will have to numerically simulate the set of equations set forward in tables 3.2–3.3. The numerical setup along with convergence tests of the numerical solution of the PDE is the topic of this section.

4.1.1 Numerical Method for Solving the PDE

In the following we will describe the numerical method used to solve the PDE in (3.49). For notational simplicity we will not include the species number i. Instead we will use index i for time discretization. The grid points w_m are distributed evenly on a logarithmic scale as discussed in section 4.2 and the time t is evenly discretisized as:

$$w_m = w_0 + \sum_{j=1}^{m} \Delta w_m \quad , \quad i = 0, 1, 2, \ldots, M-1 \tag{4.1}$$

$$t_i = t_0 + i\Delta t \quad , \quad i = 0, 1, 2, \ldots, i_{end} \tag{4.2}$$

where it is noted that the w_m grid has M points.

As in section 2.3 we have to translate between discrete and analytical derivatives. We may use the following approximations for time t and weight w derivatives:

$$\left.\frac{\partial n(w,t)}{\partial t}\right|_{t=t_i,w=w_m} = \frac{n_m^{i+1}-n_m^i}{\Delta t} + O(\Delta t) \tag{4.3}$$

$$\left.\frac{\partial g(w,N)n(w,t)}{\partial w}\right|_{t=t_i,w=w_m} = \frac{g_m^i n_m^{i+1} - g_{m-1}^i n_{m-1}^{i+1}}{\Delta w_m} + O(\Delta w_m) \tag{4.4}$$

where n_m^i denotes the density at time-step i and weight index m. Similarly for the growth function g_m^i. The approximation in (4.4) is known as the Upwind approximation because we calculate the derivative in m from m and $m-1$. This can be done since the growth function $g(w,N)$ always is positive*; remember that the problem of "shrinking fish" upon food depletion was solved by introducing a starvation mortality (section 3.4.2). We also note that the approximation in (4.4) is semi-implicit since we are using the density at time-step $i+1$. This implicit Upwind scheme of first order in both w and t is very stable, but diffusive. The problem of numerical diffusion is treated in the next section.

By using (4.3)–(4.4) we may write the PDE describing the p-state dynamics in (3.49) as:

$$\frac{n_m^{i+1}-n_m^i}{\Delta t} + \frac{g_m^i n_m^{i+1} - g_{m-1}^i n_{m-1}^{i+1}}{\Delta w_m} = -\mu_m^i n_m^{i+1} \qquad \Leftrightarrow \tag{4.5}$$

$$n_{m-1}^{i+1}\underbrace{\left(-\frac{\Delta t}{\Delta w_m}g_{m-1}^i\right)}_{A_m} + n_m^{i+1}\underbrace{\left(1+\frac{\Delta t}{\Delta w_m}g_m^i + \Delta t\mu_m^i\right)}_{B_m} = \underbrace{n_m^i}_{C_m} \tag{4.6}$$

The boundary condition $g(0,N)n(0,t)$ is equal to the reproduction R as described in (3.50). This gives us $g_0^i n_0^{i+1} = R$ and we may recast (4.5) to obtain:

$$\begin{aligned}&\frac{n_1^{i+1}-n_1^i}{\Delta t} + \frac{g_1^i n_1^{i+1} - R}{\Delta w_1} = -\mu_1^i n_1^{i+1} \qquad \Leftrightarrow \\ &n_1^{i+1}\underbrace{\left(1+\frac{\Delta t}{\Delta w_1}g_1^i + \Delta t\mu_1^i\right)}_{B_1} = \underbrace{n_1^i + \frac{\Delta t}{\Delta w_1}R}_{C_1}\end{aligned} \tag{4.7}$$

where we note the identity $A_1 = 0$. The A_m, B_m, and C_m identities in (4.6) and (4.7) may be used to easily describe the problem to be solved in a simple manner:

$$\begin{bmatrix} B_1 & & & & \\ A_2 & B_2 & & & \\ & A_3 & B_3 & & \\ & & \ddots & \ddots & \\ & & & A_M & B_M \end{bmatrix} \begin{bmatrix} n_1^{i+1} \\ n_2^{i+1} \\ n_3^{i+1} \\ \vdots \\ n_M^{i+1} \end{bmatrix} = \begin{bmatrix} C_1 \\ C_2 \\ C_3 \\ \vdots \\ C_M \end{bmatrix} \tag{4.8}$$

Naturally we are interested in solving for the vector n_m^{i+1} since this gives us the density spectrum at the next time-step. The matrix in (4.8) is bidiagonal, which

*A numerical scheme could be implemented even if fish were allowed to shrink in size. A case in the solver changing between a Down- and Upwind method should then be implemented.

means that we may easily solve for n_m^{i+1} using the simple iteration:

$$A_m n_{m-1}^{i+1} + B_m n_m^{i+1} = C_m \quad \Leftrightarrow$$
$$n_m^{i+1} = \frac{C_m - A_m n_{m-1}^{i+1}}{B_m} \tag{4.9}$$

This iteration process naturally also works for the first grid point since (4.7) gives us $A_1 = 0$.

In the following section we will perform convergence test of this semi-implicit Upwind scheme. However, to ensure stability one should obey the Courant condition (i.e. Press et al. (1992)):

$$\frac{|g_m^i|\Delta t}{\Delta w_m} \leq 1 \tag{4.10}$$

which basically states that an individual should grow less than Δw_m in the time-step Δt. The Courant condition is the same criterion as the one we used in the derivation of the PDE (3.49) to ensure that individuals grow through the grid points successively (section 2.3).

4.1.2 Convergence – Selection of Step Size and Grid Spacing

In this section we will determine the required number of grid points M in w_m and the required Δt for convergence. Cyclic states are more difficult to model than steady states and therefore a cyclic state in the one species model was located. The parameters from section 3.6 are used with the exception of $\kappa = 1.5 \cdot 10^{-4}\,\mathrm{g/m^3}$, and a regeneration rate for the background resources of $r_0 = 20\,\mathrm{g^b/year}$. The modelled species has $w_\infty = 18\,\mathrm{kg}$ and the selected parameters result in cyclic states as it will become evident in the following.

To obtain time convergence we run simulations with $M = 200$ and $\Delta t = 2/2^j$ ($j = 1, 2, \ldots, 13$). Figure 4.1(a) shows that the spectrum after 100years has converged after $j = 5$. We can extract a measure of the error by using:

$$e(\Delta t) = \frac{1}{M}\sum_{m=1}^{M}\left(n\Big(w_m, t'; \Delta t\Big) - n\Big(w_m, t'; \frac{1}{2}\Delta t\Big)\right)^2 \tag{4.11}$$

which states a measure of the error introduced by doubling Δt at a given time-step t'. Since the used implicit Upwind scheme is of first order in time we expect errors in the magnitude:

$$e(\Delta t) \propto O\Big(\Delta t\Big) - O\Big(\frac{1}{2}\Delta t\Big) = \frac{1}{2}\Delta t \tag{4.12}$$

which means that we halve the error whenever we double Δt. More explicitly the expected error will be $e(2^{-j}\Delta t) \propto 2^{-(j+1)}\Delta t$. Figure 4.1(b) shows that the observed error indeed do follow this.

Figure 4.1(a) shows that convergence is definitely reached after $j = 5$, but from 4.1(b) we may also justify the use of $j = 4$. As a result we may take a value of $\Delta t = 0.075$ in between.

As expected from the Courant condition (4.10) we need a smaller Δt as we increase M. Figure 4.2(a) shows the biomass evolution from simulations using different M calculated using (2.2). When making the plot we use smaller Δt for larger

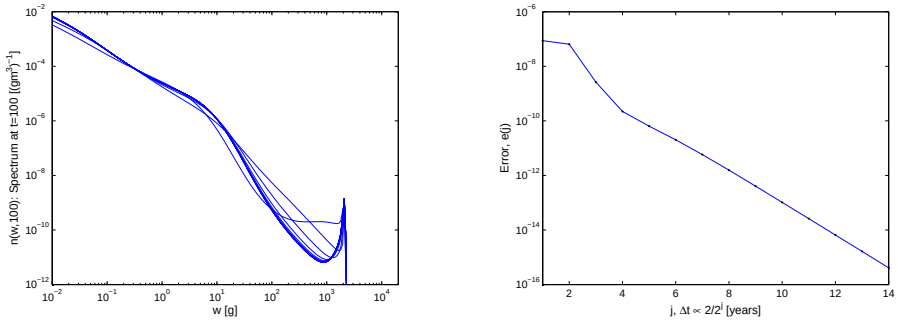

(a) (b)

Figure 4.1: Simulations using $M = 200$ grid points and $\Delta t = 2/2^j$ $(j = 1, 2, \ldots, 13)$. *(a)* For increasing j we see that the spectrum after 100years has converged for $j = 5$. *(b)* The error calculated from (4.11) for j in $\Delta t = 2/2^j$.

M to ensure that time convergence is fulfilled. From the figure we see that the solutions from differing M has different period lengths. This is mainly due to numerical diffusion in the implicit Upwind scheme, but may also partly be due to discretization errors. We may calculate the error introduced when lowering N as done in the time convergence test via (4.11). However, due to computational time we cannot double M between each run, but instead we run tests using $M = 100, 150, 200, \ldots, 600$ and calculate the error introduced by lowering M with $M_{extra} = 50$ grid points:

$$e(M) = \frac{1}{M} \sum_{m=1}^{M} \left(n\Big(w_m, t'; M\Big) - n\Big(w_{m'}, t''; M + M_{extra} \big| \, w_m\Big) \right)^2 \tag{4.13}$$

where we get the problem that we are not evaluating the simulations along the same w grid. Therefore we use linear interpolation on the solution with the larger grid to retrieve its densities at the grid points from the simulation with the smaller grid.

Figure 4.3(a) shows the error calculated at $t' = t'' = 100\,\text{years}$ (blue), and at

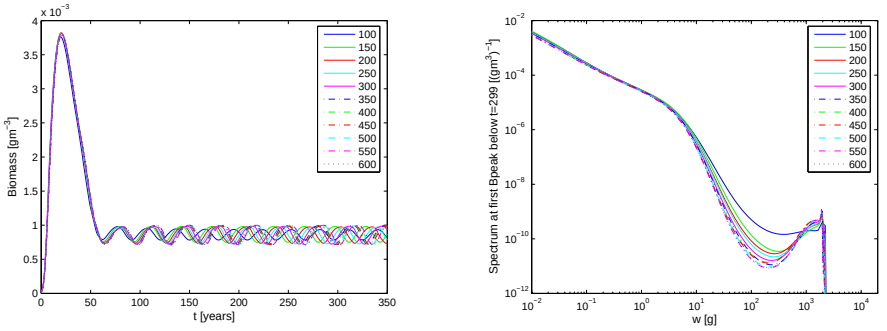

(a) (b)

Figure 4.2: Simulations for different number of grid points M. *(a)* Biomass evolution; see figure (b) for colour nomenclature. *(b)* Density spectrum at the first peak in the biomass evolution below 300years. These spectra are close to identical, but the states have different period lengths.

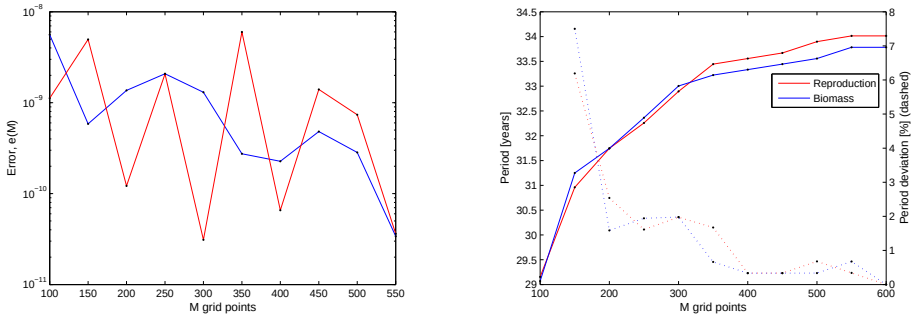

(a) (b)

Figure 4.3: Simulations for different number of grid points M. *(a)* Errors calculated using (4.13). After 100years (blue) and of the spectra in figure 4.2(b) (red). *(b)* Period lengths for reproduction and biomass, and the relative error in period length when lowering M with $M_{extra} = 50$ (dashed).

the first period top below $t = 300$ years (red). The blue curve shows a decreasing error since the difference in period lengths are getting smaller and the solutions thus become more identical. However, the red curve shows that the actual error at comparable time-steps is not getting better for increasing M. The red curve is calculated on the densities in figure 4.2(b).

So if the error is not getting smaller, then why use a larger grid? In figure 4.2(a) we saw that M infers changes on the period length of the cyclic state and from figure 4.3(a) we see that the discretization error is not the main driver for this. The reason for the changes in period length is numerical diffusion. Figure 4.3(b) shows the period length and the relative error introduced when lowering M with M_{extra}, and from that we can see no clear sign of grid convergence within the examined M range; and aiming for even higher M is unrealistic. Period lengths where calculated using Discrete Fourier Transform (DFT).

To examine the problem of numerical diffusion the Quadratic Upwind Interpolation for Convective Kinematics (QUICK) scheme was implemented using Versteeg & Malalasekera (1995) and Ferziger & Perić (2002) for computing coefficients on a non-linear grid. The QUICK scheme is a third order scheme in the w dimension, which means that the diffusion will be less pronounced. Numerical diffusion is most important in species with larger w_∞ since their longer growth trajectory leaves more time for diffusion. The simulations from the above convergence tests was repeated with the QUICK scheme for the species having $w_\infty = 18$ kg, and figure 4.4 shows the results.

From figure 4.4(a) wee see that numerical diffusion do get less pronounced with the high-order scheme since the period lengths become more similar. In figure 4.4(b) we see that the period length changes less with grid size and that grid convergence seems more clear than in the Upwind scheme in figure 4.3(b). This means that we should aim for the QUICK scheme which do not require substantially more computation time since it only requires us to invert a tridiagonal matrix compared to the bidiagonal matrix in the Upwind scheme. However, the draw-back from the QUICK scheme is that it imposes oscillations (overshoots) that may lead to small negative numbers in the density matrix. This can be circumvented by using the techniques set forward in Zijlema (1996).

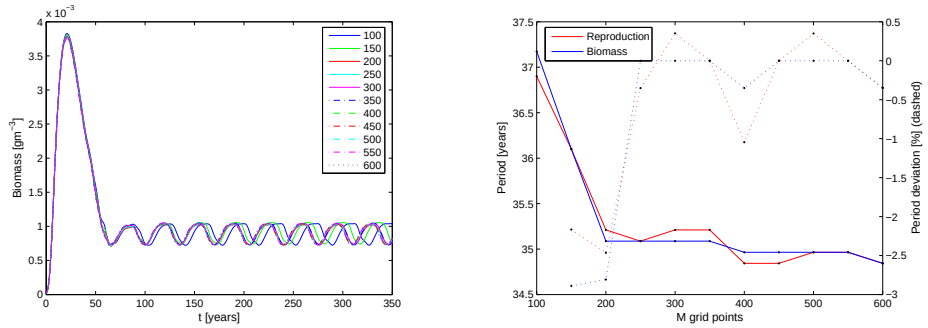

(a) (b)

Figure 4.4: Simulations for different M using the QUICK scheme. *(a)* Biomass evolution. *(b)* Period lengths for reproduction and biomass, and the relative error in period length when lowering M with $M_{extra} = 50$ (dashed).

Conclusion

The implementation has been tested in three independent ways. 1) Stationary solutions with constant growth, mortality, and boundary condition was compared to analytical results from Mathematica. 2) Two independent implementations was compared. And lastly 3) simulations from the QUICK and Upwind scheme was compared.

Numerical diffusion can be minimised by using the QUICK scheme or by adding natural diffusion (as mentioned in section 2.3.1). However, assessing a diffusional term, or any other higher order term encapsulating differing growth trajectories, for the PDE in (3.49) is out of the scope of this thesis. Also it would be nice to able to use the model without the complexity of diffusion.

A third way of avoiding diffusion would be to solve for growth trajectories (characteristics) for the super-individuals, and then make sure that the set of tracked super-individuals is dense enough to allow evaluation of the integrals involved in the model. A method for solving characteristics in Physiologically Structured Population (PSP) models is the Escalator Boxcar Train (EBT) method. However, this will require quite some implementation effort and it might be too heavy computationally. This method is not pursued in this thesis.

The convergence tests show that numerical diffusion is not strong enough to change the qualitative result of the simulations. The techniques of Zijlema (1996) have not been implemented due to time constraints. Therefore the semi-implicit Upwind scheme using $M = 200$ and $\Delta t = 0.05$ will be used in this thesis. However, actually the tests showed that $\Delta t = 0.075$ could be used, but since faster population dynamics might be encountered the smaller Δt will be used. As seen by comparing figures 4.3 and 4.4 the semi-implicit Upwind scheme is good enough, but with QUICK and the techniques by Zijlema (1996) it might be possible to use a lower M and thus also a smaller Δt, which will lead to shorter computation times which is clearly wanted for using the model as a multi-species model as in the following chapters.

4.2 Defining the Grid

The PDE is a one dimensional transport equation, which means that we need a grid in the weight w dimension. As previously discussed the density function $n_i(w,t)$ of the species is best described in a logarithmic plot. This is due to the fact that the growth function ($\sim$transport velocity) $g_i(w)$ (3.57) of the super-individuals naturally is a linear function in a double logarithmic plot.

To have the grid points for computation logarithmically evenly distributed in w space the following recursion apply:

$$\begin{aligned} &\log w_{m+1} - \log w_m = k \quad \Leftrightarrow \\ &w_{m+1} = w_m 10^k \end{aligned} \tag{4.14}$$

where k is the constant length between grid points in logarithmic space. Index m refers to the grid point number. We assume that the first grid point is w_1 and naturally it is located at the recruit size $w_1 = w_0$ (cf. table 3.5). From this we obtain:

$$w_m = w_0 10^{(m-1)k} \tag{4.15}$$

which can be used directly to calculate the grid. Often one do not have a value for k but a certain number of desired points M in the grid. From (4.15) we may retrieve k from the two end points w_0, w_{max}, and the desired number of grid points M:

$$k = \frac{1}{M-1} \log\left(\frac{w_{max}}{w_0}\right) \tag{4.16}$$

In addition to the w grid we also need $\mathrm{d}w_m$ to perform numerical evaluations of integrals in the simulations. Numerically we naturally need Δw_m:

$$\begin{aligned} \Delta w_m &= \frac{\mathrm{d}w_m}{\mathrm{d}m} = \frac{\mathrm{d}}{\mathrm{d}m} w_0 10^{(m-1)k} \\ &= k w_0 \ln(10) 10^{(m-1)k} \end{aligned} \tag{4.17}$$

If we had had a linear grid Δw_m would of course have been independent of m.

4.3 Integrals & the Background Spectrum

This section describing the numerical setup is not exhaustive since implementations of i.e. the functions in tables 3.2–3.3 is straightforward. However, to do justice it is worthwhile binding a couple of notes the modelling of the background spectrum and of integral evaluation.

Integrals of i.e. the biomass (2.2) is calculated numerically using (4.17) and summation:

$$B(t) = \int_{w_1}^{w_2} n_i(w,t) w \,\mathrm{d}w \simeq \sum_{m_1}^{m_2} n_i(w_m,t) w_m \Delta w_m \tag{4.18}$$

Integrals can be evaluated more precisely using i.e. trapezoidal numerical integration. However, doing so makes the computational load much higher, and no difference was seen in actual simulations.

The grid for the background w_{nb} is equal to the w grid from (4.15) and extended towards smaller weights using the same k distance in logarithmic space. It is extended low enough to enable the use of the food-selection function $s(w, w_p)$ (3.65) at $w_p = w_0$. When using i.e. $M = 200$ and w_{cut} from table 3.4 the w_{nb} grid will contain 117 grid points if w_{nb} should be extended three orders of magnitude below w_0.

The background spectrum is modelled by using a density-dependent growth model (i.e. semi-chemostatic or logistic growth). In each grid point of w_{nb} we have to solve an Ordinary Differential Equation (ODE). Luckily these can be solved analytically so that we can keep the computational load to a minimum (cf. section 3.5.2).

5

The Single-Species Model

In this chapter we will start investigating the size-structured model summarised in section 3.6. Before advancing to multiple species we will focus on just a single species in this chapter. This is done to gain an intuitive understanding of the model before adding the complexity of multiple species in the following chapters.

First we will look at a simplified version of the model to obtain knowledge about the steady-state single-species spectrum in the model. From this we actually also obtain the distribution of species in the model.

To gain knowledge about the dynamics of the model from chapter 3 we will examine the model with just a single species. From the examination we find that the size-structured model indeed are capable of producing dynamics that are consistent with the kind of dynamics that is observed in nature. An important discussion in this chapter is the discussion in section 5.2.5 on the maximum w_∞ that can exist when the background spectrum is truncated (cf. section 3.5.1).

5.1 Steady-state Solution in a Simple Subsystem

In the following we will determine an analytical solution to the steady-state spectrum for a single species in a reduced model of the one from chapter 3. We will also find the distribution of species spectra for different w_∞ in the community spectrum and that the biomass among species are constant.

Since the community spectrum (2.7) is the sum of all species' size spectra it should be possible to extract what these spectra will look like in a steady-state situation:

$$\frac{\partial}{\partial w}\Big(g(w)n(w)\Big) = -\mu(w)n(w) \tag{5.1}$$

In this section we will derive the form of the species' spectra by following the approach by Andersen & Beyer (2006). To allow an analytical solution we will not consider reproduction explicitly, but ignore the ontogenetic shift in the growth curve and just assume than its cost is part of the maintenance costs. Also we will assume that food is abundant so that the feeding level becomes $f_i(w, N) = 1$. This allows

us to write the growth equation (3.57) simply as:

$$\begin{aligned} g(w) &= \alpha h w^k - \left(\delta + \frac{\varrho}{\alpha}\right) w^r \\ &= \alpha h w^k - \alpha h w_\infty^{k-r} w^r \end{aligned} \tag{5.2}$$

where we for the case of generality allow an allometric scaling r of the maintenance costs, and used $g(w_\infty) = 0 \Rightarrow \delta + \frac{\varrho}{\alpha} = \alpha h w_\infty^{k-r}$.

The mortality for an individual of size w is caused by all individuals in the community spectrum that can predate on it. Predators of size w_p search the volume $v(w_p)$ per unit time, and have a concentration of $N_c(w_p)\,\mathrm{d}w_p$. The probability per unit time for size w individuals of being eating is thus $v(w_p)N_c(w_p)s(w,w_p)\,\mathrm{d}w_p$. The total mortality rate for individuals of size w is found by integration over all possible predators w_p and by adding a background mortality μ_0:

$$\begin{aligned} \mu(w) &= \int_0^\infty v(w_p)N_c(w_p)s(w,w_p)\,\mathrm{d}w_p + \mu_0 = \mu_p w^{1+q-\lambda} + \mu_0 \\ &= \mu_p w^{k-1} + \mu_0 \end{aligned} \tag{5.3}$$

where $\mu_p = \sqrt{2\pi}\kappa\sigma\beta^{1+q-\lambda}\zeta\gamma \exp\left[\frac{1}{2}\sigma_i^2(1+q-\lambda)^2\right]$ is a predation mortality rate constant [g^{1-k}/year]. The integral is derived in appendix A.3, and the relation $\lambda = 2+q-k$ from (3.48) has been employed in the last line. As in the discussion in section 3.4 we again note the allometric exponent of $k-1 = -1/4$ for size dependent predation mortality.

Now we can use (5.2) and (5.3) to solve (5.1). This derivation is carried out in appendix A.4, and the solution for a species of size w_∞ is:

$$n(w;w_\infty) = \frac{K(w_\infty)}{\alpha h} w^{-k-\frac{\mu_p}{\alpha h}} \left(1 - \left(\frac{w}{w_\infty}\right)^{r-k}\right)^{\frac{\mu_p + \mu_0 w_\infty^{r-k}}{\alpha h(r-k)} - 1} \tag{5.4}$$

where we note that the solution consists of a scaling part w^{-k-a} where $a = \frac{\mu_p}{\alpha h}$ is a constant that characterises the predation strength. The last part in the parenthesis makes sure that the spectrum is cut off as w approaches w_∞. As discussed in appendix A.4 the solution (5.4) is only approximate for small deviations around $r = 1$ when background mortality is present ($\mu_0 \neq 0$). An exact explicit formulation of the solution for a general r would be a function of the β-function. For $r = 1$ the solution is exact, and for $\mu_0 = 0$ the solution is exact for all values of r. One should of course keep in mind that values of $r \leq k$ are prohibited since w_∞ is not defined in this case.

Typical values of $a \in [0; 1.3]$ (Andersen & Beyer (2006)) are difficult to determine, but a typical value of $a \approx 0.6$ may be a good guess (Andersen (2006)). This means that the typical slope of a species spectrum is $-k-a \approx -3/4 - 0.6 = -1.35$. Again this means that the biomass in evenly distributed size classes $B \propto n(w)w^2$ is an increasing function. So, the size-classes gain more weight from predation than what is lost from predation on them.

Figure 5.1(a) shows the single species spectra (5.4) for different values of the background mortality μ_0, which is naturally seen only to affect the cut-off of the spectrum. Contrarily the predations strength a naturally affects both the slope of the scaling part and the shape of the cut-off.

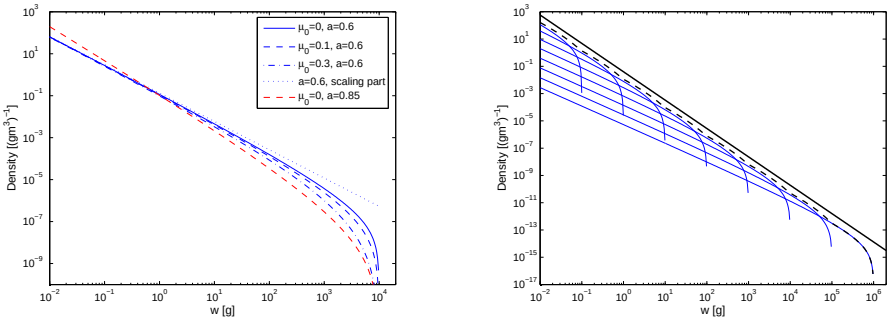

(a) (b)

Figure 5.1: *(a)* Single species spectra (5.4) for different background mortalities, and predation strengths ($w_\infty = 10\,\mathrm{kg}$). μ_0 affects the shape of the cut-off, and a naturally affects both the scaling and the cut-off part. *(b)* Single species spectra for eight species ($w_\infty = 10^n\,\mathrm{g}$, $n = -1, 0, \ldots, 6$). Dotted line shows the summation of the species' spectra, and the black line shows the corresponding community spectrum (2.7) moved up for visibility.

The prefactor $K(w_\infty)$ is a constant introduced when the solution was found by integration. $K(w_\infty)$ should be selected so that the summation of all species sum up to the community spectrum $N_c(w)$:

$$N_c(w) = \sum_{w_\infty} n(w; w_\infty) \tag{5.5}$$

In appendix A.4.2 the $K(w_\infty)$ scaling is determined from this to be:

$$K(w_\infty) \propto \kappa_c \alpha h w_\infty^{2k-q-2+\frac{\mu_p}{\alpha h}} \tag{5.6}$$

With the default parameters from section 3.6 the exponent becomes $2k - q - 2 + a = -0.73$. Figure 5.1(b) shows that this scaling indeed scales the spectra of the species so that they sum up to constitute the community spectrum.

Equation (5.6) also allows us to look at the scaling of the total biomasses of different species:

$$B_{w_\infty} = \int_0^{w_\infty} n(w; w_\infty) w \,\mathrm{d}w \propto w_\infty^{2k-q-2+\frac{\mu_p}{\alpha h}} w_\infty^{-k-\frac{\mu_p}{\alpha h}} w_\infty^2 = w_\infty^{k-q} \tag{5.7}$$

where we note that $k - q = 3/4 - 0.82 = -0.07$. This means that the biomass across species is close to constant. I.e. the total biomass of tuna like fish should equal the total biomass of anchovy like fish.

5.2 Dynamic Behaviour of the Single-Species Model

In this section we will start investigating the single-species version of the size-structured model summarised in section 3.6. This examination is by no means exhaustive, and for further in-depth treatments the reader is especially referred to the many articles by the de Roos and Persson groups on one-species size-structured models (i.e. de Roos et al. (1990), de Roos et al. (1992), Claessen et al. (2000),

de Roos & Persson (2001), de Roos et al. (2003a), de Roos & Persson (2003b), and Persson et al. (2004)). These studies are also often tightly connected to empirical studies by the Persson group in Swedish lakes.

The treatment of the single-species dynamics in this section will primarily focus on the role that the background resources play for the species spectrum dynamics. This means that the most interesting parameters are the magnitude of the background spectrum κ, and the prefactor for the regeneration rate r_0 (cf. table 3.4). Later in the section we will however also examine the roles of w_∞ and cannibalism.

First we will focus on the different kinds of dynamics present in the model. Then examples of the different dynamics are given in section 5.2.1 followed by a discussion that concludes that the dynamic states are consistent with the analytical solutions from the previous section (section 5.2.2). After this it is examined how w_∞, cannibalism, and different growth functions for the background resources affect the distribution of the different dynamic states (section 5.2.3). This is followed by more thorough examinations of cannibalism and w_∞ in sections 5.2.4–5.2.5. Section 5.2.5 more specifically examines the role of w_∞ for species persistence with a given w_{cut} cut-off of the background spectrum, and provides important discussions for the multi-species studies in the next chapter. The treatment of the single-species dynamics is rounded off by a discussion in section 5.2.6 that concludes that the dynamics exposed by the model in this thesis may very well be consistent with the kinds of dynamics that is observed in nature.

Figure 5.2 shows an approximate map of the dynamics of the one-species model using the default parameters from section 3.6. The background spectrum is present at all size ranges to give the species access to feeding resources throughout its life. One can in this case think of the background spectrum as everything in the ecosystem except the species itself with the unrealistic assumption that nobody predates on the considered species (except through cannibalism).

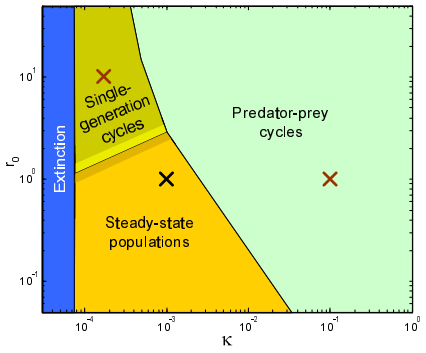

Figure 5.2: Approximate map of the dynamics in the single-species ($w_\infty = 10\,\mathrm{kg}$) model with semi-chemostatic growth rate on the background spectrum. The transition to predator-prey states is quite abrupt, and the transition from steady-state to single-generation states is more gradual. The $\times$'s mark parameters used to illustrate the different kinds of dynamics in the following sections. The black $\times$ marks the default parameters from table 3.4.

The map of the dynamics in figure 5.2 consists of four different regions. One where species go extinct because resources are too scarce to support the species. This minimum level can be predicted theoretically (next section). In the last three regions the species can persist, and the regions are constituted by a region of steady-state solutions, one with predator-prey cyclic states, and one with single-generation states. In the following sections examples of the different types of dynamics are treated more carefully. The transition from steady-states to predator-prey cycles is quite abrupt, whereas the transition from steady-state to single-generation states is more gradual (cf. section 5.2.3 and 5.2.4).

An important parameter for the dynamics is the efficiency e of turning spawning mass into recruits of size w_0. If this value is very low it naturally has the effect of being a strong damper. A large e is obtained if one aim for starting the spectrum simulation at large size w_0. Thus one removes spectrum dynamics in this process, which is not desirable. The smaller a spectrum that is modelled the closer one gets to unstructured models – this is why size-structured modelling is mostly relevant in systems where individuals grow several orders in magnitude throughout their life; and then of course if size-dependent mechanisms are present. The prefactor γ of the search volume also plays an important role for the dynamics since it sets the scaling of the predator-prey fluxes. Thus if one do not consider which parameter values of i.e. r_0 and γ that are suitable in natural systems it is possible to end up in regions of parameter space where there is very low degree or an extreme high degree of dynamics (wide vs. thin regions of steady-state and single-generation states). In this respect the modelling framework in this thesis has the advantage that its parameters in real systems can be assessed.

5.2.1 Examples of Dynamics in the Single-Species Model

In this section we will describe the different kinds of dynamics present in the model. As seen in figure 5.2 the map of the dynamics is divided into four regions: extinction, steady-state, single-generation states, and predator-prey states. In the following four sections we will treat each region in more details.

Extinction

In the region of extinction in figure 5.2 the food abundance is too scarce to support persistence of the species. In the following we will determine the minimum (critical) magnitude κ_{crit} of the background spectrum that allows a species to persist.

The minimum feeding level $f_{min}(w, N)$ required by an individual to pay full maintenance and contribute with maximum reproduction can be found by solving (3.57) for $f(w, N)$:

$$f_{min}(w, N) = \frac{\delta w^r + \psi_i(w)\frac{\varrho_i}{\alpha_i} w}{\alpha h w^k} \tag{5.8}$$

where we note that $f_{min}(w, N)$ naturally cannot become larger than 1 for $w \in [w_0; w_\infty[$ if we i.e. use the $\varrho = \varrho(w_\infty)$ formulation (3.58). The minimum feeding level $f_{crit}(w, N)$ needed for just being capable of paying maintenance is found by setting $\forall w : \psi_i(w) = 0$. By using (3.61) we may turn this into a critical food abundance needed just to sustain a species:

$$\phi_{crit}(w, N) = \frac{f_{crit}(w, N) I_{max}(w)}{v(w)\,(1 - f_{crit}(w, N))} \tag{5.9}$$

where we note that a slightly higher abundance naturally is required to enable persistence of a species since some reproduction is required for this.

If we ignore the food available from cannibalism we may combine (5.9) with (3.35) and obtain an expression for the minimum value of κ that allows the species

to reach maturation for persistence:

$$\begin{aligned}\kappa_{crit}(w_\infty) &= \frac{\phi_{crit}(w_{mat}, N)}{\sqrt{2\pi}\sigma\beta_i^{2-\lambda}\exp\left[\frac{1}{2}\sigma_i^2(2-\lambda)^2\right]w_{mat}^{2-\lambda}} \\ &= \frac{\delta w_{mat}^{\lambda+r-q-2}}{\alpha\gamma\sqrt{2\pi}\sigma\beta_i^{2-\lambda}\exp\left[\frac{1}{2}\sigma_i^2(2-\lambda)^2\right]\left(1-\frac{\delta w_{mat}^{r-k}}{\alpha h}\right)}\end{aligned} \tag{5.10}$$

Using the default parameters from table 3.5 gives $\kappa_{crit} = 6.6 \cdot 10^{-5}\,\mathrm{g}^{1+\lambda}/\mathrm{m}^3$ for a $w_\infty = 10\,\mathrm{kg}$ species. The minimum value allowing the species to persist in figure 5.2 is seen to be $\kappa \approx 7.5 \cdot 10^{-5}\,\mathrm{g}^{1+\lambda}/\mathrm{m}^3$, which is in agreement with the theoretically predicted value. We do also expect a higher value in the simulations since (5.10) does not take into account that some energy also is required for reproduction. We note that the value of κ naturally increases with w_{mat}.

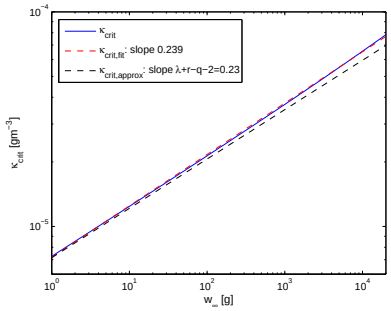

Figure 5.3: $\kappa_{crit}(w_\infty)$ plotted (blue) using relation (3.60). The plot is very close to an allometric function of $\kappa_{crit}(w_\infty) = Aw_\infty^a$ since the denominator only plays a minor role in (5.10). The approximation (5.11) is plotted as the black curve. The red curve is an allometric fit to (3.60) plotted using the prefactor from (5.11).

In figure 5.3 κ_{crit} is plotted (blue curve) against w_∞ using relation (3.60). It is seen that we almost get a straight line in a loglog plot since the denominator only plays a minor role. We may thus approximate (5.10):

$$\kappa_{crit,approx}(w_\infty) = \frac{\delta\eta^{\lambda+r-q-2}}{\alpha\gamma\sqrt{2\pi}\sigma\beta_i^{2-\lambda}\exp\left[\frac{1}{2}\sigma_i^2(2-\lambda)^2\right]}w_\infty^{\lambda+r-q-2} \tag{5.11}$$

where (3.60) has been used to express κ_{crit} in terms of w_∞. Figure 5.3 illustrates (5.11) in the black curve. It is, however, seen that a better approximation is obtained (red curve) if a scaling of 0.239 is employed instead of $\lambda + r - q - 2 = 0.23$.

Steady-State

The plot in figure 5.4 shows the case of a steady-state solution. In the plot we see that individuals pile up just after maturation since food is too scarce to allow them to grow to w_∞. This is seen by noting that $\Psi(w) < 1$ after maturation, which means that the individuals are not even capable of spending the desired amount of energy on reproduction; clearly this leaves no energy for growth as discussed in section 3.3. In section 5.2.3 (cf. figure 5.14(b)) we see that individuals are not allowed to grow to w_∞ in the steady-state region.

Single-Generation States

Figure 5.5 shows a single-generation cycle. We note that the background is in a steady-state (very low amplitudes), but that the spectrum of the species fluctuate. The fluctuations are caused by cannibalism that influences the size-dependent

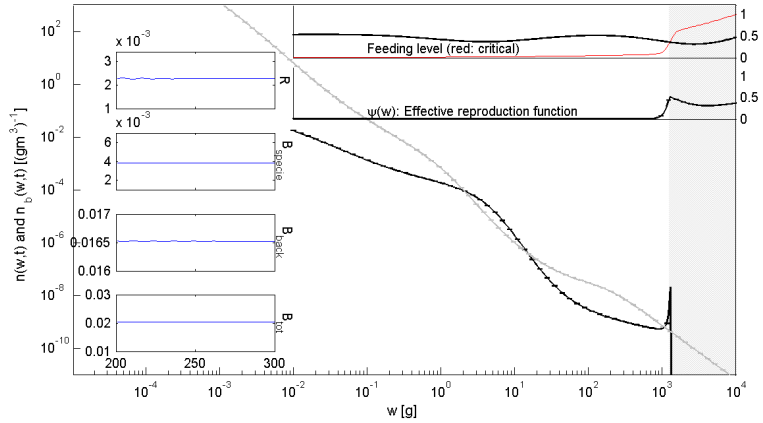

Figure 5.4: Steady-state solution. Boxplot (cf. also figure 5.5) of species and background spectrum (grey) from time $t = 200$ to $t = 300\,\text{years}$. Since we are in steady-state both spectra are constant over time. The gray shaded area marks the region of matured individuals ($\psi(w) \geq 0.5$). Insets on the left show time evolution of reproduction, total species biomass, total background biomass, and total biomass consisting of both the species and the background. Insets in the upper right corner show boxplots of the feeding level, and the effective reproduction selection function. These boxplots are naturally also constant in steady-state. We see that the somatic growth goes to zero just after maturation since not even the required energy for reproduction can be covered ($\Psi(w) < 1$ after maturation). That somatic growth goes to zero means that individuals pile up just after maturation, which is reflected in the peak in the spectrum. Parameters: $r_0 = 1\,\text{g}^\text{b}/\text{year}$, $\kappa = 10^{-3}\,\text{g}^{1+\lambda}/\text{m}^3$, and $w_\infty = 10\,\text{kg}$.

growth, mortality, and reproduction of the species. These states are termed single-generation states because their period length is correlated with species generation time from birth to w_∞.

To understand the single-generation cycle better we have zoomed in on a period from a biomass evolution top in figure 5.6. The figures show abundance spectra at various time steps. When the cycle starts at the biomass peak the intermediate size range of $10 - 300\,\text{g}$ has a low abundance level. As time passes a cohort grows into the intermediate range and we arrive at the valley of the biomass evolution (figure 5.6(a)). The abundance in the intermediate range has now increased and as time passes the individuals in the cohort grow larger and pile up at w_{mat} where the growth goes to zero. As they grow they put a higher and higher predation pressure on individuals in the intermediate size and forces the abundance down to the level at the beginning of the cycle. Now one cycle has been completed, and the process is repeated. The diet from cannibalism is most pronounced when we are in a biomass valley: here the big matured cohort feast on the abundant intermediate individuals and thus depletes them to start a new cycle.

It is noted that the spectrum cycles naturally causes cycles in the reproductive flux since the cycles changes the spectrum composition, and thus also the Spawning Stock Biomass (SSB). Size-dependent interactions at larger size-classes thus affect the entire spectrum via reproduction.

We see the largest effect of the single-generation cycle in the intermediate and large size-range since smaller individuals have smaller energy requirements and more available food from the background, and are thus not capable of starting a cycle.

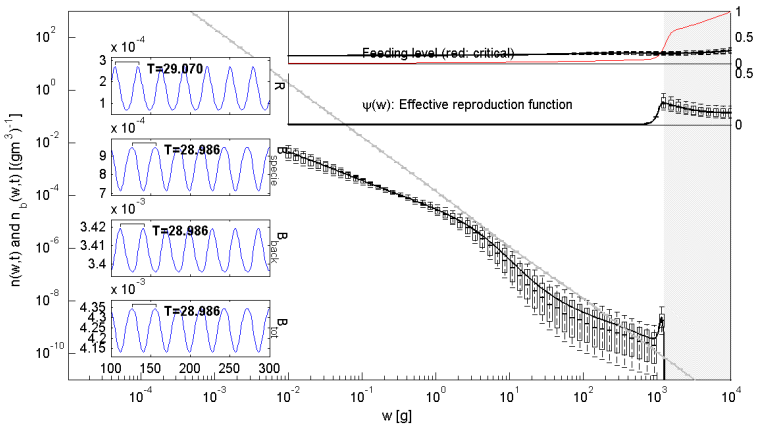

Figure 5.5: Single-generation cycle. Boxplot notation (cf. also figure 5.4): square boxes show the 25% (lower end) and the 75% percentiles (upper end) of the spectrum time series. The thicker vertical line in the boxes are the median (50% percentile). The dashed bars show the minimum (0% percentile) and maximum (100% percentile) of the time series. The thick continuous line shows the mean spectrum. As in the steady-state solution the somatic growth goes to zero upon maturation since food resources are too scarce to allow full reproduction. The amplitude of the species biomass evolution dominates over the background biomass evolution – meaning that the species biomass are in phase with the total biomass. Actually the background fluctuations are almost non-existing (in steady-state) and their low magnitude makes them non-existing in the boxplot of the background spectrum (grey). Parameters: $r_0 = 10\,\mathrm{g^b/year}$, $\kappa = 1.5 \cdot 10^{-4}\,\mathrm{g^{1+\lambda}/m^3}$, and $w_\infty = 10\,\mathrm{kg}$.

From this discussion it should be clear that species with large w_∞ show single-generation behaviour in a larger parameter space as also discussed when treating the map of the one-species dynamics (section 5.2.3).

From the upcoming discussions in section 5.2.3 on the dynamic map in figure 5.2 we will find that removing cannibalism has the effect of removing the single-generation states. However, when adding more species to the system they may effectively cause single-generation like cycles since their predation influences the size-dependent mortality and hence also growth and mortality.

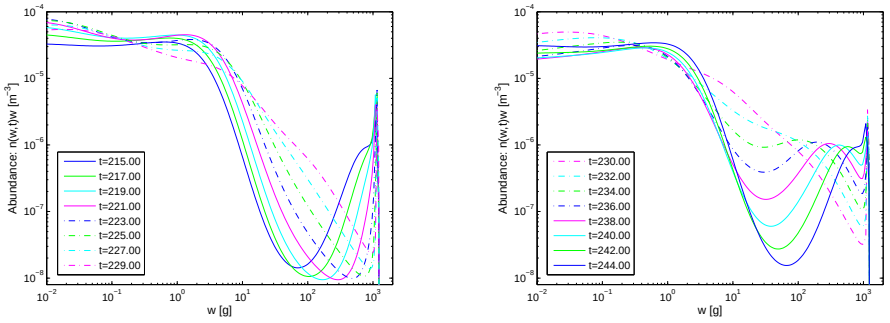

(a) (b)

Figure 5.6: Single-generation cycle originating from intra-species (cannibalism) interaction. The plots show abundances per volume in logarithmic evenly distributed size bins. The state depicted is the state from figure 5.5. *(a)* From top to valley in the biomass evolution (figure 5.5). Individuals starts occupying the intermediate size range. *(b)* Valley to top in biomass evolution (figure 5.5). Individuals from the intermediate size range become dominating predators and forces the abundance level in the intermediate size range down.

Predator-Prey States

Figure 5.7 shows an example of a predator-prey cycle. Predator-prey cycles occur when the functional response, or feeding level in the model at hand, satiate. Predator-prey cycles are characterised by the fact that the predator and prey biomasses are out of phase. Remember the example of the Canadian hare-lynx cycles based on data collected by Hudson's Bay Company that illustrated that when lynxes are abundant they deplete the hares, which then lowers the numbers of lynxes, which again causes hares to become abundant again and closes the cyclic loop (Leigh (1968)).

The predator-prey cycle looks like a mixture of a single-generation cycle and a normal unstructured predator-prey cycle where high resource abundance is followed by high predator abundance, which then depletes the resource, so that the number of predators starts decreasing and enables the start of a new cycle when the prey recovers. In the structured modelling regime the predator-prey cycle is however a bit more complex, and is not easily depicted in a 2D plot. However the above discussion of the single-generation cycle and the following description should enable an understanding of the nature of the predator-prey cycle. In the example of figure 5.7 the predator-prey relation is most pronounced in the $0.1 - 1\,\mathrm{g}$ size range. High levels of resources allow a cohort of recruits to leave w_0 quickly, but soon too many intermediate sized individuals depletes the resources so that new cohorts are hindered by having low growth rates due to scarce food resources. Cannibalism amplifies the problem for a new cohort since the low resource abundance causes the diet of the old cohort to be dominated by cannibalism meaning that individuals of a new potential cohort are prevented from forming a new cohort due to cannibalistic mortality. A new cohort is allowed to be formed when the old cohort has decreased in numbers due to mortality and grown upon the range where its diets lie in the $0.1 - 1\,\mathrm{g}$ range. When this happens the resources has recovered and the cycle starts over.

Increasing κ increases the level of fluctuations (cf. section 5.2.3) which is why

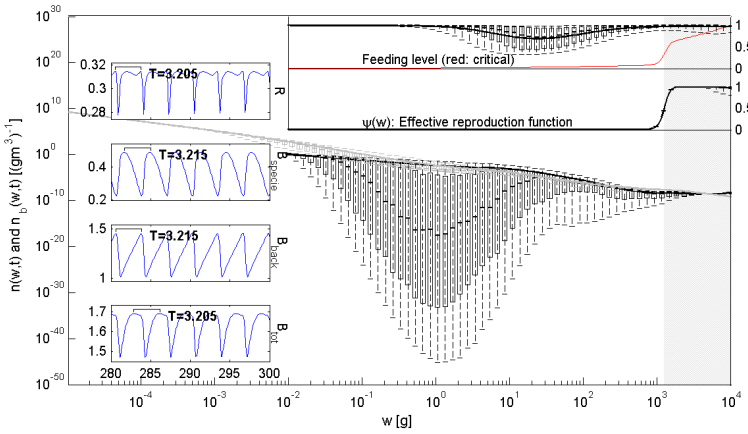

Figure 5.7: Predator-prey cycle. Boxplot notation are found in figure 5.4 and 5.5. In this state both the species and the background spectrum fluctuates, but much faster than in the single-generation example. It is seen that the background biomass fluctuations dominate since they are in phase with the total biomass evolution. The increased food availability from increased κ allows the species to grow beyond the size of maturation and reach the ultimate size of w_∞. Parameters: $r_0 = 1\,\mathrm{g^b/year}$, $\kappa = 0.1\,\mathrm{g}^{1+\lambda}/\mathrm{m}^3$, and $w_\infty = 10\,\mathrm{kg}$.

predator-prey cycles are also denoted paradox of enrichment cycles since these cycles may lead to stochastic extinction for increasing κ due to low abundance levels in the valleys of the cyclic solution. We see that the level of depletion of the intermediate size range in the predator-prey cycle in figure 5.7 is extreme. However, unlike in the case of large fluctuations in unstructured models this does not mean that the species is vulnerable to stochastic extinction since individuals in other size ranges are present at normal abundance levels.

In the size-structured modelling regime one should not put too much into the notion of *predator-prey* cycles since these naturally also show fluctuations in the spectrum composition. Predator-prey interactions will even assist in generating the fluctuations since the interactions are size-dependent and will have effects on size-dependent growth, mortality, and reproduction of the interacting species. However, such fluctuations might also have a damping effect on the predator-prey cycles.

5.2.2 Comparison of Dynamic States & Single-Species Spectra

Figure 5.8 shows mean value plots of the abundance and biomass spectrum from the time-series of the three states described above. We see that the abundance is a decreasing function due to mortality with a small pile-up at intermediate and matured size classes due to reduced growth rate. The biomass spectrum of the species on the other hand is an increasing function (consistent with the results from section 5.1 plotted as the red curve). This means that super-individuals in logarithmically evenly distributed size-classes gain more weight from predation than what is lost via mortality. In the current example only the background mortality is present, but still the results are consistent with the theoretically predicted steady-state solutions of a simpler sub-model of the model at hand (cf. section 5.1).

Figure 5.9 relate the steady-state solution to empirical data. We see that even though North Sea cod is an exploited species it is still well-represented by the

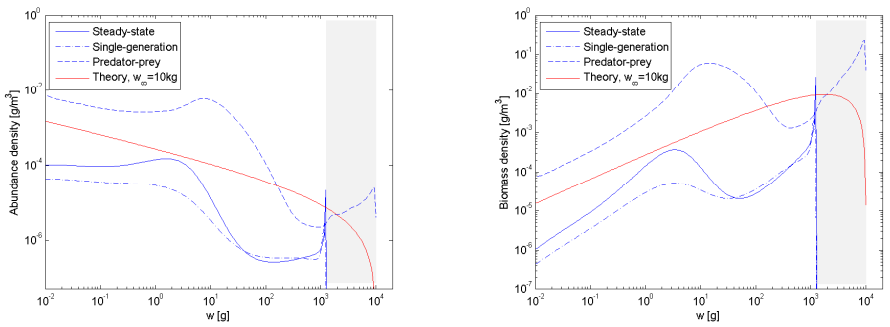

(a) (b)

Figure 5.8: Mean values of 180 years of the three different type of states. Red curve is the single-species spectrum (5.4) with $w_\infty = 10\,\mathrm{kg}$, $\mu_0 = 0$, and $a = 0.6$. *(a)* Abundance density in logarithmically evenly distributed size classes. *(b)* Biomass density in logarithmically evenly distributed size classes. The predator-prey state has the highest biomass followed by the steady-state and single-generation states due to a higher κ value (cf. figure 5.2).

steady-state single-species spectrum. This is no surprise since industrial fishing may be regarded as an increased background mortality for fishes above a given size threshold. According to (5.4) this will change the cut-off of the spectrum, but leave the scaling slope unaffected. The data gives a small, but inconclusive, indication that some pile-up occurs after maturation. By comparing the biomass and SSB curves we see that some extra biomass seems accumulated as maturity is reached. However, this indication is quite weak, and more data below maturation is required for a conclusion. That the accumulation seems weak indicates that in the case of limited food individuals will not spend as much energy as possible on reproduction, and nothing on growth; so an advancement of the growth model that will still allocate some energy for growth in scarce food conditions might be necessary for more realism.

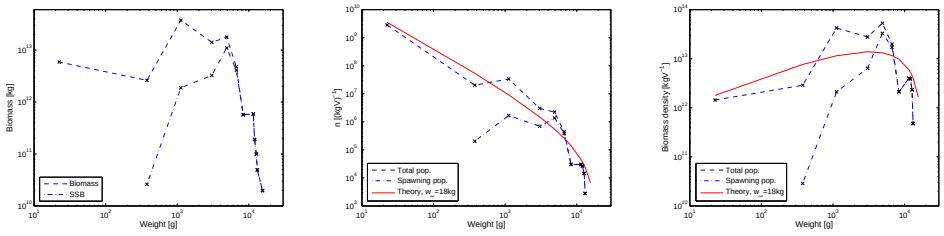

(a) (b) (c)

Figure 5.9: *(a)* Biomass composition of North Sea cod in the fourth quarter of 2004. Each data point marks the year class starting at age 0. Data from ICES (2005). *(b)* Data made size-bin independent by division with Δw, and transformed to a density by division with w. The red curve is a fit to a $w_\infty = 18\,\mathrm{kg}$ single species spectrum. *(c)* Results from (b) multiplied with w^2 to obtain the biomass density in logarithmically evenly distributed size-classes.

5.2.3 The Map of Dynamics: Detailed Discussion

In this section we will describe more carefully how the map of the dynamics in figure 5.2 has been created. It is also discussed how the map will change for different values of w_∞, and how changing the growth function for the background resources will affect the dynamics. After this we will treat enrichment and find that the transition from steady-state to predator-prey states is abrupt due to a bifurcation.

Construction of the Map of the Dynamics

The map of the dynamics in figure 5.2 are created with a 10 kg species and the default parameters given in section 3.6. In the analysis we vary the population growth rate pre-factor r_0 (cf. (3.55)), and the carrying capacity κ (cf. (3.55)) in the semi-chemostatic growth function (3.54). The last 100 years of a simulation was used to make the figures. Spectrum deviation is calculated using the standard deviation $n_\sigma(w)$ and mean value $\overline{n}(w)$ over time t:

$$\text{Spectrum deviation} = \frac{1}{M}\sum_w 100\,\frac{n_\sigma(w)}{\overline{n}(w)} \tag{5.12}$$

where M is the number of points in the discrete species spectrum. Biomass deviation is calculated using:

$$\text{Biomass deviation} = 100\,\frac{B_\sigma}{\overline{B}} \tag{5.13}$$

Figure 5.10 shows the results from these calculations where the dark blue areas represent extinction, blue areas equilibrium, and other colours represent the magnitude of oscillation. The figure shows that the transition to predator-prey cycles is quite abrupt, whereas the transition from steady-state to single-generation states is more gradual. In figure 5.11 we see that increasing the values of κ and especially r_0 has the effect of enabling the species to obtain a higher biomass; this is due to increased abundance and supply rate of resources.

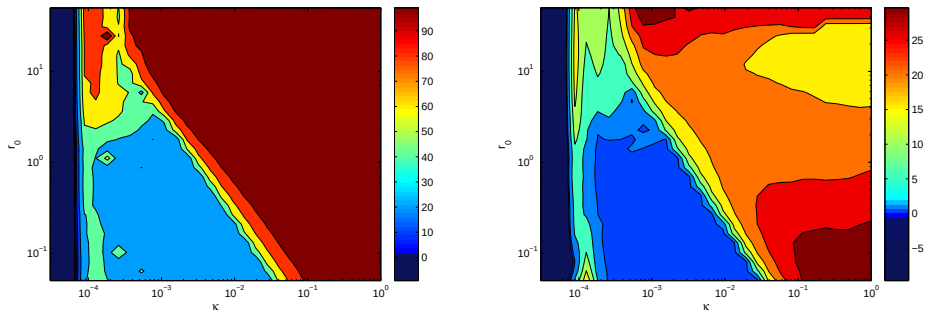

(a) (b)

Figure 5.10: Single-species dynamics with semi-chemostatic growth rate on the background spectrum. *(a)* Spectrum deviation. *(b)* Biomass deviation. In both plots we clearly see that the transition to predator-prey cycles is quite abrupt, whereas the transition from steady-state to single-generation states is more gradual.

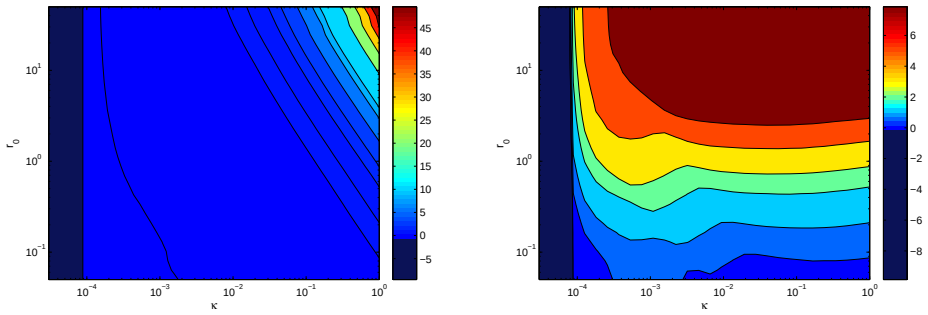

(a) (b)

Figure 5.11: Single-species dynamics with semi-chemostatic growth rate on the background spectrum. *(a)* Mean biomass indicating that the biomass of the species is increasing with r_0 and κ. *(b)* Mean biomass/κ showing that increasing r_0 increases the biomass of the species relatively to the available magnitude κ of resources.

From figure 5.12 we see that smaller species size w_∞ increases the size of the steady-state region. Predator-prey dynamics set in when the feeding level (3.61) satiates for $v(w)\phi_i(w,N) \gg I_{max}(w)$. From (3.35) and (3.62) it is known that the encountered food from the background is $v(w)\phi_{i,b}(w,N) \propto w^{2-\lambda+q} = w^{0.77}$, and from (3.63) that $I_{max}(w) \propto w^k = w^{3/4}$. This clearly means that $v(w)\phi_{i,b}(w,N) \gg I_{max}(w)$ is more easily fulfilled for large w meaning that species with large w_∞ have a narrower steady-state region. The total available food is $\phi_i(w,N) = \phi_{i,b}(w,N) + \phi_{i,c}(w,N)$ where $\phi_{i,c}(w,N)$ is the food available from cannibalism. Small species will clearly have less access to cannibalistic intake meaning that the tendency for predator-prey dynamics is further enhanced for large w_∞ species. For smaller species the minimum required value of κ to allow existence decreases as the size of maturation goes down, which is the size the background has to allow the species to reach for persistence (cf. section 5.2.1).

Removing cannibalism has the effect of removing the region of single-generation dynamics since cannibalism is the driver for pure single-generation dynamics (cf. section 5.2.4). Removing cannibalism also widens the width of the steady-state region due to decreased food availability $\phi_i(w,N)$ so that $v(w)\phi_i(w,N) \gg I_{max}(w)$ requires a larger value of κ to be fulfilled.

Changing the growth function for the background to logistic growth does not have any influence on the qualitative behaviour for values of $r_0 = 1\,\mathrm{g^b}$/year and up (cf. figure 5.13). For smaller values the problems of slow recovery (cf. section 3.5.2) starts to play a role, and makes the growth function useless. The parabolic growth function has the same qualitative behaviour as logistic growth, but with less problems in the regime of low r_0 values.

Figures 5.11 and 5.13 also show that semi-chemostatic growth has a stabilising effect (larger region of steady-state) on the species dynamics compared to logistic and parabolic growth. This is due to the fast effective population regeneration rate (cf. section 3.5.2), and is consistent with the results in de Roos et al. (1990).

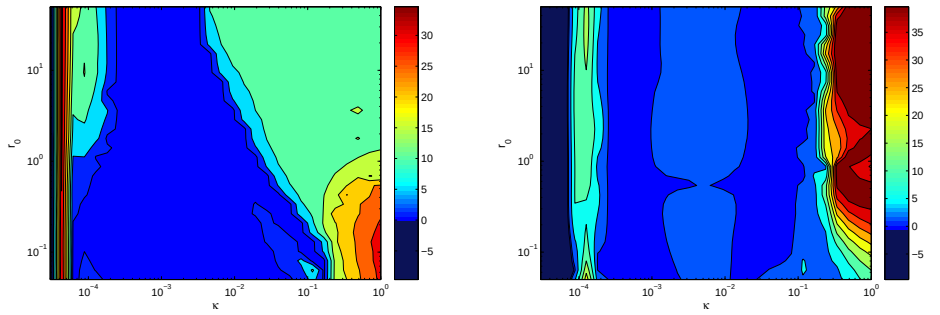

(a) (b)

Figure 5.12: Biomass deviation using semi-chemostatic growth rate on the background spectrum. *(a)* A smaller species of $w_\infty = 1\,\mathrm{kg}$ increases the region of steady-state since predator-prey dynamics set in more easily for larger species. The minimum required value of κ to sustain the species also declines since it naturally has a smaller size at maturation (cf. (5.10)). *(b)* A $w_\infty = 10\,\mathrm{kg}$ species is again studied, but its capability to cannibalise has been removed. This increases the region of steady-states since the total amount of encountered food decreases which again requires a higher κ to satiate the feeding level. In the centre of the steady-state (blue) region small oscillations of both the background and the species occur. The lighter area on the left is due to very long transients that, however, ultimately do end up in a steady-state.

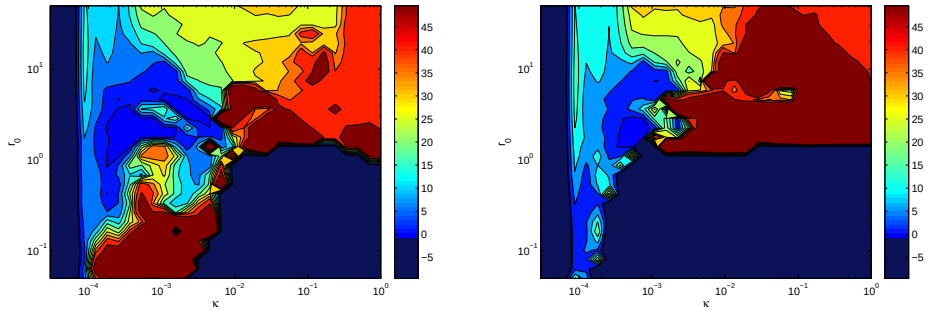

(a) (b)

Figure 5.13: Biomass deviation. *(a)* Logistic growth. From at least $r_0 = 1\,\mathrm{g^b/year}$ and up the model expose the same behaviour as the semi-chemostatic model. The different behaviour at low r_0 is due to the very slow regeneration rate upon depletion (cf. section 3.5.2). In the lower-right region this even leads to extinction because of the added effect of enrichment which destabilises the system and thus puts more severe regeneration requirements on the background. In natural systems we expect $r_0 \in [0.6;\, 19]\,\mathrm{g^b/year}$. *(b)* Parabolic growth shows the same qualitative result as logistic growth. In the lower region of r_0 parabolic growth is, however, capable of maintaining steady-state.

Paradox of Enrichment in the Size-Structured Model

Figure 5.14(a) shows an example of a vertical line in the dynamic map in figure 5.2. From this we see that the predator-prey dynamic set in in a bifurcation, which is why the transition is so abrupt. The bifurcation is due to satiation of the functional response, the feeding level in the current model, and is known as the paradox of enrichment (Rosenzweig (1971)). In the size-structured model we furthermore note from figure 5.14(b) that the species does not have enough food intake to obtain the ultimate size of w_∞ before the predator-prey region.

From the discussion on the predator-prey states in section 5.2.1 we furthermore note that the paradox of enrichment is not as critical in size-structured as in unstructured models. In unstructured models a species may go extinct due to stochastic extinction in the valley of a cycle when the amplitudes of the predator-prey cycles become very large. This is not necessarily the case in size-structured models since the cycles here mostly are the result of interspecies fluctuations, so that even though some size-classes is depleted the species is still invulnerable to stochastic extinction since other size-classes are abundant.

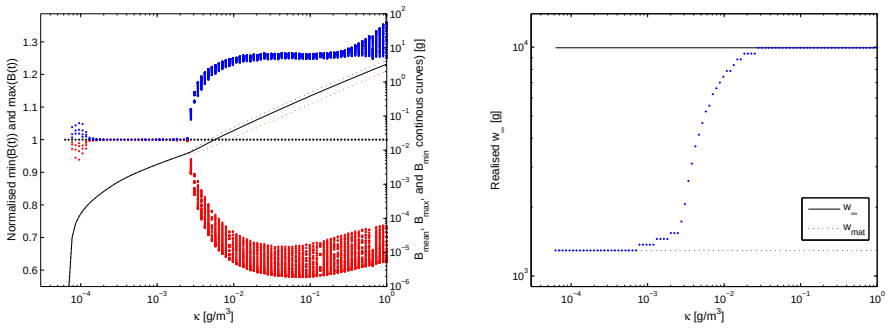

(a) (b)

Figure 5.14: Effects of enrichment using default parameters and $w_\infty = 10\,\mathrm{kg}$. *(a)* Biomass deviations as a function of κ. Mean biomass (black), local maxima (blue), and local minima (red). In the non-normalised plot only the global extremes are plotted. We see that predator-prey dynamics set in in a bifurcation. In the normalised plots we also see deviations for small κ, but these are noise from the low biomass level. *(b)* The maximum size an individual obtain for varying κ. We see that food abundance is too scarce to allow the species to reach w_∞ in the steady-state region.

5.2.4 Cannibalism

In this section we will treat the role of cannibalism further. Claessen et al. (2004) provides an extensive review of cannibalism in population models. Claessen et al. (2004) characterise cannibalism by i) victim mortality, ii) energy gain from victims, iii) size-dependent interactions, and iv) intraspecific competition. Claessen et al. (2004) attribute five effects to cannibalism: i) regulation of population size, ii) destabilisation of steady-states to cycles or chaos, iii) stabilisation by damping cycles caused by other interactions, iv) bistability; depending on initial condition the population may converge to one of two stable states, and v) modification of population size structure. Claessen et al. (2004) conclude the Physiologically Structured

Population (PSP) modelling framework to include all characteristics and effects, and hence the same is valid for the framework of this thesis.

Effects i), v), and iv) will be identified in the next section in figures 5.17(a), 5.16, and 5.19. Effect iii) cannot be identified from the dynamic map in figure 5.2 (cf. also section 5.2.3) and is not demonstrated here. Interactions from other species may however i.e. cause oscillations, which can be removed by cannibalism. Effect ii) will be demonstrated in the following.

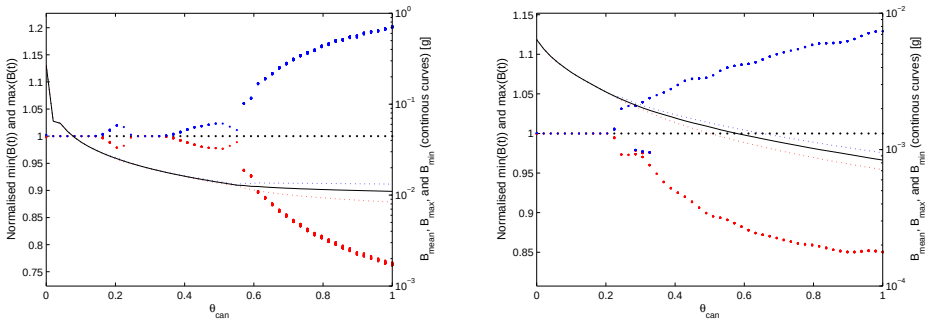

Figure 5.15: Diagrams of relative magnitude oscillations. Biomass deviations as a function of cannibalism θ_{can}. Mean biomass (black), local maxima (blue), and local minima (red). In the non-normalised plot only the global extremes are plotted. *(a)* Analysis of a steady-state (no cannibalism) that becomes a predator-prey state. Parameters: $r_0 = 10\,\mathrm{g^b/year}$, $\kappa = 10^{-3}\,\mathrm{g/m^3}$, and $w_\infty = 10\,\mathrm{kg}$. *(b)* Analysis of a steady-state (no cannibalism) that becomes the single-generation state from figure 5.5. Parameters: $r_0 = 10\,\mathrm{g^b/year}$, $\kappa = 1.5\cdot 10^{-4}\,\mathrm{g/m^3}$, and $w_\infty = 10\,\mathrm{kg}$.

Figure 5.15 shows two examples of cannibalistic destabilisation of steady-states. From the dynamic map in figure 5.2 it is seen that full cannibalism in the final state of figure 5.15(a) is a predator-prey-state, and that the resulting state in (b) is a single-generation state, which in agreement with previous discussions clearly is seen introduced by cannibalism. From the discussions on the dynamics map in figure 5.2 we know that the transition from steady-state to predator-prey states is abrupt due to a bifurcation. In (a) we clearly see this abruptness in the biomass evolution when cannibalism is introduced, whereas the transition in (b) is smooth (black curves).

The transition from zero to full cannibalism takes places through a series of bifurcations as seen in figure 5.15(a). First small-scale ($< 5\%$) oscillations set in followed by large-scale oscillations (up to 25%). At intermediate degrees of cannibalism we might have steady-states meaning that intermediate levels of cannibalism might not necessarily enhance the paradox of enrichment. In (b) there is only one pronounced bifurcation, which gradually leads to large-scale oscillations of up to 15%. The three local maxima (blue) around a 0.3 degree of cannibalism is due to introduction of small biomass evolution peaks in the valleys of the dominating peaks, and the bifurcation responsible for these does not seem to have a strong effect on the dynamics.

5.2.5 The Role of Background Length and w_∞

In the previous no cut-off w_{cut} was employed on the background spectrum meaning that the background spectrum was extended throughout the species spectrum to supply food throughout the species spectrum. However, in this section we use the default cut-off of $w_{cut} = 0.05\,\mathrm{g}$ (section 3.5.1). Since individuals are feeding with a preferred prey-predator ratio of $\beta = 0.01$ this means that the available resources will start decreasing as the predator grows beyond 5 g. However, food will still be available via the log-normal food selection function (3.65) due to the selection width σ. In this section we will examine how large w_∞ that can exist for the given cut-off w_{cut}.

In the examination we will also find that cannibalism give rise to bistability in the model. Depending on the initial species spectrum two different states might be reached. Either a state (mostly steady-state) with a low biomass level, or a high biomass state that is cyclic. The high biomass state is propelled by cannibalism, and is reached by having a high biomass initial spectrum since a given spectrum structure is needed to enter the high biomass cannibalistic driven state.

Determining $w_{\infty,max}$

Figure 5.16 shows the resulting species spectrum from different simulations with differing w_∞. All spectra come from steady-states. We see that the species have decreasing densities at w_0 for increasing w_∞ as we expect from the discussion on steady-state solutions in section 5.1. However, we expect slopes of $-k-a \approx -3/4-0.6 = -1.35$ of the single species spectra. If regression lines are made only the three smallest cannibalistic species have comparable slopes of $[-1.35; -1.23]$. The $w_\infty = 280\,\mathrm{g}$ species has an incomparable slope of -0.66 due to severe food limitation as w_{mat} is approached. The non-cannibalistic species have slopes of $[-0.55; -0.15]$. Thus also only the three smaller cannibals come close to obeying the (5.6) scaling of $K(w_\infty) \propto w_\infty^{-0.73}$ with their scaling exponent of -0.57. The cannibals' spectra come closer to the theoretically expected since they come closer of having feeding items of suitable size range throughout their life. Thus, when more species are added to the spectrum even non-cannibals are expected to have spectra comparable to the predicted steady-state spectra.

It may at first seem counterintuitive that the cannibalistic species have the highest densities at the smaller size ranges, since the densities could be lowered by cannibalistic predation. However, cannibalism has the effect that the increased food abundance from cannibalism makes it possible to produce more recruits. Fur-

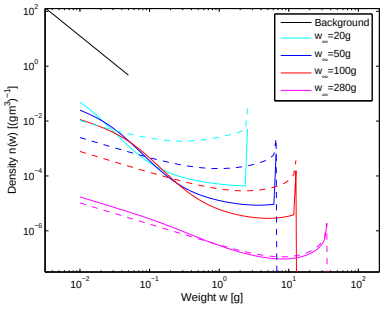

Figure 5.16: Steady-state spectra for different w_∞. Each spectrum is from an independent simulation. Solid curves represent cannibalistic spectra, and dashed curves are from non-cannibals. Background spectrum (black) have $w_{cut} = 0.05\,\mathrm{g}$ and is plotted at the carrying capacity. The different spectra have different exploitation levels on the background.

thermore, more resources will be available from large-sized resource items since competition for these resources are lowered since larger species retrieve parts of their food from cannibalism.

We may predict how large species that are capable of persisting in a system with a given cut-off w_{cut}. A species has to have a feeding level upon maturation that exceeds a critical feeding level of (5.8) with $\forall w : \psi_i(w) = 0$:

$$f_{crit}(w_{mat}; w_\infty) = \frac{\delta w_{mat}^r}{\alpha h w_{mat}^k} \tag{5.14}$$

The realised feeding level due to background resources is calculated via (3.61):

$$f_{rea}(w_{mat}, n_b; w_\infty) = \frac{v(w_{mat})\phi_i(w_{mat}, n_b)}{v(w_{mat})\phi_i(w_{mat}, n_b) + I_{max}(w_{mat})} \tag{5.15}$$

Thus from $f_{rea}(w_{mat}, n_b; w_\infty) \geq f_{crit}(w_{mat}; w_\infty)$ we may retrieve the maximum w_{mat} or w_∞ via (3.60) that is capable of persisting when resources from the background is dominating. An analytic solution for w_∞ by setting $f_{rea}(w_{mat}, n_b; w_\infty) = f_{crit}(w_{mat}; w_\infty)$ is not possible since the available food from a truncated background spectrum $\phi_i(w_{mat}, n_b)$ is a function of the error function $\text{erf}(\cdot)$. In figure 5.17(a) (left axis) $f_{crit}(w_{mat}; w_\infty)$ (red) and $f_{rea}(w_{mat}, n_b; w_\infty)$ (blue) are plotted.

Figure 5.17(a) (right axis) shows the biomass level for varying w_∞ using a stepping function at w_{mat} for the reproductive selection function $\psi(w)$ (black curves). We see that the maximum w_∞ species that can exist with the given w_{cut} is explained by $f_{rea}(w_{mat}, n_b; w_\infty) = f_{crit}(w_{mat}; w_\infty)$. The green curves show the biomass for varying w_∞ using the gradual Fermi-Dirac distribution (3.59). We see that larger species can exist with the smooth $\psi(w)$ since some individuals here mature before w_{mat}.

From figure 5.17(a) we see that the same pattern is seen from a cannibalistic species. We might expect that cannibalistic species could persist with larger w_∞. From figure 5.8(b) and section 5.1 we know that the biomass density in logarithmically evenly distributed size-classes is an increasing function for the single species spectrum. Prey are selected with the log-normal selection function (3.65) meaning that larger size-classes have to cannibalise on size-classes with lower biomass densities than themselves, which clearly does not allow the cannibals to exist in a steady-state at larger w_∞ since the maintenance requirements scale with body weight and thus also biomass.

Figure 5.17(a) has been produced with the default value for the magnitude κ of the background spectrum (section 3.6). If κ is increased more food will be available, and we will expect that species with larger w_∞ can exist since an increased amount of food clearly will give an increased $f_{rea}(w_{mat}, n_b; w_\infty)$ (5.15). The reverse is naturally expected for lower κ values. In figure 5.17(b) the maximum w_∞ species that can exist for a given κ has been retrieved numerically from $f_{rea}(w_{mat}, n_b; w_\infty) = f_{crit}(w_{mat}; w_\infty)$ (black curve) and we see that $w_{\infty,max}(\kappa)$ indeed is an increasing function. To find the maximum w_∞ with the smooth $\psi(w)$ (3.59) simulations were carried out for 25 different w_∞ close to the biomass collapse. From these simulations the maximum w_∞ was found, and the result from this investigation for nine values of κ is illustrated with the red curve in figure 5.17(b).

The red curve is shifted to higher κ values compared to the theoretically devised (black). This shift is due to the fact that we strictly should require $f_{rea}(w_{mat}, n_b; w_\infty)$

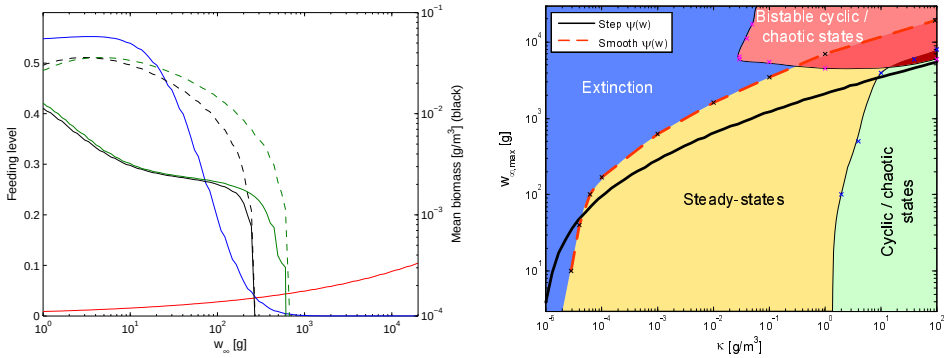

(a) (b)

Figure 5.17: *(a)* Blue and red curves (left axis) show realised and critical feeding level at w_{mat} for varying w_∞. Black curves (right axis) show biomass levels in the steady-state for cannibals (solid) and non-cannibals (dashed) using a step function at w_{mat} as the reproductive selection function $\psi(w)$. The green curves show the corresponding biomass levels when the smooth reproductive selection function $\psi(w)$ (3.59) is used. Larger w_∞ is possible with the smooth $\psi(w)$ since some individuals matures below w_{mat}. Maximum $w_\infty \approx 630\,\mathrm{g}$. *(b)* The maximum w_∞ cannibalistic species that can exist for a given magnitude κ of the background spectrum. The black curve is for a stepping function, and the red using the smooth (3.59) reproductive selection function. The resulting states are mainly steady-states that of course becomes cyclic with enrichment when the feeding level satiates. The red region marks a region where alternative states are possible. These dwarf-giant cyclic states are driven by cannibalism and may be emerged if the simulations are started with a high total biomass of the species spectrum. The boundaries between the different regions are only approximate since no full analysis for all parameter combinations were carried out. The points marked with $\times$ were used to draw the boundaries.

$> f_{crit}(w_{mat}; w_\infty)$ to allow room for reproduction – a higher κ is required for a given w_∞. However as κ increases the red curve exceeds the black due to the before mentioned width of the gradual reproduction selection function $\psi(w)$ (3.59).

Species having w_∞ above the red curve in figure 5.17(b) will naturally go extinct, and species with a w_∞ on or below the curve will be in a steady-state in a large range of κ. However for increasing κ cyclic states emerge due to satiation of the feeding level (paradox of enrichment, section 5.2.3). The parameters γ and h are important parameters for the location of the steady-state to cyclic boundary since predator-prey states set in when the feeding level (3.61) satiates.

Bistability from Cannibalism

Above we argued that cannibalism will not allow species to exist in steady-states with larger w_∞ than the non-cannibals for a given κ. However, a cyclic state where reproduction is cyclic due to cohorts growing beyond w_{mat}, may produce such states since the matured cohort may be kept alive on cannibalistic intake. Such states are denoted dwarf-giant cycles (Claessen et al. (2000)) since cohorts might be able to grow just to w_{mat} if the food from cannibalism is limited, or closer to w_∞ if sufficient food is available.

In figure 5.17(b) a red region of bistable cyclic states is found. These states are cannibalistic dwarf-giant cycles which may be reached if the simulation is started with a high initial biomass of the species. We see that the red region below the

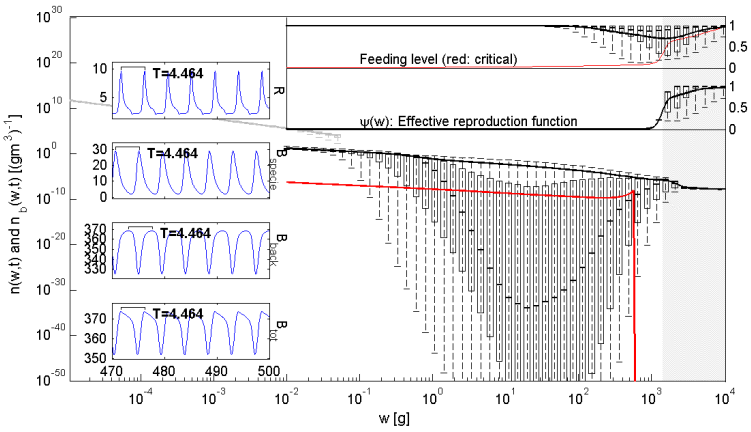

Figure 5.18: Depending on initial conditions one of two different states are reached. The boxplot shows the dwarf-giant cyclic state due to high initial total biomass of $1\,\mathrm{g/m^3}$. The red spectrum in the plot is the steady state from a low initial total biomass of $10^{-4}\,\mathrm{g/m^3}$. Apparently it seems that the steady state persists with no matured population, but the small pile-up do indeed fall into the range where the Fermi-Dirac distributed maturation function has increased from zero $\psi(w) > 0$ (3.59). The gray-shaded area marks the transition where 50% of all individuals at size w have matured: $\psi(w) = 0.5$. Boxplot notations are found in figure 5.4 and 5.5. Parameters: $r_0 = 1\,\mathrm{g^b/year}$, $\kappa = 3 \cdot 10^1\,\mathrm{g^{1+\lambda}/m^3}$, and $w_\infty = 11.390\,\mathrm{kg}$.

red line marks a region of bistable states, where we can either have low biomass solutions or high biomass dwarf-giant cycles. Figure 5.18 shows an example of such two states.

The bistable region above the red line allow presence of species that for low initial biomass spectra will go extinct due to too low food abundance. However, when starting the simulation with a high biomass spectra the alternative cyclic state may be reached. Thus the criterion for entering a dwarf-giant cycle is that it is introduced at a high concentration or that it may eat its way to a proper density distribution on alternative food items such as other species. That the ladder is possible is shown in section 6.2.2. Figure 5.19 shows that the alternative dwarf-giant states indeed allow species with a larger w_∞ to exist for lower values of κ.

It is noted that the bistable region only is present for large species. This is due to the fact that cannibalism is more helpful for larger species. If an individual is not cannibalised before it has reached a larger size then it has obtained a higher energy content, which the cannibal cannot encounter from any resources due to its size selective prey-predator ratio β. This gives the large individuals the required energy for reaching maturation. The effect of sparing victims till they have become more nutritious is known as the *Hansel and Gretel* effect (Claessen & de Roos (2003)). The effect is not due to any individual choice or strategy, but merely dependent on the species spectrum distribution.

It is difficult – if at all possible – to separate the dwarf-giant and the predator-prey states from section 5.2.1. Apparently, only the dynamic map in figure 5.17(b) can be used to separate the states. Separation might, however, not be important since predator-prey states as discussed earlier have a different nature than the unstructured models' counterparts. In the size-structured modelling regime the inter-species cohort fluctuations give rise to total biomass cycles on top of – or counteracting – the predator-prey contribution.

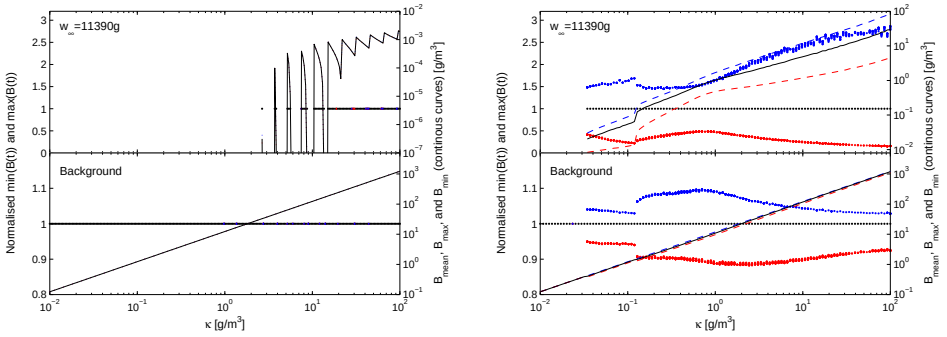

(a) (b)

Figure 5.19: Enrichment study for a $w_\infty = 11.390\,\mathrm{kg}$ species. *(a)* The transition from extinction to steady-state with a low initial biomass spectrum. It seems that the transition takes place through a series of bifurcations indicating that the dynamic map in figure 5.17(b) indeed only is approximate. The upper right region of 5.17(b) is difficult to assess due to dynamic richness. However, we do see the general trend that increased κ allows the species to reach a higher biomass. *(b)* The transition from extinction to dwarf-giant cycles with a high initial biomass spectrum. At $\kappa \approx 3 \cdot 10^{-2}\,\mathrm{g}^{1+\lambda}/\mathrm{m}^3$ the intake from the background of the smaller individuals is high enough to allow the species to persist via cannibalism in the larger size range. At $\kappa \approx 10^{-1}\,\mathrm{g}^{1+\lambda}/\mathrm{m}^3$ another bifurcation takes place. The nature of this bifurcation has not been examined.

Summary

To sum up this section we have seen that the maximum species size w_∞ that can sustain in a system where the background spectrum has been cut off is a function of β, but that species beyond $w_\infty = w_{cut}/\beta$ may persist due to the width σ of the size selection function. The ultimate size that can persist in the system have a realised feeding level at maturation size that comes close to the critical feeding level. The maximum w_∞ species that can exist with the default parameters (section 3.6) for varying κ can be found in figure 5.17(b).

Alternative states are also possible. If the initial spectrum distribution has a high enough magnitude then alternative dwarf-giant states might be reached. These states are driven by cannibalistic intake, and allow species with higher w_∞ to exist than if a low magnitude intial spectrum is used.

5.2.6 Model Dynamics vs. Dynamics in Nature

In the previous sections we have surveyed the different kinds of dynamics that the size-structured model expose. It was found that cyclic states show fluctuations in the spectrum composition in the form of cohorts. Figure 5.20 shows that cycles of advancing cohorts do indeed occur in nature. The figure shows relative differences from year to year in the Norwegian cod composition, which displays cohort cycle behaviour. Whether the cohorts are from single-generation, predator-prey, dwarf-giant cycles or a mixture from more complicated interactions is difficult to tell. However, the long period time indicates that it might be closely related to the single-generation cycles.

Empirical evidence from Kendall et al. (1998) show that population cycles are indeed common. Among fish almost half of the recorded populations are cycling.

Kendall et al. (1999) provides methods for studies and validates mechanisms for cycling. Murdoch et al. (2002) examines how often different cycles occur. They find that predator-prey cycles almost only occur in specialist predators and that single-generation and delayed-feedback cycles (I do not differ between these cycles in this thesis) are normal for generalists, which covers most fish species. That specialists should expose more predator-prey dynamics is also what we would expect since specialist interactions have stronger interactions that cannot be damped through other links (McCann et al. (1998)).

From the discussions in this chapter it is evident that the size-structured model indeed is capable of producing dynamics that are consistent with the dynamics observed in nature.

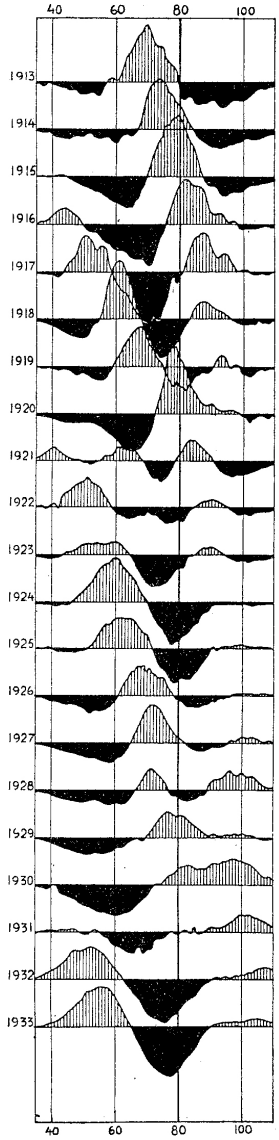

Figure 5.20: Relative differences in the average distribution in the Norwegian cod spectrum composition (in cm) from 1913 to 1933. It is seen that cohorts are advancing in time and is being replaced by new dominating cohorts. The graph is taken from Sund (1934). It might be interesting to do a similar study today to see how industrial fishing has affected these cohort cycles.

6

Multi-Species Coexistence Using the Trophic Ladder

The size-structured model from chapter 3 does not include any explicit description of a food web structure. Everybody can eat everybody if they fall into a suitable size range. In this chapter it is shown that we may have species coexistence in this completely mixed environment setting. In chapter 7 we initiate examinations of how an actual food web configuration enhances the possibilities for coexistence.

Larger species need the possibility of feeding on smaller species to reach the size of maturation, which is clearly required for a species to maintain itself. This mechanism is treated in this chapter and is denoted the *trophic ladder*. Section 6.1 is an introduction to the concept of the trophic ladder, which is examined in detail in section 6.2 where it is also found that species may be present in between the steps of the trophic ladder. Examples of coexistence of up to six species are given. Perspectives for even more coexisting species without introducing an explicit food web structure in the size-structured model are discussed in the last section 6.4.

6.1 Coexistence by Just Adding More Species?

The simplest thing that can be done to start studying coexistence in the model from chapter 3 is to add more species. The only trait that characterises a species is the ultimate size w_∞. The first experiment will be to add 100 species with logarithmically evenly distributed w_∞ in the range 1 g–19 kg and see what happens when a simulation is started.

Figure 6.1(a) shows the result of this experiment. The figure shows the time evolution of the biomass of the 100 species. First a ~ 1000 years transient is seen where two clusters of species of high biomass evolve towards smaller sizes. When the smaller cluster reaches 1 g it is being excluded by the larger size cluster that predates heavily on the smaller cluster since the larger cluster consists of species of a size that cannot exist purely on the background spectrum. Species in the larger size cluster around 10^3 g cannot sustain without the smaller species since the prey-predator ratio β and the width σ of the size selection function (3.65) does not allow them to feed on the background (cf. figure 5.17). When the smaller cluster is being excluded a niche for a new smaller cluster has appeared in the 10^1 g–10^2 g range.

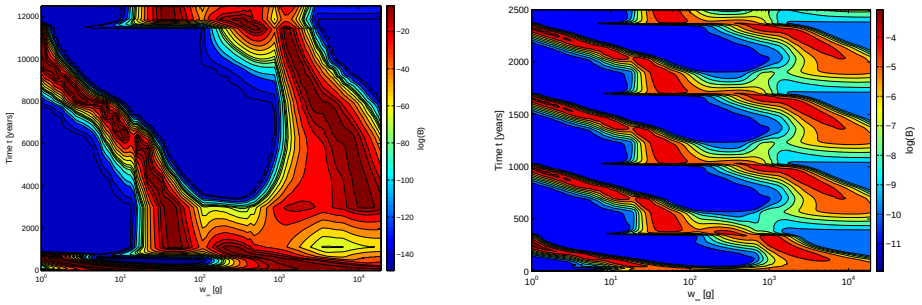

(a) (b)

Figure 6.1: Time evolvement of biomass (per volume) distributions for 100 species logarithmically evenly distributed in the range $[1\,\mathrm{g};\ 19\mathrm{kg}]$. *(a)* Using default parameters (section 3.6). Two distinct size clusters are seen to evolve towards smaller species sizes. When the cluster of the smaller species come close to $1\,\mathrm{g}$ it goes to a low biomass and a new smaller size cluster is started in the $10^1\,\mathrm{g}$–$10^2\,\mathrm{g}$ range. The pattern is repeated with a period length of $\sim 11,000\,\mathrm{years}$. *(b)* A flux consisting of the spectrum of $n_i(w,t) = 10^{-14}w^{-2}$ is added to all species. This corresponds to a constant small inflow of the 100 species from a species pool. It is seen that this mechanism speeds up the time evolution of the two size clusters to $\sim 700\,\mathrm{years}$, and shows that the pattern from (a) is cyclic and not a long transient.

This niche is available since the potential larger predators are at a low biomass level. The larger size cluster continues evolution towards a smaller size that can exist solely on background resources. However, it is soon being excluded 1) by the smaller size cluster that has a more appropriate prey-predator ratio of the background resources, and 2) by a new larger size cluster that is being formed with a diet based on the smaller size clusters. The two new size clusters now evolve towards smaller species sizes and the process repeats itself.

This experiment can be seen as a succession experiment where the superior species diminishes the less superior species. However, since all species are constantly present then the diminished species will have the possibility of reemerging if their surrounding environment consisting of the other species allows them to do so. In natural systems it is not likely that the species will survive at the very small biomass levels since they are very vulnerable to stochastic extinction. Instead we may regard the very small biomasses as influxes from a surrounding species pool, and thus regard the experiment as an invasion experiment. To study this more explicitly we repeat the experiment with one modification. A small inflow of the 100 species is allowed by adding the small amplitude spectrum $n_i(w,t) = 10^{-14}w^{-2}$ to all species at each time step. The result of this experiment is depicted in figure 6.1(b), and it is seen that the same pattern is produced at a faster time scale. In the first experiment computational time makes it difficult to determine whether the pattern is periodic. The second experiment shows a period time of $\sim 700\,\mathrm{years}$, and it seems that the period time for the first experiment is $\sim 11,000\,\mathrm{years}$.

What does this experiment say about coexistence? We see that two distinct size clusters can persist on a long time-scale, but that invasion or succession makes this pattern periodic with evolvement towards smaller size-clusters, that are replaced by two new size-clusters when these become superior. Thus it seems that species can coexist 1) if they are very different in the form of a large difference in species size w_∞, or 2) if they are sufficiently similar in species size w_∞. This result is

similar to the recent result by Scheffer & van Nes (2006) who also in an invasion experiment finds that species may co-evolve in clusters on an abstract niche axis. The evolvement in Scheffer & van Nes (2006) is however not periodic, but instead the clusters evolve along constant niche values. The niche axis of the Scheffer & van Nes (2006) experiment corresponds to the w_∞ axis in the current experiment, and the clusters in Scheffer & van Nes (2006) thus do not evolve in the direction of the horizontal niche axis.

Even though the experiment by Scheffer & van Nes (2006) gives results similar to the current experiment the mechanisms behind are quite different. Scheffer & van Nes (2006) examines an unstructured Lotka-Volterra competition model where species with similar niche values compete strongest, and competition decreases for species with quite different niche values. The competition strength is determined by a normal distribution that has a width similar to the length of the niche axis so that competition do exist between the clusters. Competition give rise to increased mortality but no energy gain is coupled to the competition mortality. In the size-structured model in this thesis competition is implemented in a more realistic manner. All species compete for the same background resources in the smaller end of the species' spectra. Also every species is capable of eating of any species' individuals if they are of a suitable size. Thus smaller species have the advantage that they can reach maturation solely on background resources and thus sustain their populations. Larger species cannot do so due to the size selective predation intake, which means that they must feed on other species to reach maturation. One can say that the larger species must use the smaller species as a *trophic ladder* to obtain the role of a large sized predator. The maximum species size that can persist solely on background resources is discussed in section 5.2.5, and for the default parameters (section 3.6) the maximum size is approximately 630 g (cf. figure 5.17(a)). Thus in the size-structured model the total competitive effect between species on the w_∞ axis is more difficult to asses since it is the result of size-dependent processes throughout the lifetimes of the individuals in all species.

In Scheffer & van Nes (2006) the clusters exist in a long transient, and as time passes each cluster is eventually constituted by just a single species. The very long time-scales do, however, indicate that quite weak forces are sufficient for stabilising the clusters, and indeed they show that self-interference competition stabilises the clusters. Self-interference competition is basically a mortality term for a species that increases with increasing population when the population exceeds a given threshold. No other species gain energy from this term, which may thus be regarded as a damper. The interference term can be thought of as a top-down control from natural enemies that prevent the populations from becoming very abundant. It is also argued that other weak forces stabilise the cluster pattern. Scheffer & van Nes (2006) also carry out an evolutionary experiment where species can evolve along the niche axis. Here it is seen that species do indeed evolve into clusters, so that the clusters is a self-organised pattern.

In the experiment at hand the cluster width is stable due to the periodic pattern that the concrete niche value w_∞ give rise to. The pattern is robust. If the influx of species i.e. is removed and a constant influx of w_0 recruits is used the same pattern is seen.

Omnivory – the case where a species feeds upon more trophic levels – is most common in aquatic food webs (i.e. Pimm et al. (1991)). Everybody is capable of eating everybody in the size-structured model if the victims are of a suitable size. This an extreme case of omnivory since i.e. the anchovy like fish may predate on

large cod like predator's offspring. This clearly shows that one should be careful when assigning species to trophic levels in aquatic ecosystems since the trophic level is more closely linked to body size (Jennings et al. (2001)). However, even in this everybody-eats-everybody scenario we see a division of species into clusters that display a structure similar to the concept of trophic levels. Instead of being the direct result of a who-eats-whom differentiation the 'trophic levels' displayed in figure 6.1 is the result of size-dependent processes where the smaller species are required as a trophic ladder for the larger species.

In this chapter the concept of the trophic ladder in regards to species coexistence is studied more thoroughly. In section 6.2.1 it is shown that two species, one from each cluster, can coexist without any invaders present. It is also discussed what combinations of small and larger species that can coexist. With this result established it is shown that the trophic ladder indeed can lead to stable species coexistence in the size-structured model. The stability of the coexistence is then studied in regards to enrichment (section 6.2.2) which is clearly interesting since it is food limitation that determines whether both the smaller and the larger species can exist. Subsequently (section 6.2.3) it is shown that the pattern from figure 6.1 can be scaled to more than two 'trophic levels', but that the presence of many such 'trophic levels' in nature is unlikely. In general two very alike species will only exist in a long transient as in the experiment of Scheffer & van Nes (2006) since the competitively superior eventually will outcompete the less superior. However in section 6.3 it is shown that species with w_∞ in between the species constituting the trophic ladder indeed can coexist in stable states without any modifications of the model. Finally the chapter is rounded off by a discussion on the perspectives for more species coexistence in the model (section 6.4).

6.2 Coexistence Using the Trophic Ladder

In the previous section it was found that clusters of different w_∞ sized clusters coexisted over long time scales in an invasion experiment. In this section we will describe the stable states that can be found in the absence of invasion.

6.2.1 Two Species Coexistence

From the clusters in figure 6.1 two species may be picked out, one from each cluster, and it is seen that they can exist in stable states. Figure 6.2 shows the example of a steady-state. It is easily tested that the larger species uses the smaller species as a trophic ladder since it cannot exist if the smaller species is removed.

For a given size of the smaller species $w_{\infty,1}$ there is an upper level for the size of the larger species $w_{\infty,2}$. The upper level is determined by the possibility of reaching the size of maturation on the smaller species. We may regard the smaller species' spectrum as a continuation of the background spectrum and then we can find the maximum $w_{\infty,2}$ by using the methods from section 5.2.5 where the maximum w_∞ that can exist for a truncated background spectrum is found. Figure 6.3(a) shows an example of two species' capability of coexisting when the size of the larger species is varied while the smaller is fixed at $w_{\infty,1} = 10\,\mathrm{g}$. In the figure it is seen that the larger species is close to its maximum size at $w_{\infty,2} = 19\,\mathrm{kg}$ since the biomass starts dropping off dramatically. We see coexistence from $w_{\infty,2} = 400\,\mathrm{g}$ even though species up to 630 g are capable of living solely on background resources.

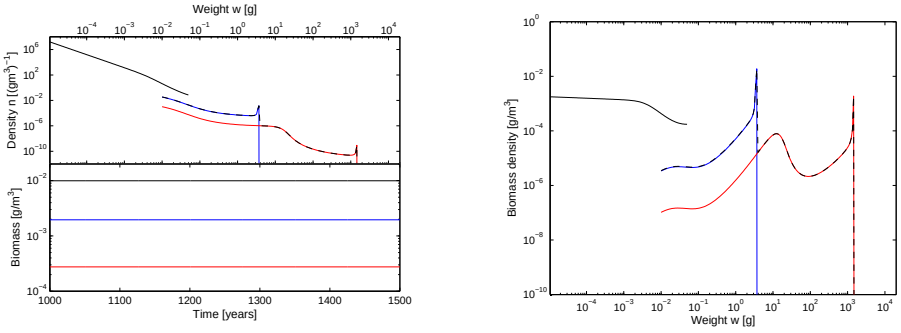

(a) (b)

Figure 6.2: *(a)* Two species of sizes $w_{\infty,1} = 30\,\mathrm{g}$ and $w_{\infty,2} = 11.390\,\mathrm{kg}$ in a steady-state. Without the smaller species the larger species cannot exist since it is needed as a trophic ladder. *(b)* The biomass spectrum of the state in (a) in logarithmically evenly distributed size bins. A pile-up of the larger species is seen at $w \approx 10\,\mathrm{g}$, and is due to scarce abundances of food items in the preferred size range of $w = \beta \cdot 10\,\mathrm{g} = 0.1\,\mathrm{g}$. The dashed black curves show the summation of the two species' spectra.

The coexistence in the $400 - 630\,\mathrm{g}$ is not due to the 'pure' trophic ladder since both species are capable of living solely on background resources in the absence of each other. In section 6.3 it is discussed that states can exist in between the steps of the trophic ladder. However, since species start suffering from reduced access to background resources from a size of $w_{cut}/\beta = 5\,\mathrm{g}$ the coexistence mechanism is similar to the trophic ladder since the smaller species allows the species in the $400 - 630\,\mathrm{g}$ to exist at a larger biomass level. From $630\,\mathrm{g}$ the larger species coexist with the smaller due to the trophic ladder, and no lower level of the larger $w_{\infty,2}$ thus exist.

When the roles are reversed and the larger species is kept constant at $w_{\infty,2}$ and the size of the smaller species is varied then both a lower and an upper level for $w_{\infty,1}$ are present for coexistence. The lower level is due to the same mechanism as before since a minimum size of the smaller species naturally is required for the larger species to reach maturation. The upper level is a bit more complicated. Increasing $w_{\infty,1}$ will decrease the magnitude of the species' spectrum as predicted by $K(w_\infty)$ in (5.6) since the same amount of resources basically have to be distributed to individuals over a larger size range. Thus the larger species will have access to less food resources at a given size w, which may be insufficient for reaching the size of maturation since the growth may drop to zero at an earlier stage since no excess energy is available for growth once maintenance costs have been paid. This may be illustrated by observing the biomass spectrum in figure 6.2(b) where it is seen that individuals pile up around $w \approx 10\,\mathrm{g}$ due to scarce abundances of food items in the preferred size range of $w = \beta \cdot 10\,\mathrm{g} = 0.1\,\mathrm{g}$. If $w_{\infty,1}$ is increased further the lower valley in the biomass spectrum will soon be too low to allow any growth of the individuals that pile up, and once this happens the species can no longer exist. Figure 6.3(b) shows an explicit example of the lower and upper level of the smaller species for coexistence.

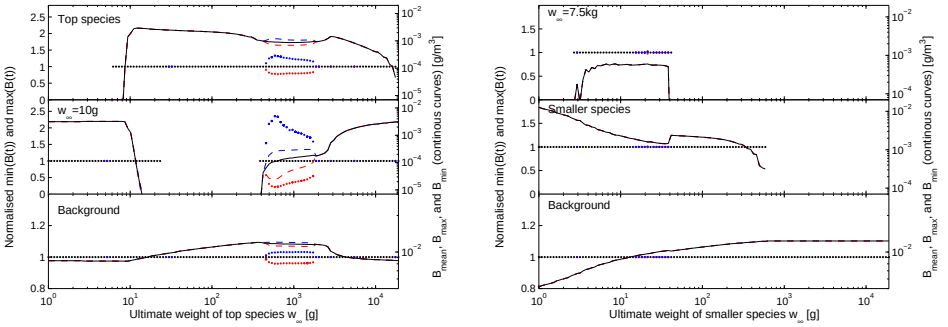

(a) (b)

Figure 6.3: Left axis: normalised biomass deviations; mean biomass (black), local maxima (blue), and local minima (red). Right axis: Non-normalised plots where only the global extremes are plotted. *(a)* The size of the larger species is varied while the smaller species size is fixed at $10\,\mathrm{g}$. The apparent coexistence in the $5 - 10\,\mathrm{g}$ range is only due to a long transient, and ultimately only the $10\,\mathrm{g}$ species will be present. The plotted data are the last $150\,\mathrm{years}$ of a $2150\,\mathrm{years}$ simulation. When the larger species has the same size as the smaller species of $10\,\mathrm{g}$ both species are naturally present at equal biomass levels since they then comprise the same species. The larger species outcompetes the smaller species in the size range $10 - 400\,\mathrm{g}$. For a large species size above $400\,\mathrm{g}$ both species are present. From $630\,\mathrm{g}$ and up the two species coexist due to the trophic ladder, and it is seen that we are emerging the maximum size of the larger species at $19\,\mathrm{kg}$ since the biomass level drops of. *(b)* The size of the smaller species is varied while the larger species size is fixed at $7.5\,\mathrm{kg}$. Below $3\,\mathrm{g}$ the the larger species is unable to reach the size of maturation and is thus not capable of existing. The larger species in (a) is close to this destiny at $19\,\mathrm{kg}$. Above $3\,\mathrm{g}$ the larger species can exist by using the smaller species as a trophic ladder. However, when the size of the smaller species exceeds $40\,\mathrm{g}$ the larger species can no longer persist due to zero growth in some size range below the size of maturation (see text). The smaller species is naturally capable of persisting with a size up to $630\,\mathrm{g}$ which is the maximum size that can exist on the truncated background spectrum (cf. figure 5.17(a)).

6.2.2 Enrichment of the Two Species Trophic Ladder

Coexistence using the trophic ladder has now been demonstrated, and the requirements in regards to the ultimate body weight w_∞ for two species to coexist have been discussed. In the following the stability of coexistence of the trophic ladder in response to enrichment is discussed.

Figure 6.4(a) shows the response to enrichment of the state from figure 6.2. From the previous discussions it is readily understood why the smaller and larger species is allowed to exist from two different levels of enrichment. The smaller can exist when the resource abundance is high enough for it to reach maturation. The larger species uses the smaller species as a trophic ladder and the smaller species' spectrum magnitude increases with κ, and when the abundance is high enough as discussed in the previous section the larger species can coexist. When enriching the system further the steady-states becomes cyclic due to satiation of the functional responses at smaller body sizes.

Continuing enrichment leads to species loss. From section 5.2.5 we know that two different states are possible due to bistability at high levels of κ for the larger species (cf. figure 5.17(b)). In the absence of the smaller species at high κ the larger

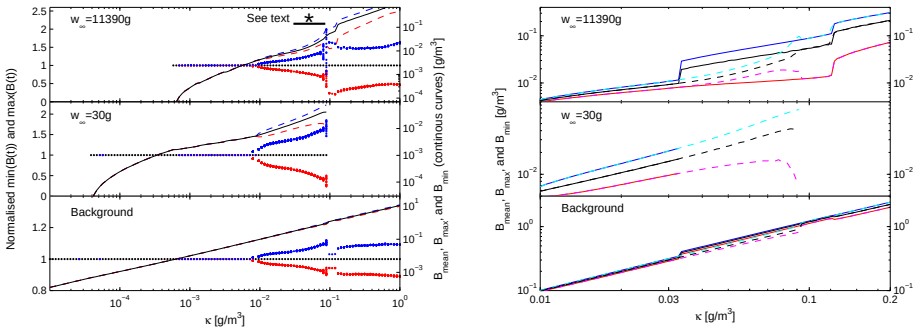

(a) (b)

Figure 6.4: Responses to enrichment. *(a)* Normalised (left) and non-normalised (right) biomass deviations. A lower κ is needed for both the smaller and larger species to exist. When the system is enriched further cycles are introduced to the system due to satiated functional responses at the smaller body sizes w. At $\kappa \approx 9 \cdot 10^{-2}\,\mathrm{g}^{1+\lambda}/\mathrm{m}^3$ the smaller species is lost since the larger species drives it out by entering the alternative dwarf-giant state (cf. section 5.2.5). Depending on initial conditions the smaller species may even be excluded in the beginning of the * marked region. The smaller species can be excluded at two different levels of enrichment due to bistability. Figure 6.5 shows the two different possibilities, and *(b)* shows the biomass levels of the two different states. The solid curves show the case where the large species is introduced at high biomass level, and the dashed when it is introduced at a low level. It is noted that the two states converge at the location of the extinction of the dashed state since the states resulting from the two different initial conditions then both are the dwarf-giant state.

species may i) go extinct if the initial biomass of its spectrum is low, or ii) enter a cyclic cannibalistic driven dwarf-giant state if its initial biomass is high. At very high levels of κ the species may enter i) a steady-state, or ii) the dwarf-giant state. The resulting state thus depends on initial conditions. In figure 6.4(a) both species are introduced at a low biomass, but the larger species may in the transient increase its biomass, enter the dwarf-giant state, and outcompete the smaller species since the dwarf-giant state does not need the smaller species for existence.

The larger species may enter the dwarf-giant state at a lower level of enrichment if the initial biomass of its spectrum is high. This gives two different routes to extinction for the smaller species. Figure 6.5 shows a zoom-in on the region where the extinction takes place in the two cases. When the large species is introduced at a low level the dynamics undergoes a series of period-doublings before the smaller species goes extinct. The extinction takes place in just a single bifurcation when the large species is introduced at a high biomass. By comparison of the two plots with figure 5.19(b) it is seen that the resulting state indeed is the dwarf-giant state, and it is also noted that the bifurcation at $\kappa \approx 0.12\,\mathrm{g}^{1+\lambda}/\mathrm{m}^3$ is not due to inter-species interactions, but a bifurcation in the dwarf-giant state. In figure 6.4(b) the biomass levels of the two alternative routes are shown in the same plot for visibility.

It is interesting to note that the smaller species indirectly assists in its own extinction. Without the smaller species the larger species could not enter the dwarf-giant state, and thus it would not be possible for the larger species to drive out the smaller before $\kappa \approx 3\,\mathrm{g}^{1+\lambda}/\mathrm{m}^3$ where the larger species is capable of surviving solely on background resources (cf. figure 5.19(a)).

The results of this enrichment study is apparently equivalent to the result of

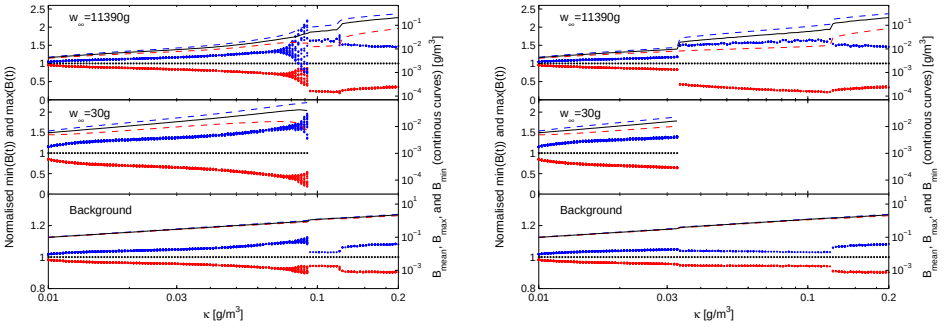

Figure 6.5: Zoom-in on the * marked region in figure 6.4(a). *(a)* The route to extinction of the smaller species when the species are introduced at low biomass levels (i.e. $10^{-10}\,\mathrm{g/m^3}$), and *(b)* when the larger species is introduced at a high biomass level (i.e. $1\,\mathrm{g/m^3}$). The high initial biomass level allows the larger species to enter the dwarf-giant state at a lower level of enrichment. Figure 6.4(b) shows the biomass levels from (a) and (b) in a combined plot.

Mylius et al. (2001) where an Intraguild Predation (IGP) system is studied. An IGP system is a tri-chain system of a predator, a consumer, and a resource where the predator is allowed also to feed on the resource. In the system of the current experiment both consumers can predate on each other, and they are both cannibals. Experiments (results not shown) show that removing both the smaller species cannibalistic behaviour and its capability of predating on the larger species does not change the qualitative result of the experiment. However, removing the larger species cannibalistic behaviour changes the result. The studied extinction points are due to the cannibalistic driven dwarf-giant states, which naturally are absent when cannibalism is not included. The smaller species is of course still driven to extinction, but not until after $\kappa \approx 3\,\mathrm{g}^{1+\lambda}/\mathrm{m}^3$ where the larger species can live solely on background resources. Before this point is reached the cyclic behaviour becomes extreme. This means that the smaller species is driven extinct at a lower level of enrichment when cannibalism is included.

Mylius et al. (2001) conclude that stable food chains cannot involve strong competition between the intermediate consumer and the predator for resources since this will drive the consumer to extinction over a large range of enrichment. The experiment at hand shows that coexistence for the two considered species is possible in the range $[6{\cdot}10^{-4}; 9{\cdot}10^{-2}]\,\mathrm{g}^{1+\lambda}/\mathrm{m}^3$ which does not seem too worrying considering that the estimated value for a typical level of enrichment in a marine environment is $\kappa = 10^{-3}\,\mathrm{g}^{1+\lambda}/\mathrm{m}^3$. If cannibalism is excluded coexistence is possible over an even larger κ range. It should of course be noted that strong competition only is present at the smaller size w stages. More worrying seems the lower level for existence via the trophic ladder which is not too far away from the estimated typical value. That the parameters of the model in principle easily can be compared to empirical values is a strong advantage of this experiment. The experiment based on the size-structured modelling framework includes more realism, and from the experiment in this section it seems likely that strong competition for food items between a predator and an intermediate consumer at smaller life stages indeed is possible in natural systems. However, before making a final conclusion research should be put into determining the range of expected values for κ in nature.

6.2.3 Extending the Ladder to More Than Two Species

In this section it is shown that the pattern of the two evolving clusters from figure 6.1 can be extended to more clusters. Trophic ladders with three species in a steady-state, and four species in a cyclic state are demonstrated. The ladder configuration is studied in an enrichment experiment for comparison with the result from the two species example.

By considering figure 6.1 smaller σ and β are clearly needed to have more than two clusters in the used grid. The invasion experiment with a small species influx is repeated in figure 6.6(a) with $\sigma = 0.5$ and $\beta = 0.1$. Still only two clusters are seen. From the previous section it is known that food limitation can keep the number of species down. Therefore the experiment is repeated with an increased enrichment of $\kappa = 0.1\,\mathrm{g}^{1+\lambda}/\mathrm{m}^3$. The result of this experiment is depicted in figure 6.6(b) where it is seen that a more irregular pattern is produced, but that the start of a period show three and the end of a period four 'trophic levels'. It is noted that the increased food abundance speeds up the period length to $\sim 130\,\mathrm{years}$.

The trophic ladder states may also be found by a simple algorithm. First a trophic ladder state with a small larger $w_{\infty,2}$ species is found. Then a third $w_{\infty,3}$ species is added. If it outcompetes $w_{\infty,2}$ it is replaced with a larger species. This continues till the third species is established. The process is now repeated for a fourth species. It should be checked that the final state indeed is a trophic ladder state. This is done by removing species $w_{\infty,n}$ and observing that species $w_{\infty,m>n}$ goes extinct. Figure 6.7(a) shows that this indeed makes it possible to locate a three species trophic ladder using the default $\sigma = 1$, $\beta = 0.01$, and a modest enrichment value of $\kappa = 0.01\,\mathrm{g}^{1+\lambda}/\mathrm{m}^3$. Using the smaller $\sigma = 0.5$, $\beta = 0.1$, and a higher level of enrichment of $\kappa = 0.1\,\mathrm{g}^{1+\lambda}/\mathrm{m}^3$ allowed location of a four species trophic ladder state (figure 6.7(b)).

In figure 6.8 the four species state from figure 6.7(b) is used in an enrichment experiment. As in the two species example it is seen that the species are allowed existence subsequently for increasing food abundance. At high levels of enrichment

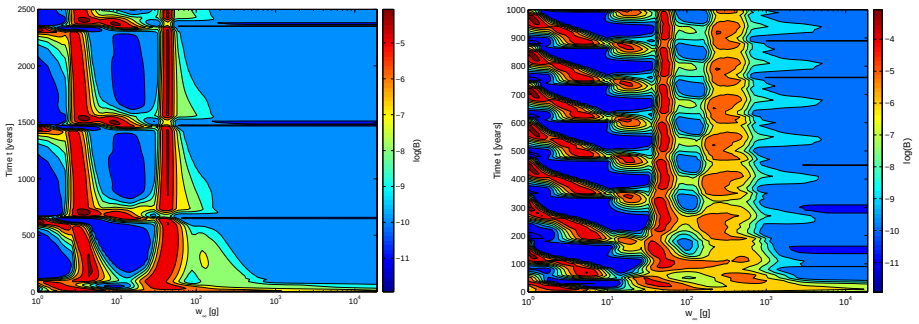

(a) (b)

Figure 6.6: The invasion experiment from figure 6.1 using $\sigma = 0.5$ and $\beta = 0.1$. Still the 100 species are logarithmically evenly distributed in the range $[1\,\mathrm{g};\ 19\mathrm{kg}]$, and an influx of $n_i(w,t) = 10^{-14}w^{-2}$ is added to each species' spectra at each time step. *(a)* The smaller σ and β still only provides two distinct size clusters. *(b)* The system is enriched to $\kappa = 0.1\,\mathrm{g}^{1+\lambda}/\mathrm{m}^3$, which speeds up the period time to $\sim 130\,\mathrm{years}$. The cluster pattern becomes more irregular, but provides hope of finding trophic ladder states with at least three to four species.

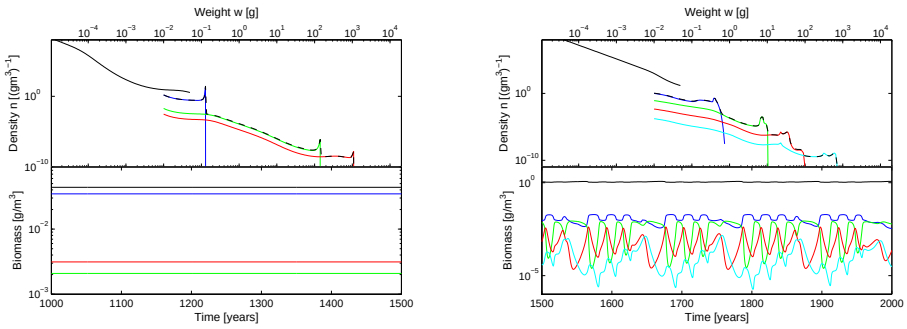

(a) (b)

Figure 6.7: Examples of trophic ladder states with more than two species coexisting. The states were found with the search algorithm described in the text. *(a)* Three species of $w_\infty = \{1\,\mathrm{g}, 900\,\mathrm{g}, 9.5\,\mathrm{kg}\}$ in steady-state. Parameters: $\sigma = 1$, $\beta = 0.01$, and $\kappa = 0.01\,\mathrm{g}^{1+\lambda}/\mathrm{m}^3$. *(b)* Four species of $w_\infty = \{1\,\mathrm{g}, 50\,\mathrm{g}, 250\,\mathrm{g}, 5\,\mathrm{kg}\}$ in a cyclic state. The plotted spectra are the mean spectra of the time series. Parameters: $\sigma = 0.5$, $\beta = 0.1$, and $\kappa = 0.1\,\mathrm{g}^{1+\lambda}/\mathrm{m}^3$.

a species is lost. Further enrichment does not lead to more species loss, but cascades take place where the extinct species changes to another.

It is not likely that the trophic ladder mechanism is responsible for major parts of the biodiversity that is seen in nature since this would require many 'trophic levels'. And if the trophic ladders should account for many species large values of κ would be required. However, the trophic ladder states may play a role in the structure of size-structured food webs. The trophic ladder can be seen as a food web structure that emerges from lower level processes and assists in species coexistence.

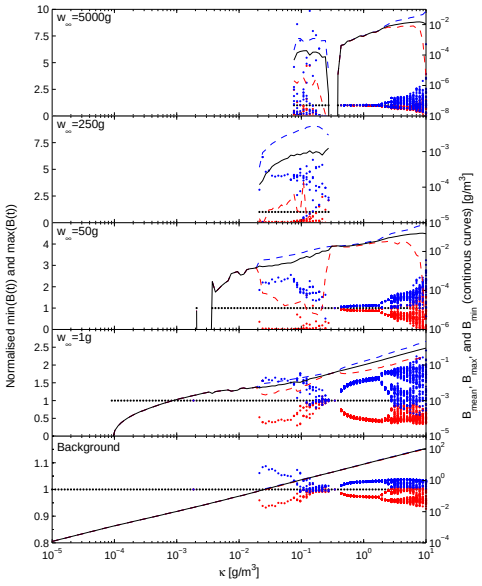

Figure 6.8: Enrichment study of the four species state from figure 6.7(b). As in the two species experiment (figure 6.4(a)) enrichment leads to species loss. Further enrichment leads to cascades where the extinct species changes to another. At $\kappa = 10^6\,\mathrm{g}^{1+\lambda}/\mathrm{m}^3$ still only one species was extinct. However, around $\kappa \approx 3 \cdot 10^{-1}\,\mathrm{g}^{1+\lambda}/\mathrm{m}^3$ the two largest species goes extinct and the remaining species exist in a steady-state; actually the $250\,\mathrm{g}$ species persists at a very low biomass level till the larger species can persist without it. Around $\kappa \approx 2.2 \cdot 10^{-3}\,\mathrm{g}^{1+\lambda}/\mathrm{m}^3$ the $50\,\mathrm{g}$ species is capable of persisting in at least a very long transient. $2000\,\mathrm{years}$ simulations were used for the experiment.

6.3 Random Invasion: States Between Ladder Steps

In the previous it has been shown how the trophic ladder leads to species coexistence. In this section it will be showed that more states than the trophic ladder states actually are possible without any modifications of the model.

To try locating such states a random invasion experiment was carried out using just 10 species. Every five years in the simulation it was checked if any species had gone extinct, and extinct species were replaced with new species having a random w_∞. Details of the experiment is given in figure 6.9(a) along with the result of such a simulation. In the plot it is seen that the surviving species are clustering in size ranges comparable to the clusters in figure 6.1, and that more species are present at both steps of the trophic ladder. It is seen that the clusters are coexisting for thousands of years before, by random, new species are capable of disturbing the system and starting new clusters. If ultimate species sizes w_∞ from a horizontal line is taken and used in an independent simulation without any invasion up to six species are often seen to coexist over a long transient (typically $500 - 1500$ years) indicating as in the Scheffer & van Nes (2006) experiment that only very weak forces are needed to stabilise the system. Figure 6.9(b) shows the result from such a run where actually three species end up in a stable state. This state is not entirely due to the trophic ladder, since the two larger species clearly need the smaller for existence, but the two larger species may exist along with the smaller without each other. The stability of the state was tested by varying w_∞ of the species, and the result was that the state might turn cyclic but remain stable for some variation as in section 6.2.1.

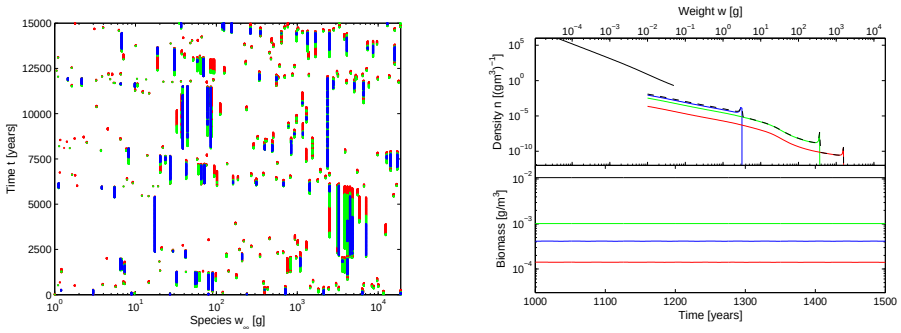

(a) (b)

Figure 6.9: *(a)* Random invasion using ten species. Ten species are added evenly distributed in the $[1\,\mathrm{g};\ 19\mathrm{kg}]$ range. Every five years it is checked if any species are extinct. Extinct species are then replaced with new species having $w_\infty = 10^n$ where n is randomly chosen in the $[\log(1\,\mathrm{g}); \log(19\mathrm{kg})]$ range. New species are introduced at low biomass levels ($10^{-8}\,\mathrm{g}$). Blue colour marks species present at high biomass levels ($> 10^{-6}\,\mathrm{g}$), green colour marks species at intermediate to low biomasses that may be close to extinction ($10^{-8}\,\mathrm{g} - 10^{-6}\,\mathrm{g}$), and red marks species with a biomass lower than when it was introduced ($10^{-13}\,\mathrm{g} - 10^{-8}\,\mathrm{g}$). Species are removed when their biomass has dropped five orders of magnitude below the introduced biomass ($10^{-13}\,\mathrm{g}$). It is seen that some clustering is appearing in size ranges comparable to the clusters in figure 6.1, and that more states are present at each trophic ladder step. *(b)* Example of three species ($w_\infty = \{23.46\,\mathrm{g}, 3.036\,\mathrm{kg}, 13.87\,\mathrm{kg}\}$) coexistence where the two larger species can survive without each other, but both are dependent on the smaller species. Parameters: default (section 3.6).

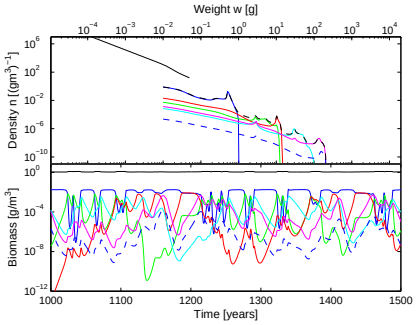

Figure 6.10: A stable six species ($w_\infty = \{1.625\,\mathrm{g},\ 34.81\,\mathrm{g},\ 70.45\,\mathrm{g},\ 359.7\,\mathrm{g},\ 997.2\,\mathrm{g},\ 1.164\,\mathrm{kg}\}$) chaotic state originating from an invasion experiment with $\sigma = 0.5$, $\beta = 0.1$, and $\kappa = 0.1\,\mathrm{g}^{1+\lambda}/\mathrm{m}^3$. The six species are not in a pure trophic ladder state since parts of the species survive if an intermediate species is removed. The shown spectra are the mean spectra of the time series.

To try locating states with more coexistence the random invasion experiment was repeated with an increased enrichment of $\kappa = 0.1\,\mathrm{g}^{1+\lambda}/\mathrm{m}^3$ and $\sigma = 0.5$, $\beta = 0.1$. From this a state was located where six of ten species were stable in a chaotic state. This state is depicted in figure 6.10.

Above it has been demonstrated that additional coexistence from the trophic ladder states is possible without any modification of the model. It is, however, likely that coexistence can be made easier by incorporating the parallel to the interference competition incorporated by Scheffer & van Nes (2006) to stabilise the coexistence of more species. This does indeed bring optimism for making an assembly algorithm that can build communities in the completely mixed environment setting. Such an algorithm will, however, not be devised in this thesis.

6.4 Perspectives for More Species

In the previous sections the concept of a trophic ladder has been shown to produce coexistence, and it has been demonstrated that additional states may be located in between the steps of the ladder. The trophic ladder mechanism gives rise to some coexistence, but it cannot account for the biodiversity seen in nature, since this would require many 'trophic levels' and high values of κ. However, from Loeuille & Loreau (2005) it can be learned that the number of states between distinct trophic levels depends on both niche width and interference competition intensity. Scheffer & van Nes (2006) show that self-interference is important for the stability of the previously discussed clusters. This means that it can be expected that incorporation of a parallel mechanism of interference will enhance coexistence. In short interference is the effect that two similar species will affect each other negatively in addition to the fact that they often compete for the same resources.

Everybody is capable of eating everybody if they are of a suitable size in the completely mixed environment setting of the size-structured model. Clearly a food web structure consisting of preferences for eating of some species, but not others can be expected to yield further coexistence. This is the topic of the next chapter. However, assemblies of food webs are often based on higher-level emergent properties of food webs (i.e. connectance) instead of examining the lower-level mechanisms that give rise to coexistence. One can think of the trophic ladders as an emerging food web structure from lower-level processes since it was i.e. argued in section 6.2.1 that not all inter-species links were important for the qualitative result of the coexistence pattern.

It may be possible to gain even more coexistence in the mixed environment setting. The only trait that characterises a species is its ultimate size w_∞, and this trait lead directly to the trophic ladder mechanism. It may be speculated that adding more traits can introduce other mechanisms for coexistence. The w_∞ implies a trade-off on the individuals strategy: aiming for a large w_∞ implies that a smaller percentage of body size will be used for reproduction while the larger size provides a refuge from size dependent predation (cf. section 3.2.3). Identification of other important traits should likewise often be linked with trade-offs in the bioenergetic model. Traits that could be studied are i.e. i) the role of specialisation vs. generalisation, ii) predation vs. sit-and-ambush strategies where the last is possible at a lower metabolism, iii) development of protection mechanisms that requires high maintenance, and iv) the role of differing spawning seasons. The possibility of adding more traits are discussed further in chapter 8.

7

Size-Structured Food Webs

Food webs reflect the structure of ecosystem predator-prey interactions – that is: food webs are graphs of who eats whom in an ecosystem. In this chapter we will use the model from chapter 3 to construct a size-structured food web.

In the previous chapter it was demonstrated that multiple species can coexist in the case of a completely mixed environment where everybody is capable of eating everybody if they are of a suitable size. However, coexistence from the mechanism denoted the trophic ladder was argued only to be partly responsible for ecosystem biodiversity, and it was argued that i.e. the food web structure will play a role for the biodiversity. In this chapter it is demonstrated that the structure of the food web indeed makes coexistence more common.

The first section 7.1 generalises the model from chapter 3 to be used in a size-structured food web framework. After this it is demonstrated that cannibalism can promote coexistence (section 7.2). This is followed by demonstrations of food web structures that show that the structure (who eats whom), and the strength of the interactions are important for the number of coexisting species (section 7.3). In section 7.4 the multi-species states from this and the previous chapter are compared to the analytical results of the reduced steady-state model in section 5.1. The structure of a food web is not likely to be constant over time since species may start consuming of other species if they for some reason become very abundant, and in the final section 7.5 it is demonstrated that this kind of switching behaviour indeed can play a role for coexistence.

7.1 Constructing a Size-Structured Food Web

The model from chapter 3 needs a couple of small modifications before it can be used as a food web modelling framework. To enable feeding preferences of different species we introduce the function $\Omega_i(N)$:

$$\Omega_i(N) = \theta_{i,b}(N) n_b(w,t) + \sum_j \theta_{i,j}(N) n_j(w,t) \tag{7.1}$$

which we denote the *experienced total spectrum* for species i. This name is inspired by the *total spectrum* $N(w,t)$ (3.51) which is the total spectrum of all species and the background resources (the community spectrum). $\theta_{i,b}(N) \in [0;1]$ is species i's

preference (or coupling strength) for the background spectrum. $\theta_{i,j}(N) \in [0;1]$ is species i's preference for species j. The preferences are in the $[0;1]$ range since values above 1 would scale the available densities in (7.2) to higher densities than what is actually available. By using this notation species may be disconnected ($\theta_{i,j} = 0$) or have preference couplings of different strengths towards both other species and the background resources; $\Omega_i(N)$ thus gives the total spectrum that species i encounters or *experiences*.

The θ preferences are functions of the environment (denoted as the total spectrum $N(w,t)$) to allow studies of e.g. switching (a species may change its diet from one species to another depending on abundance levels). However, in this thesis we will mainly examine constant preferences $\theta_{i,b}(N) = \theta_{i,b}$ and $\theta_{i,j}(N) = \theta_{i,j}$:

$$\Omega_i(N) = \theta_{i,b} n_b(w,t) + \sum_j \theta_{i,j} n_j(w,t) \tag{7.2}$$

where we note that $\Omega_i(N)$ of course still is a function of the environment, since the *experienced total spectrum* is a subset of the *total spectrum* $N(w,t)$.

We may think of the preference couplings $\theta_{i,j}$ as interaction strengths in classical unstructured food webs; see e.g. Martinez et al. (2005) for an introduction to unstructured dynamical food webs. However, in this thesis I will refrain from this notation since it may cause confusion. The preference is *not* an interaction strength since the actual interaction strength is the preference times the size selection function $s(w, w_p)$ (3.65). Furthermore the resulting interaction strength is also a function of the feeding level $f_i(w_p, N)$ (3.61) and the available food $\phi_i(w_p, N)$ (3.64) which we have to generalise to:

$$\phi_i(w_p, N) = \int \Omega_i(N) w s_i(w, w_p)\, \mathrm{d}w \tag{7.3}$$

Likewise we have to modify the mortality rate for species i $\mu_i(w, N)$ (3.66) to:

$$\mu_i(w, N) = \sum_j \theta_{j,i}(N) \mu_{p,j}(w, N) + \mu_{i,s}(w) + \mu_{i,0} \tag{7.4}$$

as well as the mortality of the background:

$$\mu_b(w, N) = \sum_j \theta_{j,b}(N) \mu_{p,j}(w, N) \tag{7.5}$$

After these mathematical details of the size-structured food web we will now illustrate the differences from a traditional unstructured food web. Figure 7.1 shows a small unstructured and a small size-structured food web. The links in the size-structured web are of a more general nature since the interaction strength is a function of both the actual preference and the size-selective function. This means that even though there is a connection between two species then parts of the spectrum may not experience the link if the size-selective function is very weak; this would for instance be the case for a smaller species connected to a larger species. Self-interactions such as cannibalism is also more naturally incorporated in the size-structured web since this is easily modelled with the size-selection function. In both webs we can see dynamics of the interacting species in biomass abundances, but in the size-structured web we also have intra-species dynamics in the species density function.

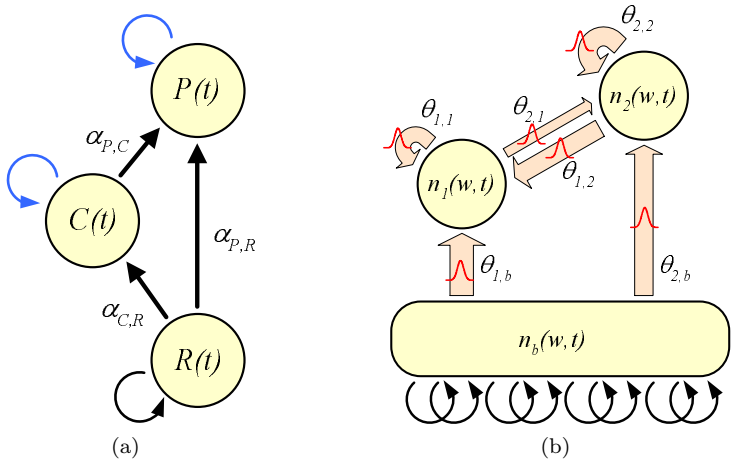

Figure 7.1: Examples of small food webs. *(a)* Traditional unstructured food web with predator, consumer, and resource. *(b)* Size-structured food web. The black arrows indicate self-regulation in primary production. Self-interactions (i.e. cannibalism) are rarely used in unstructured models whereas cannibalism naturally is implemented in size-structured models. Size-structured links are drawn wide to illustrate that individuals of differing size may experience different effective interaction strengths due to the size-selection function. In unstructured webs $\alpha_{i,j}$ is interaction strengths, whereas $\theta_{i,j}$ is denoted preferences in size-structured webs; interaction strengths are obtained both through the preferences and the size-selective function.

7.1.1 Interpretation of the Experienced Total Spectrum $\Omega_i(N)$

The inter-species preferences part $\theta_{i,j}$ of $\Omega_i(N)$ is a matrix, which means that we may use the computationally convenient formulation:

$$\boldsymbol{\theta}_{i,j} = \begin{bmatrix} \theta_{1,can} & \theta_{1,2} & \theta_{1,3} & \cdots & \theta_{1,S} \\ \theta_{2,1} & \theta_{2,can} & \theta_{2,3} & \cdots & \theta_{2,S} \\ \theta_{3,1} & \theta_{3,2} & \theta_{3,can} & \cdots & \theta_{3,S} \\ \vdots & \vdots & \vdots & \ddots & \vdots \\ \theta_{S,1} & \theta_{S,2} & \theta_{S,3} & \cdots & \theta_{S,can} \end{bmatrix} \tag{7.6}$$

where S is the total number of species.

Row i is species i's preferences towards species 1...S. The diagonal is self-interactions and thus the preferences for cannibalism. Different interpretations are available for the rest of the matrix. Below the three most intuitive are discussed.

1) Spatial overlaps: The off-diagonal may be regarded as a measure of how geographically accessible the different species are to each other. If i.e. species 1 and 3 have no spatial overlap then $\theta_{1,3} = \theta_{3,1} = 0$, and in general it is clear that the matrix becomes symmetric ($\theta_{i,j} = \theta_{j,i}$). A preference of 1 means that the two species are completely mixed among each other.

2) Temporal overlaps: The interpretation in 1) is directly translatable to a temporal interpretation where a coupling of 1 means that the two species are present at the same location all the time and vice versa. In this case the matrix will naturally also be symmetrical.

3) Diet preferences: The size of the preferences $\theta_{i,j}$ may also be understood as a dietary preference. Maybe species 3 has a preference $\theta_{3,1} = 0.5$ for species 1,

while species 1 is not feeding on species 3 $\theta_{1,3} = 0$. In this interpretation the matrix is in general asymmetric, but can be symmetric if preferences between two species always are mutualistic.

For further generality the preference matrix should be a function of w so that preferences towards different species could change with size. This is partly included with the size selection function. Even though i.e. a large predator like cod is connected to zooplankton then it will only feed on this resource when it is small since the food selection otherwise is zero. A generalisation with a size dependent preference matrix would however be too complex for this thesis.

The three interpretations naturally do not exclude each other. One might divide $\boldsymbol{\theta}_{i,j}$ into three matrices:

$$\boldsymbol{\theta}_{i,j} = \boldsymbol{\theta}_{i,j,diag} + \boldsymbol{\theta}_{i,j,overlap} + \boldsymbol{\theta}_{i,j,pref} \tag{7.7}$$

where the first matrix only contains the diagonal (cannibalism) and the two latter have zero diagonals. The second matrix contains couplings due to spatial and/or temporal overlaps, and the third couplings due to dietary preferences. The second matrix is as discussed above symmetric whereas the third may be symmetric, but asymmetric in most cases.

The preferences $\theta_{i,b}$ towards the background in (7.2) may equivalently be divided into two terms:

$$\overline{\theta}_{i,b} = \theta_{i,b,const} + \overline{\theta}_{i,b,pref} \tag{7.8}$$

where the first term is the largest scalar that the S background preferences have in common, and the second the remaining vector where at least one element is zero. The constant term $\theta_{i,b,const}$ thus corresponds to an effective scaling of the magnitude of the background spectrum κ, and $\overline{\theta}_{i,b,pref}$ then represents the actual difference in preferences of the background between the S species.

7.1.2 The Concept of Connectance

In classical unstructured food webs connectance is mostly defined as $C = L/S^2$, where L is the number of links and S the number of species in the food web. Clearly S^2 links is the maximum number of links a food web can have if cannibalism is included. Thus $C \in [0; 1]$. A link is either present '1' or not present '0' in classical food webs. In the framework presented in this chapter species i has a preference $\theta_{i,j} \in [0; 1]$ towards species j. The concept of connectance may in the framework at hand be defined equivalently as:

$$C = \frac{1}{S^2} \sum_{i,j} \theta_{i,j} \tag{7.9}$$

Where we note that the connectance says nothing about the background preference $\theta_{i,b}$, but denotes a property of the preference matrix (7.6). Naturally we also have $C \in [0; 1]$ in the size-structured framework. The connectance of a single species can also be defined ($C = \frac{1}{S} \sum_i C_i$):

$$C_i = \frac{1}{S} \sum_j \theta_{i,j} \tag{7.10}$$

7.2 Cannibalism Can Promote Coexistence

In this section it is demonstrated that cannibalism promotes coexistence in a manner similar to the self-interference term in i.e. Scheffer & van Nes (2006) (cf. section 6.1). The difference from the self-interference term, which can be seen as an increased mortality rate for increasing populations, is that cannibalism also gives rise to an energy gain.

To study the effect of cannibalism ten species are studied ($w_\infty \in [1\,\mathrm{g};\ 300\mathrm{g}]$) that in solo are capable of reaching the size of maturation and thus exist solely on the background spectrum. The study is started by using a zero preference matrix, so that no species interact and none are cannibals. Figure 7.2(a) shows that this produces a system with two coexisting species where the other goes extinct due to resource competition which does not allow them to grow to the size of maturation.

The index $BMS_{log} = \frac{\Delta \log(B)}{\Delta t}$ is introduced to easily illustrate whether a species is capable of persisting in a given system. BMS_{log} is the slope of the species biomass (B) evolution in a semi-logarithmic plot, and a persisting species will thus have $BMS_{log} = 0\,\mathrm{years}^{-1}\log(\mathrm{gm}^{-3})$.

Now the diagonal θ_{can} in the matrix that determines the species' preferences for cannibalism is varied from 0 to 1. Figure 7.2(b) illustrates that this experiment results in an increasing numbers of coexisting species. At $\theta_{can} = 0.5$ nine of the ten species coexist. The largest species is not capable of persisting even for full cannibalism since its capability of feeding on the background spectrum is too weak with the default β and σ for the size selection function (cf. section 5.2.5). Cannibalism allows the species to coexist due to 1) increased capability of retrieving suitable food

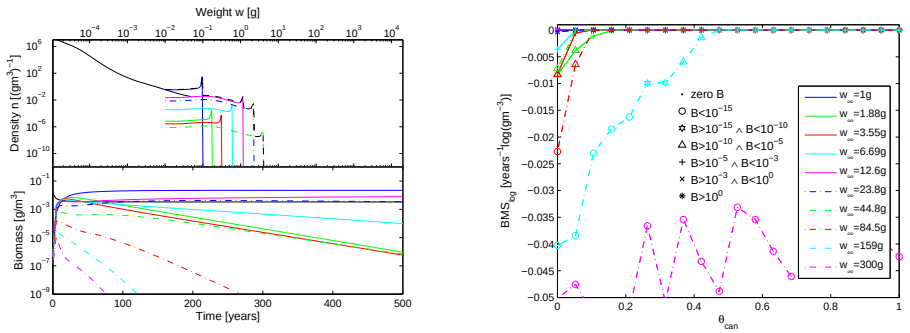

(a) (b)

Figure 7.2: Examination of cannibalism for 10 species having their w_∞'s logarithmically evenly distributed in the range $[1\,\mathrm{g};\ 300\mathrm{g}]$. *(a)* The species spectra at time step $t = 500\,\mathrm{years}$ and the biomass evolution for the case where the preference matrix is a zero matrix. It is clearly seen that only three species is not diverging to extinction due to exclusion from resource competition. However, the blue dotted species is also diverging towards extinction at a very slow rate leaving only two coexisting species. The index $BMS_{log} = \frac{\Delta \log(B)}{\Delta t}$ is the slope of the species biomass (B) evolution in a semi-logarithmic plot. A species having $BMS_{log} = 0\,\mathrm{years}^{-1}\log(\mathrm{gm}^{-3})$ is capable of persisting in the system. *(b)* Plot of biomass evolution slopes BMS_{log} for the 10 species for varying strength of the preference for cannibalism θ_{can}. It is seen that more species can coexist for increasing θ_{can}. At $\theta_{can} = 0.5$ nine species coexist where only the largest species cannot persist due to food limitation from resource competition. All coexisting species for all θ_{can} preferences are in steady-state.

items, and 2) due to decreasing abundance levels competing for the same resources since cannibalism effectively is a damper since the energy fraction $e(1-\alpha)$ is not utilised for new recruits (cf. equations (3.3) and (3.58)).

In the previous chapter cannibalism was not seen to stabilise the clusters in section 6.1 since cannibalism did not play a dominating role because a preference of 1 was present towards all species.

7.3 Food Web Assembly

The most challenging part of using the food web framework presented above is the problem of determining how the food web should be assembled. This problem will not be tackled in this thesis. However, in section 7.3.1 a null model will be used to show that random food webs with random preferences enhances the coexistence pattern seen in the last chapter where the completely mixed environment (all preferences equal to 1) setting was used. Section 7.3.2 uses the niche model (Williams & Martinez (2000)) to show that food webs where not all species are connected allow more species to coexist. Finally in section 7.3.3 different approaches for assembly are outlined.

The preferences towards the background resources $\theta_{i,b}$ will not be studied, hence $\forall i : \theta_{i,b} = 1$. Only the essential structure of inter-species who-eats-whom relations are considered in the following.

7.3.1 Preference Strength is Important

The simplest way that the preference matrix $\boldsymbol{\theta}_{i,j}$ (7.6) can be constructed is by using a null model where all preferences are selected randomly from [0; 1]. Often this reduces to systems where one to three species are surviving, but within a few runs where the w_∞ of 25 species were logarithmically evenly distributed in the [1 g; 19kg] range a stable state consisting of 7 species was located.

Following the procedure from the previous chapter the extinct species were removed and a simulation with the 7 species was made to check that the system is stable. The state is depicted in figure 7.3 and the preference matrix is:

$$\boldsymbol{\theta}_{i,j} = \begin{bmatrix} 0.9717 & 0.6835 & 0.8536 & 0.0657 & 0.6029 & 0.5517 & 0.8809 \\ 0.7398 & 0.9716 & 0.0180 & 0.0488 & 0.9963 & 0.6269 & 0.4193 \\ 0.0107 & 0.0415 & 0.1565 & 0.9573 & 0.4431 & 0.4706 & 0.3915 \\ 0.5280 & 0.3616 & 0.6795 & 0.8132 & 0.0726 & 0.1309 & 0.4654 \\ 0.5207 & 0.2553 & 0.1884 & 0.3223 & 0.4552 & 0.6165 & 0.7560 \\ 0.2567 & 0.6248 & 0.1299 & 0.1236 & 0.2917 & 0.3263 & 0.7733 \\ 0.7380 & 0.8878 & 0.0602 & 0.8221 & 0.1396 & 0.0439 & 0.2473 \end{bmatrix} \tag{7.11}$$

From figure 7.3 it is seen that the null model has produced a state with 7 species that coexist with low biomass oscillations. This may be due to the fact that weak couplings are expected to stabilise food web structures (McCann et al. (1998)). Removing links with a preference below 0.1 does not alter the system, but removing links below 0.2 causes two species to go extinct and leaves a 5 species state that still have low amplitude oscillations. Making the weakest links stronger does not produce more extreme states either. From this example it is difficult to prove that the many links of varying strength dampens the system. Many links of weak to intermediate strength are, however, important for promotion of community

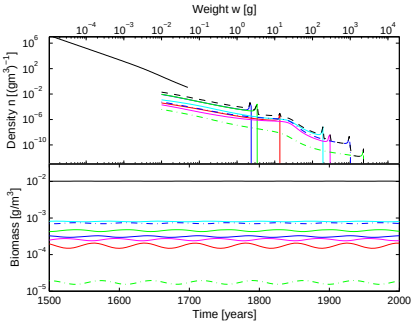

Figure 7.3: Resulting 7 species stable state from a 25 species simulation where the w_∞'s were logarithmically evenly distributed in the range $[1\,\mathrm{g};\ 19\mathrm{kg}]$. The preference matrix was created by drawing random preferences in $[0;\ 1]$. The resulting state has connectance $C = 0.46$, $w_\infty = \{17.7\,\mathrm{g},\ 26.7\,\mathrm{g},\ 138\,\mathrm{g},\ 1.62\,\mathrm{kg},\ 2.44\,\mathrm{kg},\ 8.36\,\mathrm{kg},\ 19\,\mathrm{kg}\}$, and preference matrix (7.11).

persistence and stability, and empiric seems to agree that natural food webs are characterised by many weak and a few strong interactions (McCann et al. (1998)). Weak interactions can dampen dynamics by providing alternative energy routes (McCann et al. (1998)), and it is clear that if only weak preferences are present towards certain species then these will clearly be less vulnerable to predators.

The null model produces states with a high connectance value compared to typical food web statistics. The expected connectance from the null model is:

$$C_{null,exp} = \frac{1}{S^2}\frac{1}{2}S^2 = \frac{1}{2} \tag{7.12}$$

where typical food web statistics indicate connectances of $0.1 - 0.3$ (Williams & Martinez (2000)). It may, however, also be expected that the connectance of the preference matrix should be higher than in classical interaction matrices since the actual interaction strength in the preference matrix is the preference times the size selection function (3.65).

Only very few runs have been made so no conclusion can be made to how likely the null model is to result in communities of multiple species, and how likely the model is to expose only small amplitude oscillations. However, from the example above it has been demonstrated that variation in preference strength can lead to stable communities of several interacting species. It has also been discussed that we may expect the preference matrix to have higher connectance values than classical interaction matrices.

7.3.2 Constructing Food Webs using the Niche Model

Above it was seen that variation in preference strength can lead to stable communities. In this section it will be shown that the structure of the food web also leads to multi-species communities. To study the effect of food web structure preferences will be considered either present '1' or absent '0'. This is done since methods for constructing such food webs are readily available. That both food web structure and preference strengths are important for coexistence calls for methods incorporating both in the food web assembly process. This is discussed in more detail in section 7.3.3.

In brief four methods for constructing food webs from a top-down approach are available. Constructing webs from a top-down approach means that the entire web is constructed from some algorithm that do not consider how the web may actually have evolved through evolution and/or invasions, and if the resulting web indeed

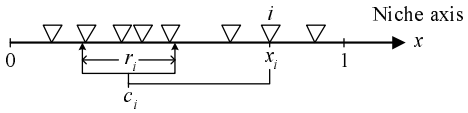

Figure 7.4: The niche model (Williams & Martinez (2000)). Each species i is assigned a niche value x_i drawn uniformly from $[0; 1]$. Species i can predate on species having niche values in the r_i range with the centre c_i. The centre of the preferred niche value c_i is drawn uniformly from $[r_i/2; x_i]$, and the range r_i of niche values that the species is connected to is drawn with a β-distribution ($\alpha = 1$) from $[0; 1]$ with expectation value $2C$ and multiplied with x_i to obtain an expectation value of C. All species are allowed a preference of 1 towards the background spectrum since all species need the background in the early life stages.

is possible to occur in nature. The methods are qualified by testing how well they reproduce statistics of natural food webs, and are typically used only for studying static food webs. The four methods are the null random model where all links are equally likely to occur, the cascade model (Cohen & Newman (1985)), the niche model (Williams & Martinez (2000)), and the nested hierarchy model (Cattin et al. (2004)).

In the cascade model all species are given a rank number $1...S$ and all species are allowed to predate on a random number of species with a lower rank than themselves. This clearly does not allow cycles as i.e. cannibalism. This problem was solved by the niche model which has been proven to reproduce food web statistics much better (Williams & Martinez (2000))*. The most recent model is the nested hierarchy model which improves the capability of reproducing food web statistics. In this thesis only the niche model will be used to examine the food web structure, since the nested hierarchy model is more problematic to implement in the framework at hand and since it is not widely used in the literature. The niche model has also been used in studies of unstructured dynamic food webs (i.e. Martinez et al. (2005)).

Outline of The Niche Model

The niche model (Williams & Martinez (2000)) is similar to the cascade model, but its algorithm encapsulates more ecological realism. As in the cascade model each species i is given a rank called a *niche*. The niche value x_i is drawn randomly from $[0; 1]$ (uniform distribution), and each species is allowed to feed on species having niche values in an interval r_i around the centre of a preferred niche value c_i (cf. figure 7.4). The preferred niche value c_i for species i is drawn uniformly from $[r_i/2; x_i]$ to allow cannibalistic cycles and some feeding on some species with a higher niche value. The range of the niche values r_i is drawn from a β-distribution ($\alpha = 1$) in $[0; 1]$ with an expectation value of $2C$, and multiplied with x_i to obtain the expected connectance of C. The probability density function for the β-distribution is given by:

$$P_\beta(y) = \frac{(1-y)^{\beta-1} y^{\alpha-1}}{B(\alpha, \beta)} \quad , \quad \text{for } y \in [0; 1] \tag{7.13}$$

*This is however mainly due to the development in the procedures used for collecting food web data. Earlier cycles and omnivory was i.e. not seen in real food webs, whereas it today is generally agreed upon that both are quite common in natural food webs. See i.e. Drossel & McKane (2003) for a small review.

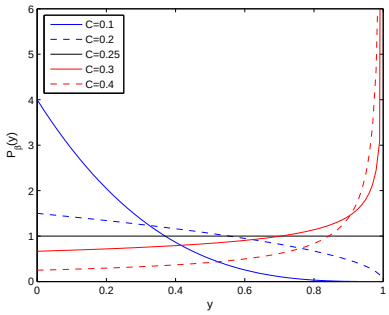

Figure 7.5: The probability density function for the β-distribution using $\alpha = 1$ (7.14). Low connectance values $C < 0.25$ give rise to narrow widths of the preferred range of niche values r_i. Connectance $C = 0.25$ gives the uniform distribution, and large connectance values $0.25 < C < 0.5$ give rise to larger r_i's.

where $B(\alpha, \beta) = \frac{(\alpha-1)!(\beta-1)!}{(\alpha+\beta-1)!}$ is the beta-function. For $\alpha = 1$ the beta-function reduces to $B(1, \beta) = \beta^{-1}$. This means that the probability density function (7.13) may be written simply as:

$$P_\beta(y) = \beta(1-y)^{\beta-1} \quad , \quad \text{for } y \in [0;\, 1] \tag{7.14}$$

The expectation value of the β-distribution is given by $E(Y) = \frac{\alpha}{\alpha+\beta} = \frac{1}{1+\beta}$, which means that $\beta = \frac{\alpha}{E(Y)} - \alpha = \frac{1}{2C} - 1$ should be used to obtain an expected value of $2C$. The probability function (7.14) is seen only to be defined for $C < 0.5$, and figure 7.5 shows the distributions for different connectance values.

In the niche model the resource is given the niche value $x_R = 0$ so that not all species are connected to the resource, but most likely species with low niche x_i values. This makes sense in unstructured models since the abstract niche here may be regarded as a trait like body size, and clearly it seems more likely that mainly smaller species use the primary production as a food source. In the size-structured framework it makes no sense to interpret the niche value as ultimate body size, and clearly all species needs to have links to the background spectrum since the smallest individuals in a species only can feed on the background. In the size-structured framework the niche value is an abstract one-dimensional quantity that determines the feeding relations among species. That such a one-dimensional trait should exist is of course highly hypothetical, and it could be interesting to study the effect of multi-dimensional niche values for the generation of preference matrices.

A Stable Community from the Niche Model

Figure 7.6 shows an example of the preference matrix $\boldsymbol{\theta}_{i,j}$ (7.6) for 100 species constructed using the niche model. Two different permutations of the matrix are shown. One where the species are ordered according to their niche value x_i, and one where the species are ordered according to their ultimate body weight w_∞. The w_∞ of the species were assigned logarithmically evenly in the range [1 g; 19kg]. From the niche ordered matrix it is seen that species with large niche values have more prey species since more species with a lower niche value clearly are available. The size ordered matrix shows that all species in general are connected to a wide range of w_∞ species, and that the notable difference between the species is the number of links.

A simulation with the matrix from figure 7.6 was carried out. Species that went extinct were removed till a stable system was located. From this process the 14

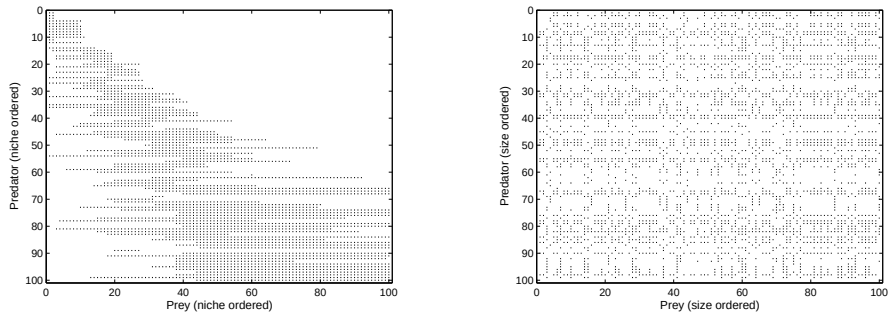

(a) (b)

Figure 7.6: 100×100 preference matrix $\boldsymbol{\theta}_{i,j}$ constructed using the niche model with $C = 0.4$. Realised connectance $C_r = 0.347$. A black dot indicates a link, and the species used for the simulation have their w_∞'s logarithmically evenly distributed in the range $[1\,\mathrm{g};\ 19\mathrm{kg}]$. *(a)* The preference matrix where the species are ordered increasingly after their niche value x_i. It is noted that species with low niche values only have few links since few species with a smaller niche value is present. *(b)* The same preference matrix where the species are ordered increasingly according to ultimate size w_∞.

species state from figure 7.7 was located. It is, however, possible that stable states of more than 14 species can be located from the 100 species system since some species could have been lost in the process if they for some reason were excluded in the transient and have a very long time for recovery. Also removing one species that is actually stable can cause a cascade that makes additional species go extinct.

Figure 7.7(a) shows the resulting preference matrix for the 14 species state. From the matrix it is seen that all species are cannibals, which in section 7.2 was demonstrated to promote coexistence. The niche model can generate stable food webs where some species are non-cannibals, but still the majority are seen to be cannibals.

The pattern in the reduced preference matrix in figure 7.7(a) is equivalent to the pattern in the generated matrix (figure 7.6) since the main difference between the preferences of the w_∞ species is the number of links. The 100×100 matrix

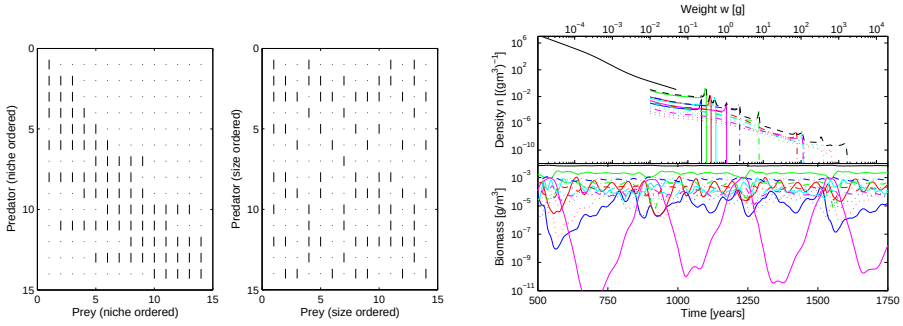

(a) (b)

Figure 7.7: The 14 species stable state that originates from the simulation of the preference matrix in figure 7.6. $C_r = 0.408$ and $w_\infty = \{1.82\,\mathrm{g},\ 2.45\,\mathrm{g},\ 3.30\,\mathrm{g},\ 4.45\,\mathrm{g},\ 8.93\,\mathrm{g},\ 19.8\,\mathrm{g},\ 72.2\,\mathrm{g},\ 528\,\mathrm{g},\ 787\,\mathrm{g},\ 869\,\mathrm{g},\ 960\,\mathrm{g},\ 3.17\,\mathrm{kg},\ 5.21\,\mathrm{kg},\ 15.6\,\mathrm{kg}\}$. *(a)* The resulting preference matrix. *(b)* Mean spectra and biomass evolution of the state.

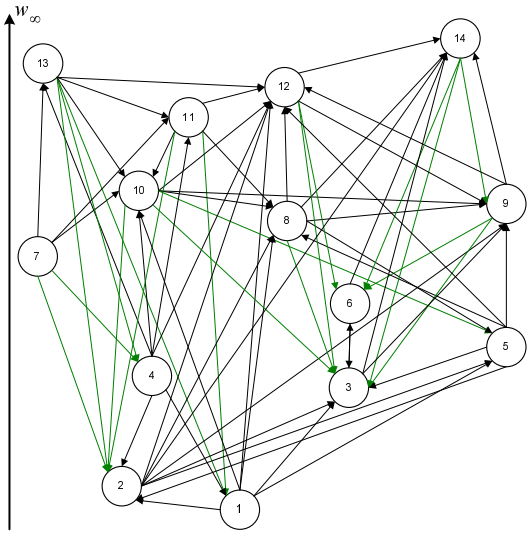

Figure 7.8: Visualisation of the food web from the 14 species state in figure 7.7. Cannibalistic links and links to the background are not drawn for visibility. Green links are links to smaller species eating on species that have at least a 10 times higher weight. The species are ordered increasingly upwards according to ultimate body weight w_∞.

was created with a high connectance of $C = 0.4$, and a high realised connectance of $C_r = 0.347$ was returned by the niche model. As discussed above in section 7.3.1 a high connectance is used since the preference matrices are expected to have higher connectance values than classical interaction matrices since the interactions in the preference matrix is the product of the preference and the size-selection function (3.65). The resulting 14 species state has a high connectance of $C_r = 0.408$.

In figure 7.8 the 14 species states from figure 7.7 is visualised. From the food web it is easily seen that the niche model also is capable of producing cycles in the food web. This is true since the r_i range may be located so that a species can feed on some species with higher niche values. Examples of cycles are species 2–5–2 and 2–8–5–2.

From the food web species no. 4, 7, and 14 are recognised of having a link composition different from the other species. Species no. 4 is seen only to have links to species that are at least 10 times larger than itself. This means that its prey not will suffer notably from predation mortality in the largest 3 orders of magnitude due to the prey-predator ratio β. Species no. 14 is seen to be a top predator since it only has enemies of smaller w_∞ species. Removal of species no. 4 or 14 results in cascades where several species goes extinct. Finally species no. 7 is recognised of only feeding on the background and via cannibalism. It is a prey for five species, where species no. 13 depends heavily on it since removal of it causes species no. 13 to go extinct.

If 0.2 is added to the zero elements in the 14 species preference matrix from figure 7.7(a) species no. 4, 5, and 13 are lost, and the resulting 11 species community coexist in the steady-state in figure 7.9. Simulation of the 11 species without the 0.2 preferences results in a cyclic 9 species state. This is another example that shows that many weak links dampens oscillations. The state do indeed have many links since it has a high connectance of $C_r = 0.557$. It is noted that the wildly fluctuating species no. 5 from figure 7.7(b) (magenta, 8.93 g) goes extinct, which is not surprising since its fluctuations indicate that it could go extinct for small changes in the food web structure. The new food web structure does not allow species no. 4 and 13 to gain enough suitable food intake to reach maturation which then causes their extinction.

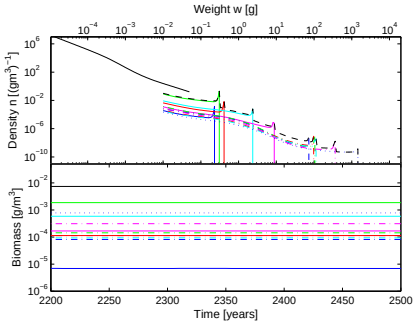

Figure 7.9: Resulting 11 species steady state when a 0.2 preference is added to the zero preferences in the 14 species state in figure 7.7. The 11 species: $w_\infty = \{1.82\,\mathrm{g},\ 2.45\,\mathrm{g},\ 3.30\,\mathrm{g},\ 19.8\,\mathrm{g},\ 72.2\,\mathrm{g},\ 528\,\mathrm{g},\ 787\,\mathrm{g},\ 869\,\mathrm{g},\ 960\,\mathrm{g},\ 3.17\,\mathrm{kg},\ 15.6\,\mathrm{kg}\}$. The state has a high connectance of $C_r = 0.557$. Notice that 4 species are present around $w = 100\,\mathrm{g}$, and that the red and red dashed species' biomass evolution coincide.

7.3.3 Assembly Models: Bottom-up or Top-down?

In the two previous sections it has been demonstrated that the strength of the preferences, and the structure of the food web plays an important role for coexistence. Furthermore it was shown that the weak links also serve as dampers to avoid extremely fluctuating populations that are very vulnerable to stochastic extinction.

A top-down approach was used for the construction of the preference matrix. The top-down 'assembly' of i.e. the niche model does not give any explanation for the observed structure of a food web – it is merely capable of producing webs with statistics similar to empirical food webs. Also it is not possible to tell whether the constructed community could have evolved in nature.

Food webs in nature are formed by their history from species invasion, extinctions, cascades, and evolutionary mutations on the even longer time-scale. Thus to understand the structure of food webs two time-scales are needed in a bottom-up assembly model that examines the emergence of food web structures. The time-scales needed are naturally the ecological time-scale already present and some longer time-scale for species invasions and/or evolution. To avoid complexity species invasions and evolution should be considered independently. However, the concepts are in general not expected to yield very different results since the species available for immigration in surrounding communities in general not are expected to be very different from the ones already present.

The second time-scale can also be important for coexistence. In the simulations it was often seen that species are going extinct in a long transient, which indeed can be stabilised by processes on the longer time-scale (e.g. Scheffer & van Nes (2006)). The second time-scale may also prove important when studying human interactions with natural systems. Human interactions often occur at a much faster time-scale than the natural assembly process, which means that selection pressures towards new niches may be increased so that evolution will play a larger role at a faster time-scale than usually.

Drossel & McKane (2003) give a nice review of present approaches in the assembly of dynamical food webs along with many useful references. This along with the book by de Ruiter et al. (2005) contains many useful lessons and references for the development of an assembly model for the size-structured food web framework in this thesis.

In conclusion the two different approaches for constructing preference matrices are relevant for different questions. The intensive two-scale bottom-up approach is important to understand the structure and emergence of food webs, whereas the

ad-hoc top-down approach is needed for less computer-intensive studies of ecological problems. A next step with the size-structured framework from this thesis could be 1) to study it using the bottom-up approach, and 2) to study an extended niche model for the top-down approach where multi-dimensional abstract niches determines the inter-species feeding relations.

7.4 Multi-Species Spectra vs. the Analytical Results

In this section the obtained multi-species spectra are compared to the analytical results for the shape, distribution, and biomass of steady-state species spectra in the reduced model of section 5.1. The chaotic 14 species state from figure 7.7, and the 6 species chaotic state from the completely mixed environment setting in figure 6.10 are used as test cases. These are picked out since they include the highest number of coexisting species of the two different settings of a) having a food web structure, and b) having a completely mixed environment.

To compare the species spectra of the two cases with the analytical result the slopes and magnitudes were computed using allometric fitting. The peaks upon maturation due to reduced growth naturally play a role for the obtained slopes and magnitudes. To study the influence of the peaks the slopes and magnitudes were computed 1) where the peaks are included, and 2) when the spectra have been cut-off before the peaks. Figure 7.10 shows the results of this process for the 14 species state. It is seen that whether or not the peaks are included the same qualitative result is obtained. Therefore only the case that includes the peaks is included in figure 7.11(a) that shows the slopes and magnitudes for the 6 species state.

The analytical solutions of the reduced steady-state model predicts spectra

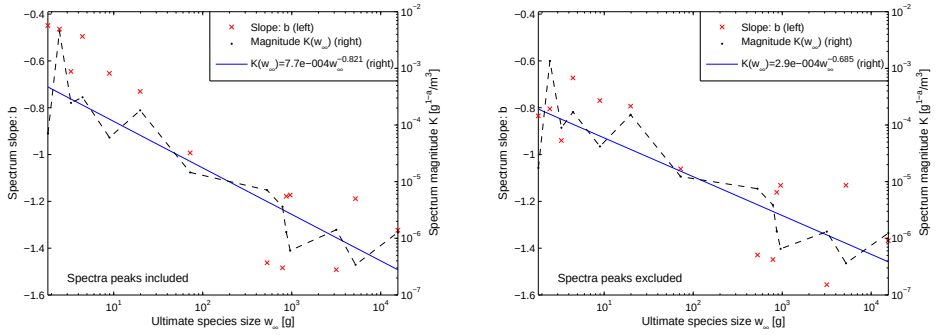

(a) (b)

Figure 7.10: Spectra slopes (left axis) and magnitudes (right axis) for the 14 species chaotic state from figure 7.7. The slopes and magnitudes are obtained by fitting an allometric function to the species spectra. The blue curve is an allometric fit to the spectra magnitudes. *(a)* Spectrum peaks upon maturation are included in the allometric fits. Species slopes are located in the $[-1.49; -0.45]$ range, and the magnitudes of the spectra follow an allometric function with an exponent of -0.821. *(b)* Spectrum peaks upon maturation are excluded in the allometric fits. Species slopes are located in the $[-1.56; -0.67]$ range, and it is noted that it is primarily the slopes of smaller species that differ from the case where the spectra peaks are included. This is naturally the case since the peaks play a larger role for shorter spectra. The magnitudes of the spectra follow an allometric function with an exponent of -0.685.

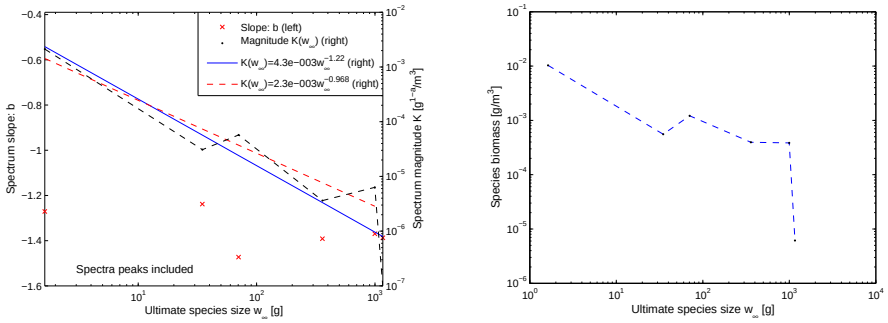

(a) (b)

Figure 7.11: Properties of the 6 species chaotic state from figure 6.10 which was obtained in the completely mixed environment setting. Spectrum peaks upon maturation are included in the allometric fits. *(a)* Spectra slopes (left axis) and magnitudes (right axis). Species slopes are located in the $[-1.47; -1.24]$ range, and the magnitudes of the spectra follow an allometric function with an exponent of -1.22. If the magnitude of the largest species is excluded the allometric fit yields the exponent -0.968 (red dashed curve). *(b)* Mean biomass showing a decreasing dependency of w_∞. If the biomasses of the smallest and largest species are ignored then no w_∞ correlation is seen. The smallest and largest species may be speculated to obtain lower and higher biomasses, respectively, if the w_∞'s of the state were more evenly distributed.

slopes of $-k - a \approx -3/4 - 0.6 = -1.35$ when the typical value of $a = 0.6$ is used for the predation strength. The slopes of the 14 species state show a decreasing dependency of w_∞. With and without the spectra peaks the slopes are located in the ranges of $[-1.49; -0.45]$ and $[-1.56; -0.67]$. The decreasing w_∞ may be attributed to the food web structure since the slopes of the 6 species state from the mixed environment show no strong w_∞ correlation, and since its slopes in the $[-1.47; -1.24]$ range are much closer to the analytical result.

Equation (5.6) using $a = 0.6$ predicts that the magnitudes should be distributed with an allometric w_∞ exponent of $2k - q - 2 + a = -0.73$. The 14 species state is close to this result with its exponents of -0.821 and -0.685 when peaks are included and excluded (figure 7.10). The mixed environment 6 species state show a steeper exponent of -1.22, but it is seen that the largest species has a much lower magnitude (figure 7.11). However, exclusion of the largest species still yields a steep exponent of -0.968. The disagreement may be due to the uneven distribution

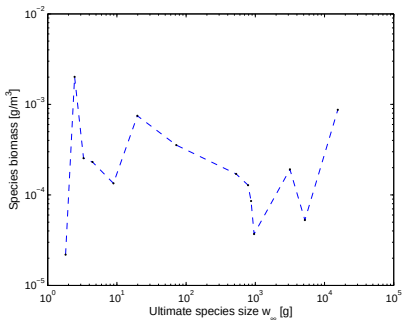

Figure 7.12: Mean biomasses of the 14 species from figure 7.7. The analytical results from the reduced steady-state model predicts equal biomass for all w_∞ species. In the 14 species chaotic state the mean biomasses show no correlation with ultimate body weight w_∞.

of the coexisting w_∞ species. The smallest species could be speculated to have a lower magnitude, and the largest a higher magnitude if the w_∞'s were more evenly distributed.

The theory of the reduced model in equation (5.7) predicts that the total species biomasses should be close to constant across the species ultimate size w_∞. Figure 7.12 shows that the 14 species state shows no biomass correlation with w_∞. The 6 species state shows a decreasing biomass dependency of w_∞ (figure 7.11(b)). However, as discussed before a more even species distribution can be speculated to produce a lower biomass for the smallest species, and a higher biomass for the largest species. If the biomasses of the smallest and largest species are ignored then no w_∞ correlation is seen.

One of the key assumptions in the derivation of the analytical results of the reduced steady-state model is that food always is abundant. This is definitely not the case in the multi-species simulations of the full model since low feeding levels are present, which i.e. causes the peaks that are seen in the species spectra. In the reduced model no ontogenetic shift in the growth trajectory of the individuals occur since the energy contribution to reproduction is not modelled explicitly. This ontogenetic shift amplify the problem of reduced growth since the energy requirements increase upon maturation if growth is to continue. However, in spite of these discrepancies of the two models it can indeed from the above discussion be concluded that the species composition in the full dynamic model is consistent with the predictions from the reduced steady-state model in section 5.1.

7.5 Prey Switching

Yodzis (1989) among others stress that the diet of real animals – compared to the model species – have quite variable feeding habits. This problem is partly solved by the size-structured model since it incorporates that the diet changes throughout the life history through size-dependent predation. Furthermore animals may switch prey type if their favourite prey becomes scarce. Thus real communities may be more plastic compared to their model counterparts.

The role of prey switching is studied in a simplified case in this section where each individual of size w_p is allowed only to feed on the background and the single species that provides the highest amount of suitable food items. This does indeed promote coexistence, and figure 7.13 shows the result of such a simulation where 25 of 25 species are coexisting. The species are capable of coexisting since the switching prevents exclusion. If a species i.e. starts to become very abundant everybody will start eating of it, and if a species becomes rare it is likely to have no enemies. Larger w_∞ have no refuge either since that if they become very efficient spawners their recruits will suffer from a high mortality, which eventually will decrease the adult population and its total reproductive capability.

The effect of switching is that the magnitudes of the species spectra become very similar. The biomass evolution also shows low amplitude fluctuations that, however, expose a more noisy behaviour due to the constant switching.

In a switching experiment it may be impossible for some species to exist if they fail to reach maturation due to lack of suitable food items (cf. section 6.2.1). This may happen even though individuals feed of the species that provides the largest amount of food since the spectrum magnitudes of the victims may be too low. In the previous studies of coexistence this problem often get less pronounced since

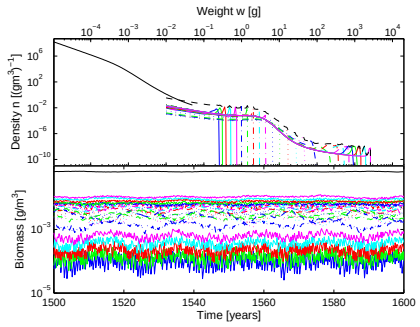

Figure 7.13: 25 species coexisting due to switching behaviour. The ultimate sizes w_∞ are logarithmically evenly distributed in the range $[1\,\mathrm{g};\ 19\mathrm{kg}]$. It may be impossible for some species to exist in a switching experiment if they fail to reach maturation due to lack of suitable food items (see text). Parameters: $\kappa = 0.01\,\mathrm{g}^{1+\lambda}/\mathrm{m}^3$.

a species can feed of multiple spectra. In the switching experiments the species spectra have comparable magnitudes, which amplifies the problem since this means that the magnitude of the most abundant species often is lower than in the non-switching experiments for a given κ. If the value of κ in figure 7.13 is lowered to $\kappa = 0.001\,\mathrm{g}^{1+\lambda}/\mathrm{m}^3$ some intermediate sized species cannot persist due to food limitation that prevents them from reaching maturation.

Figure 7.14 shows more details of how switching takes place. In figure 7.14(a) the prey species of all different individuals are shown, and figure 7.14(b) shows an example of the switching behaviour for individuals of size w_p. The intermediate sized individuals that feed heavily on the smallest w_p's switch most frequently since all species are available, whereas fewer species are available to switch between for large sized w_p's.

Switching behaviour should more realistically be incorporated in a food web structure. It is likely that a species may not have access to some species, and hence it cannot switch its diet to those if they become abundant. The 'food web' in this case should then present all possible feeding items for a species. An individual of size w_p may then switch between the possible links depending on which resources that are most abundant. It is also more realistic that a switch will not be a distinct preference shift from 0 to 1 and vice versa why the effect of maintaining weak links to more rare species could be interesting to examine.

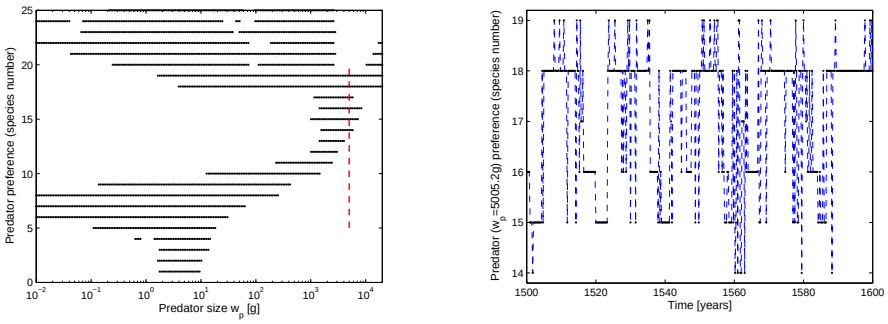

(a) (b)

Figure 7.14: Elaboration of the switching behaviour responsible for the state in figure 7.13. *(a)* The y-axis marks which species numbers (ordered increasingly for w_∞) a given individual of size w_p predates on. *(b)* Time series of the diet of the $w_p = 5\,\mathrm{kg}$ species marked with a red dashed line in (a).

8

Discussion

In this chapter the main results of the work in this thesis are discussed along with suggestions for future research. The discussion is divided into three parts. The first dealing with the model, the second part goes into the mechanisms that have been shown to enable coexistence, and the third part discusses the numerical setup.

8.1 The Simple Size-Structured Population Model

In chapter 3 a simple size-structured model for marine ecosystems was derived. This model encapsulates much more ecological realism than typical unstructured models since it takes into account size dependent processes, which are very important in aquatic ecosystems since individuals may grow six orders in magnitude throughout their life and thus become their own enemy (cf. chapter 2). The model is denoted *simple* since only one parameter, the ultimate body weight w_∞, is used to distinguish species.

The three key components for the model are the functions for growth, mortality, and reproduction. The growth function determines how much energy that should be allocated to somatic growth, maintenance, and reproduction depending on the actual intake. Mortality is imposed on individuals from either direct predation mortality from other individuals, starvation, or through a constant background mortality that takes into account other sources of mortality, and makes sure that mortality is present for the largest individuals. The starvation mortality has not been recorded to play any substantial role in the results of the simulations. As discussed in section 3.4.2 the starvation mortality only plays a role in the transient of a simulation, and should not play a substantial role for the results of a simulation since the starvation mortality has not been validated with empirical data since such data are missing. New recruits enter the species spectrum at the smallest spectrum size w_0 via the function for reproduction that takes into account the mortality individuals experience before they reach the recruit stage.

Since food intake is a size-dependent process a background spectrum is implemented to provide suitable food items for the smallest individuals of all species. The background spectrum represents smaller food items in the marine ecosystem as i.e. (zoo)plankton, and is modelled by a series of semi-chemostatic growth equations (cf. section 3.5). The background spectrum constitutes the lower half, and the species spectra the upper half of the community spectrum.

The environment that an individual encounters is completely determined by all species' spectra and the background spectrum. From this the available food, and thus intake and growth is calculated. This also gives the reproduction and the mortality for each individual. These lower level processes are described by individual level functions, and from the individual level processes the population dynamics are returned. This is another great advantage of size-structured models compared to their unstructured counterparts. In unstructured models the dynamics are implied by direct descriptions of the population dynamics whereas the population dynamics from the size-structured models emerge from individual level processes that are more naturally described. The individual level parameters are also more easily assessed.

All parameters for the individuals and the background spectrum were derived to allow use of the model in a biologically plausible region of parameter space. The only parameter that distinguishes species is the ultimate body weight w_∞, and all size dependent processes as i.e. the search volume of an individual are described with functions of w_∞ and w. Section 3.6 provides a summary of all equations in the model along with the derived default parameters.

In the following two sections some important properties are described followed by a discussion of how well the model describes natural systems, and how it can be improved.

8.1.1 Important Properties of the Model

In chapter 5 the model was examined using just a single species. Following Andersen & Beyer (2006) an analytical solution for the steady-state spectrum was derived in a reduced model. An analytical solution was also found for the distribution of the different w_∞ spectra that constitutes the community spectrum. Finally it was found that in steady-state the theory of the simpler model predicts all species to have the same total biomass.

The analytical derivations were followed by examinations of the dynamics of the model using just a single species. From this several lessons were learned. In the model steady-state, predator-prey cycles, single-generation cycles, and dwarf-giant cycles were located and demonstrated, and it was discussed that the model is capable of producing dynamics consistent with the kinds of dynamics that are observed in nature. Common for the three cycle types is that they expose intra-species cohort cycles. The dynamic states were compared and concluded consistent to the theory of the reduced steady-state system.

For the predator-prey cycles it was noted that size-structured models often are less vulnerable to stochastic extinction compared to their unstructured counterparts. When the biomasses of the predator-prey cycles reach low levels some individuals in the species spectrum may be present at large abundance levels to counteract stochastic extinction.

Theory was established to find the maximum w_∞ that can exist on a background spectrum that has been cut-off at w_{cut}. Predators have a preferred prey-predator ratio of β, and the lognormal size dependent food selection function (3.65) has the width σ. This means that less and less food will be available from the background when the predator grows beyond w_{cut}/β, but that some food will be available due to the width σ. This result proved important when describing simple coexistence patterns when moving to multiple species (discussion follows in section 8.2). Large w_∞ species may, however, circumvent the theory established for finding the maximum w_∞ for a truncated spectrum if a simulation is started with a high biomass

spectrum, since large species have alternative states that allow the species to enter a cyclic dwarf-giant state. The alternative states are due to bistability from cannibalism in the model. Figure 5.17(b) (page 73) shows the maximum w_∞ that may exist on a truncated background spectrum for a given κ, and that alternative dwarf-giant states are possible for large w_∞ species. Without the alternative cannibalistic driven dwarf-giant states some of the large species would only be capable of persisting in the system for very high values of κ.

8.1.2 The Model vs. Nature

In this section it is discussed how well the model represents natural systems, and suggestions are given for advancing the model to an even higher level of realism. First the bioenergetic growth model is discussed since it incorporates the energetics of the individuals. The predation mortality is just a matter of bookkeeping that makes sure that individuals that are consumed via the growth model indeed are removed. Starvation mortality has been discussed above not to be important, and the energy to reproduction is also determined by the bioenergetic model. After a discussion of the growth model it is discussed how realism can be enhanced by using more than the single trait of ultimate size w_∞ to describe a species.

The bioenergetic growth model is the most important part of the model since it takes care of the most important task of allocating the acquired energy into somatic growth, maintenance, and reproduction. As described in section 3.2.3 where the growth model is derived more research should be put into the allocation. In the used $\varrho(w_\infty)$ formulation (3.58) the cost of obtaining a large ultimate size w_∞ is a reduced capability of reproducing. The capability of reproducing is measured as how large a percentage of body weight that is used for reproduction. This trade-off seems to be physiologically reasonable. The problem in the model is that growth upon maturation is stopped completely if food intake is not large enough for ideal reproduction. Energy is first allocated to maintenance requirements, and if full maintenance cannot be paid the missing energy is translated into a starvation mortality. Then, if the individual has matured, energy is allocated to reproduction. Finally, if excess energy is available after reproduction the remainder is used for somatic growth. Thus if the acquired energy does not allow full ideal reproduction nothing is spend on growth, and this has the effect of a pile-up of individuals upon maturation as seen in i.e. figure 5.4 (page 61). Such extreme pile-ups do not seem likely to occur in nature since some continuation of body growth could be expected with the cost of reduced reproduction. Modifying the growth model to allow some minimum growth when costs of ideal reproduction cannot be paid is, however, not straightforward since it is difficult to find a rule to how much energy that should be ensured to growth depending on both the available energy and body size. The pile-up is due to a low feeding level due to limited available food, and it might just be so that this does not occur in a natural ecosystem since it may organise to prevent this. If this is the case research should of course be put into how this can be modelled.

Individuals of a given size w are assumed identical in the model. This is clearly not the case in natural systems since individual differences are present. This individual diversity is a third way in which the pile-ups at maturation may become less extreme. Other effects can also emerge from individual diversity, and the diversity could be implemented with a higher-order term in the PDE (3.49) describing the p-state. Expanding the model with such a term would, however, not be recommend-

able at this stage since it may be more fruitful to explore and develop the current model before complicating it further.

Advancing the Model to More Traits

In the model the only trait that characterises a species is its ultimate body weight w_∞. In nature more traits seem to identify species. This can be seen both by looking on the physiological structure and the behaviour of species. In addition to the ultimate weight the physical appearance of a species may be characterised by body shape, colour markings, and special body features as i.e. defence mechanisms in the form of spines. The body shape may be included in a behavioural trait since body shape often reflects a species swimming and predation strategy. Colour markings may be less important since most species can be expected to have the colour that provides the best camouflage in a given ecosystem. Defence mechanisms costs energy, but lowers the risk for predation and could thus also be modelled as a behavioural trait. In the following different behavioural mechanisms that could be implemented in the model are discussed:

- *Foraging strategies.* Species may have different strategies for foraging where the two extremes are continuously foraging predators and predators that use a sit-and-wait strategy where passing prey is ambushed. This strategy can be implemented by modelling the used energy for activity (3.17) separately in the growth model where the sit-and-wait predators have the advantage of lower activity requirements, but the cost of a reduced food intake due to a smaller search volume. Foraging strategy also has an indirect effect on predation mortality since individuals may try to escape predation by aiming for a high growth rate, which, however, may intensity the predation risk if the individual exposes itself to more predators when foraging.

- *Defence strategies.* In the model predation mortality is only a function of the predators search volume and not the strategy of the prey. Reduced mortality due to a certain strategy (i.e. spines) can be implemented by utilising the food web framework so that predators become more weakly coupled to defence strategists. The defense strategists costs for reduced mortality should be increased maintenance requirements so that less energy is available for growth, reproduction, and activity if this is modelled separately.

- *Specialisation vs. generalisation.* The role of specialisation vs. generalisation in regards to selection of food items can be studied by varying the width σ while requiring a fixed value of the integral of the food selection function (3.65). This might, however, not be a very important trait in aquatic environments since the lognormal size selection function is valid for i.e. both copepods and cods (cf. section 3.2.1), but investigations should naturally be carried out to ensure that it is not so that the food selection of many species cannot be described with the default parameters.

- *Different spawning periods.* Species may spawn at different times during the year and/or have very different spawning habitats. To include different spawning periods the time resolution of the model should be enhanced since the model is expressed in time-steps of years. Different spawning grounds may be incorporated via the food web structure, and should per see not be regarded as a trait.

- *Size/age at maturation.* Species may have different relationships or a different proportionality than the used proportional relation (3.60) between w_{mat} and w_∞. Using age of maturation instead of size at maturation can be more realistic for some species, but is not expected to play an important role for the qualitative results. Early maturation has the advantage of a low mortality risk before maturation, and the cost of a reduced reproductive capability.

It is of course possible to list even more traits, but only the most important should be modelled to enable simple models that encapsulates a high degree of ecological realism.

The two first behaviourial mechanisms require incorporation into the bioenergetic growth model, and the foraging strategy mechanism is more easily implemented since it may be incorporated by using the trade-off that increasing values of the prefactor γ in the search volume (3.62) should lead to an increasing prefactor for the activity requirements (3.17). The defense mechanism involves a trade-off between an energetic maintenance term and the dimensionless coupling to predators, which may be more difficult to quantify. Specialisation vs. generalisation is not expected to be very important in aquatic ecosystems. Different spawning periods require implementation of a finer time-scale, and the possibility of different spawning grounds is already included in the food web structure. Size/age at maturation is interesting when studying the evolutionary effects of harvesting, and is not expected to play a significant role in promotion of coexistence since it may play a role similar to differing w_∞.

From this discussion it may be concluded that that the most obvious first extra trait to incorporate in the model would be a trait to describe foraging strategy since this is most easily implemented. The foraging strategy could be interesting since an individual may use up to 80% of the available energy on activity meaning interesting patterns could emerge from such studies; in the next section it is discussed that such further traits might lead to food web structures that enforces coexistence. As discussed above predation risk may be regulated by the activity of the prey, and including an activity dependent refuge could thus be interesting as well.

8.2 Coexistence in the Size-Structured Model

In this section the mechanisms that have been located for coexistence in the developed model are discussed. First the possibilities for coexistence in the completely mixed environment setting is treated (section 8.2.1), and secondly food web structure induced coexistence is discussed in section 8.2.2.

Before advancing to the mechanisms for coexistence it is noted that section 7.4 concluded that the spectra shape and distribution in the dynamic model is consistent with the predictions in the reduced steady-state model of section 5.1. The full dynamic model produces consistent spectra even though one of the key assumptions of the reduced model is violated. In the reduced model food is assumed abundant, which definitely is not the case in the full model where i.e. the observed peaks in the spectra upon maturation are due to low feeding levels. The full model includes an ontogenetic shift in the growth trajectory upon maturation which amplify the problem of a low feeding level due to increased energy requirements upon maturation.

8.2.1 Coexistence in the Completely Mixed Environment

In chapter 6 it was shown that coexistence is possible in the setting of a completely mixed environment where everybody is capable of eating everybody if they are of a suitable size. Coexistence is possible in this setting due to the trophic ladder mechanism. Small species can reach the size of maturation and thus exist purely on the truncated background spectrum. Larger species cannot do this and thus need the smaller species as a trophic ladder for existence. This pattern enables coexistence, and it was shown that the mechanism can be generalised to more than two species. It was also demonstrated that coexistence with species in between the steps of the trophic ladder is possible. In the following the results of the examinations of the trophic ladder mechanism is discussed further along with perspectives for obtaining even more coexistence in the mixed environment setting.

The trophic ladder mechanism was studied more thoroughly in the two species case. When the size of the smaller species is kept constant the larger species can coexist up to a maximum w_∞. This higher level is determined by the theory that describes the maximum w_∞ on a truncated background spectrum since the smaller species can be seen as an extension of the background spectrum. A lower level for the size of the large species does not exist since it can coexist down to the size that allows it persist on its own. Actually coexistence is possible further down to a w_∞ where the smallest species becomes competitively superior. This is an example of coexistence without the trophic ladder mechanism; the smaller species do, however, assist the larger species in obtaining a higher biomass. When the size of the larger species is hold constant there is a lower, and an upper level for the w_∞ of the small species that allow coexistence. The lower level is due to the same mechanism as before since the background spectrum has to be extended to a certain length to enable existence of the larger species. The upper level is due to decreasing food availability for the larger species. As w_∞ of the small species is increased its spectrum magnitude decreases since the same amount of food has to be distributed to a larger size range of individuals within the species. When the magnitude drops below a certain level the food available for the large species drops to a level that does not allow it to reach maturation.

An enrichment experiment of the two-species system was performed. Comparable to the results of the studies of Intraguild Predation (IGP) by Mylius et al. (2001) it was found that the smallest species is driven to extinction at high levels of enrichment. The smaller species link to the larger species and its cannibalistic capability can be removed without changing the qualitative results of the experiment, which thus enables comparison with the Mylius et al. (2001) study. The large species cannibalistic capability is, however, important since the smaller species is driven to extinction because the large species enter the alternative dwarf-giant state that allows it to exist without the smaller species. The large species can enter the dwarf-giant state even on a low initial biomass spectrum since it may enter the state by increasing its biomass through predation on the smaller species in the transient of the simulation, meaning that the smaller species actually assists in its own extinction. Bistability allows extinction of the smaller species at two different levels of enrichment since the large species may enter the dwarf-giant state at a lower level of enrichment if the simulation is started with high biomass spectra. Without cannibalism the smaller species is still driven to extinction, but not until a very high level of enrichment where the large species can exist purely on the background spectrum. Mylius et al. (2001) conclude that food chains cannot involve strong competition

between an intermediate consumer and a predator since the consumer is driven to extinction over a large range of enrichment. The conclusion of the experiment using the size-structured model is that coexistence indeed is possible for two species that have strong competition in earlier life stages. If cannibalism is removed the species are even allowed to coexist over an even larger range of enrichment. If the two species are to have strong competition over a large size w range the species should have comparable w_∞. In this case clearly only the competitively superior species will sustain.

Even though the trophic ladder can be extended to multiple steps it is not likely that the mechanism is responsible for major parts of the biodiversity that is seen in nature. The trophic ladder can however play a role in the structure of size-structured food webs and thus assist in species coexistence. As discussed in chapter 6 the addition of a parallel mechanism of interference competition (i.e. Loeuille & Loreau (2005) and Scheffer & van Nes (2006)) in the size-structured model might increase the possibility of having states in between the steps of the trophic ladder. Cannibalism partly plays the role of self-interference with the notable difference that cannibalism also attributes to an energy gain of the species.

The trophic ladder is a food web structure that emerges from lower-level processes and that assists in species coexistence. It may be speculated that addition of more species trait can lead to other mechanisms for coexistence in the completely mixed environment. Having differing foraging strategies might i.e. lead to coexistence between different strategists since they can be expected only to interfere weakly. Performing research into trait induced coexistence could thus be interesting to locate additional lower-level processes that assist in generating food web structures.

8.2.2 Coexistence from Food Web Structure

Chapter 6 generalises the model from chapter 3 so that it can be used to study food web structures. The concept of an *experienced total spectrum* for a species is introduced to enable the possibility that not all species are capable of predating on each other. Preferences in the range [0; 1] determine how strongly coupled a species is to both the background and other species. Preference strengths are different from interaction strengths in classical unstructured food webs since the resulting interaction strength in the size-structured framework is the product of the preference and the size-selection function. This is also why preference matrices can be expected to have higher connectance values than classical interaction matrices. A high connectance value was used when constructing food webs, and the resulting system of coexisting species also had high connectance values compared to classical unstructured food webs. In the thesis the role of the background preferences was not examined since they only play a smaller role in the food web structure where intra- and inter-species preferences primarily are of interest. All species need access to the background spectrum to provide food for the smallest individuals and differing background preferences will thus give different growth opportunities. In all experiments a background preference of 1 was used.

The most challenging part of using the food web framework is the problem of determining how the food web should be assembled. This problem has not been tackled in this thesis, but two simple approaches have shown that a food web structure indeed enhances the possibilities for coexistence.

The simplest method to construct the preference matrix is a null model where all

preferences are selected randomly from [0; 1]. In section 7.3.1 this method resulted in a state where 7 species coexist with low biomass fluctuations. No investigation has been carried out to how likely the null model is to produce multi-species states, but the example illustrates that *differing preference strengths* indeed can promote coexistence.

As a second approach food webs were constructed using the niche model (Williams & Martinez (2000)) to show that the *structure* of a food web indeed induces coexistence. The generated preferences only have links either present '1' or absent '0', and a resulting 14 species cyclic state was demonstrated in section 7.3.2. Common for the resulting stable preference matrices of the niche model is that most species are cannibals, which in section 7.2 was shown to promote coexistence due to 1) increased capability of retrieving suitable food items, and 2) that cannibalism plays the role of a damper since energy is dissipated from intake to production of new recruits. As an experiment a 0.2 preference was added to the zero preferences in the 14 species preference matrix, and this resulted in a 11 species steady-state.

Both the null model and the 0.2 preference addition in the niche model experiment produced communities with low biomass oscillations. Both are examples that many weak links dampens oscillations so that the risk of stochastic extinction is lowered. Weak links can thus be important for stability and species persistence, and empiric seems to agree that natural food webs indeed are characterised by many weak and fewer strong interactions (McCann et al. (1998)).

That both food web *structure* and *preference strengths* play a role for coexistence calls for methods that incorporate both along with many weak links in a top-down method for constructing food webs. Also it will be interesting to extend the niche model. The niche model constructs the preference matrices by assuming that some abstract one-dimensional niche trait determines the feeding relations among species. Thus it could be interesting examine the role of introducing a multi-dimensional niche trait to describe inter-species feeding relations.

The top-down approaches for food web construction does not provide any explanation for the structure of a food web, but are merely capable of producing webs with statistics similar to empiric food webs. It might even be so that the produced webs could not have evolved in nature. Natural food webs are formed by their history from species invasion, extinction, cascades, and evolutionary mutations on an even longer time-scale. A bottom-up assembly approach that takes into account a longer time-scale is needed to study the emergence of food web structures. The cases of species invasion and evolution should be considered independently to keep complexity down, but the concepts are not expected to yield very different results since species for invasion in surrounding communities not are expected to be very different from the species already present. As shown in e.g. Scheffer & van Nes (2006) the second time-scale may even assist in coexistence since species that goes extinct in a long transient can be stabilised by the weak forces taking place on the long time-scale. The second time-scale can also be interesting when studying human interactions since these may take place on a short time-scale that can increase selection pressures towards new niches so that processes on the longer time-scale plays a larger role on shorter time-scales. Such studies could hence allow assessment of the relative importance of i.e. ecological and evolutionary consequences of human interactions.

Species may have variable feeding habits. This is partly implemented in the size-structured model since individuals changes food items throughout their life history through size-dependent predation implemented with the size-selection function.

However, species may also change their diet if i.e. their favourite prey becomes rare. Such a mechanism is referred to as switching, and in section 7.5 a simple example of switching is studied. In the study each size w individual is only allowed to feed on the background and the single species that provides the largest amount of suitable food items. This promotes coexistence since no species are allowed to suddenly explode in abundances, and since species populations that are decreasing will experience a decreasing predation mortality. Biomass oscillations are low, but noisy, in the switching experiment since the constant diet shifts stabilises the biomass level. This extreme degree of switching is of course quite unnatural, and it would be interesting to study more realistic impacts of switching where switches i.e. do not take place in '0' to '1' jumps and vice versa, but that some weaker links will be maintained to less abundant species. Also the switching behaviour should be incorporated in a food web structure since a species is not likely to be capable of switching its diet to all species.

To conclude the discussion on food web structure induced coexistence the most interesting future studies are summarised: 1.a) Development of top-down methods for constructing food webs that produce food web *structures* with *differing preference strengths* that include many weak links. 1.b) Examination of the role of introducing multi-dimensional niche traits to describe inter-species feeding relations in a model similar to the niche model (Williams & Martinez (2000)). 2.a) Studies of the emergence of size-structured food webs from bottom-up assembly processes using two time-scales. 2.b) Studying promotion of coexistence via the second time-scale. 2.c) Studies of the ecological and evolutionary effects of human interactions. 3) More realistic studies of switching induced coexistence. 4) Empirical research into the structure of preference matrices in natural size-structured food webs to validate theoretical results.

8.3 Numerical Setup

The computational load of the size-structured model is naturally much higher than for the unstructured models since for each time-step a PDE is solved for each species along with +100 ODEs for the dynamics of the background spectrum. Luckily the ODEs can be solved analytically, and implementing the numerical setup with care do indeed allow the model to be used as a size-structured food web framework. A 10 species 1000 years simulation can i.e. be run in one minute on a Pentium M 760 (2.0 GHz, 2 MB L2 cache, 533 MHz FSB, 1.0 GB DDR2 SDRAM) using Matlab. Implementation in a more computationally efficient programming language can speed up computation further.

To solve the PDEs the semi-implicit Upwind scheme is used, and as discussed in chapter 4 implementation of the QUICK scheme along with the techniques by Zijlema (1996) can be expected to speed up simulations further since fewer grid points and smaller Δt's then can be used. This will furthermore reduce the numerical diffusion compared to the semi-implicit Upwind scheme. It should, however, be noted that numerical diffusion in the semi-implicit Upwind scheme was concluded not to play any qualitative role for the results of simulations.

9

Conclusion

A simple size-structured model of marine ecosystems has been developed. The model is denoted *simple* since only one trait, the ultimate body weight w_∞, is used to distinguish species. The most important part of the model is the bioenergetic growth model that allocates the acquired energy from food intake into somatic growth, maintenance, and reproduction. Individuals obtain their food intake from size-dependent predation through a size-selection function, and a background spectrum is included to provide suitable food items for the smallest individuals. The environment of an individual is completely determined by the background spectrum and the spectra of all species. From the environment the food intake is calculated, and from this the mortality and reproduction of the individuals are obtained.

Coexistence has been demonstrated in the setting of a completely mixed environment where everybody is capable of eating everybody if they are of a suitable size. Individuals of a small species can reach the size of maturation solely on background resources and thus maintain the species population. Large species cannot do so, and need the possibility of predation on larger food items as i.e. the smaller species. Large species thus uses the smaller species as a *trophic ladder* to reach the size of maturation. The trophic ladder mechanism gives rise to coexistence among different sized w_∞ species. Even though it is possible also to have coexisting species in between the steps of the ladder the mechanism is not expected to be responsible for major parts of the biodiversity that is seen in nature. The trophic ladder is a food web structure that emerges from lower level processes, and in the discussion it is suggested that adding more traits to distinguish species might lead to other mechanisms for coexistence.

The structure of a food web plays an important role for multi-species coexistence. The size-structured model was generalised to be used as a framework for size-structured food webs. In the model species can have preferences in $[0; 1]$ for both other species and the background resources. The preferences times the size-selection function correspond to interaction strengths in classical food webs why preference matrices are expected to have higher connectance values than interaction matrices. It was demonstrated that both the *structure* and *preference strengths* are important for coexistence. Generated food webs consists mainly of cannibalistic species since cannibalism promotes coexistence. In the discussion it was suggested that top-down approaches of food web construction that produce food web *structures* with *differing preference strengths* would be interesting to develop since both

are important for coexistence. The examined food web structures were produced with the niche model (Williams & Martinez (2000)) which uses a one-dimensional niche trait to describe inter-species feeding relations, and it was suggested that the niche model should be extended so that the role of multi-dimensional niche traits can be studied.

Top-down approaches for food web construction provides no explanation for the structure of a food web, and the discussion suggests research into bottom-up assembly processes where size-structured food web structures emerge from processes on a longer time-scale due to species invasions and/or evolutionary mutations on an even longer time-scale. This second time-scale can also play a role for coexistence since the weak forces on the longer time-scale may stabilise species that goes extinct on a long ecological time-scale. The second time-scale will also enable studies of ecological and evolutionary consequences of human interactions.

Species may have variable feeding habits, which is partly included in the size-structured model via the size-selection function since individuals change food items throughout their life history. A species may however also change its diet if i.e. its favourite prey becomes rare. A simple version of this switching behaviour was demonstrated to promote existence in the case where a size w individual only feeds on the background spectrum and the single species that provides the largest amount of food. It would be interesting to examine more realistic switching behaviour where the preference switches do not occur with '0' to '1' transitions, and where a food web structure is included so that species cannot switch to all species.

In conclusion three different mechanisms has been located for species coexistence: 1) the trophic ladder mechanism, 2) food web structure and preference strengths, and 3) environment dependent food web structures that allow i.e. switching behaviour. This clearly shows that the size-structured model of this thesis can be used as a more realistic multi-species modelling framework, compared to the classical unstructured models, for ecosystems where size-dependent processes are important.

Glossary

This list clarifies some words and definitions used in the thesis. This is mainly to help engineers in understanding biological terms, and to clarify some technical definitions for biologists.

Benthic species

Species that are confined to the sea floor. Mostly species that have limited moving capabilities in their 2D environment. See also *Demersal* and *Pelagic species*.

Demersal species

Species that spend most of their time on the sea floor. See also *Benthic* and *Pelagic species*.

Density dependence

When the size of a population is regulated by the size of the population itself. I.e. through food limitations.

Determinate growth

See *Indeterminate growth*.

Euryhaline species

Species living in waters with high variation in salinity.

Gonad

Sexual gland. That is an organ that produces gametes (ova and sperm).

Indeterminate growth

Species that continue growth after maturation are said to display indeterminate growth. Conversely determinate growth means that the species stops growth upon maturation (often one-time spawners).

Irreversible mass

The part of the individual's body mass that cannot be reduced (also known as somatic mass); this means, organs, skeleton, and to a high degree muscles ($\sim$ the structural biovolume of the individual). See also *Reversible mass*.

Mean value

Defined by: $\bar{f} = \frac{1}{\tau}\int_t^{t+\tau} f(t)\,\mathrm{d}t$. See also *Standard Deviation*.

Ontogenetic growth/development/shift

The life history of an individual from egg/embryo to adult. An ontogenetic shift means that the individual undergoes a sudden shift in its life trajectory; e.g. metamorphosis (i.e. egg stage to juvenile), maturation (juvenile to adult stage where reproduction starts), etc.

Pelagic species

Species that forage in the entire water column. See also *Benthic* and *Demersal species*.

Percentile

Percentiles are often used in i.e. boxplots, which are statistical plots used to illustrate time series of 2D plots (i.e. a spectrum). As an example a 25% percentile marks the level along the y-axis where no more than 25% of the points in the time series at x lie below. The term percentile is equivalent with the term quantile, which however is attributed with different notations and terminology (cf. a standard statistical textbook). Special percentiles are 50% (median), 0% (minimum), and 100% (maximum) percentiles.

Poikilothermic organisms

Organisms where the internal temperature primarily follows the temperature of the environment. Fish belongs to this group compared to i.e. humans who are endotherms, which means that they keep a constant internal temperature (also known as homeotherms). Like endotherms ectotherms (i.e. terrestrial reptiles) require constant internal temperature but unlike endotherms they cannot control the temperature themselves, but has to use environmental heating and cooling sources.

Reversible mass

The mass of an individual that can be reduced; this means lipids (fat reserves), gonads, and to some parts the liver and muscles. The reversible mass can be considered a reserve that can be consumed when food resources are sparse. An individual with zero reversible mass is very vulnerable for starvation death. Reversible mass is often referred to as lipid mass, which is clearly not strictly correct. See also *Irreversible mass*.

Somatic growth/tissue

Growth that causes increase of the individual's weight and size. Instead of somatic growth energy may be allocated into reproduction and maintenance of the metabolic requirements. So somatic tissue is the structural biovolume of the individual. See also *Irreversible mass*.

Standard deviation

Defined by: $\sigma = \sqrt{\frac{1}{\tau}\int_t^{t+\tau}(f(t)-\bar{f})^2\,\mathrm{d}t}$. See also *Mean value*.

Trophic ladder

The concept used when studying coexistence in chapter 6. Small species can reach the size of maturation solely on background resources and thus maintain their population. This is not possible for larger species since the size selectivity in the choice of food items required intake from the smaller species to obtain enough energy to grow to maturation size. The larger species thus uses the smaller species as a trophic ladder.

Trophic transfer efficiency

A measure of how efficient energy is transferred between trophic levels. If a species i.e. has high loss of energy due to maintenance of body temperature then it will have a low trophic efficiency. Considering efficiency compared to resource input may however often be more informative. Species high up in the trophic hierarchy will thus have the lowest efficiency since they feed on species that have transfer loss in lower trophic transfers.

Acronyms

DDE	Delay Differential Equation
DEB	Dynamical Energy Budgets
DFT	Discrete Fourier Transform
EBT	Escalator Boxcar Train
IGP	Intraguild Predation
ODE	Ordinary Differential Equation
PDE	Partial Differential Equation
PSP	Physiologically Structured Population
QUICK	Quadratic Upwind Interpolation for Convective Kinematics
SSB	Spawning Stock Biomass

References

1. K. H. Andersen. Description of the ecosystem model. May 3, 2005. Working note. Danish Institute for Fisheries Research (DIFRES).
2. K. H. Andersen. Personal conversation. Danish Institute for Fisheries Research (DIFRES), 2006.
3. K. H. Andersen and J. E. Beyer. Asymptotic size determines species abundance in the marine size spectrum. *The American Naturalist, to appear*, 2006.
4. K. P. Andersen and E. Ursin. A Multispecies Extension to the Beverton and Holt Theory of Fishing, with Accounts of Phosphorus Circulation and Primary Production. *Meddelelser fra Danmarks Fiskeri- og Havundersøgelser, N.S*, 7: 319–435, 1977.
5. N. G. Andersen. Personal conversation. Danish Institute for Fisheries Research (DIFRES), 2006.
6. N. G. Andersen and J. Riis-Vestergaard. Alternative model structures for bioenergetics budgets of a cruising predatory gadoid: incorporating estimates of food conversion and costs of locomotion. *Can. J. Fish. Aquat. Sci.*, 61: 2413–2424, 2004.
7. J. R. Banavar, A. Maritan, and A. Rinaldo. Size and form in efficient transportation networks. *Nature*, 399:130–132, 1999.
8. J. R. Banavar, J. Damuth, A. Maritan, and A. Rinaldo. Supply-demand balance and metabolic scaling. *PNAS*, 99(16):10506–10509, 2002a.
9. J. R. Banavar, J. Damuth, A. Maritan, and A. Rinaldo. Modelling universality and scaling. *Nature*, 420:626, 2002b.
10. J. E. Beyer. Recruitment stability and survival – simple size-specific theory with examples from the early life dynamics of marine fish. *Dana*, 7:45–147, 1989.
11. P. A. Biro, J. R. Post, and M. V. Abrahams. Ontogeny of energy allocation reveals selective pressure promoting risk-taking behaviour in young fish cohorts. *Proc. R. Soc. B*, 272:1443–1448, 2005.
12. L. Blueweiss, H. Fox, V. Kudzma, D. Nakashima, R. Peters, and S. Sams. Relationships between Body Size and Some Life History Parameters. *Oecologia (Berl.)*, 37:257–272, 1978.

13. P. R. Boudreau and L. M. Dickie. Biomass Spectra of Aquatic Ecosystems in Relation to Fisheries Yield. *Can. J. Fish. Aquat. Sci.*, 49:1528–1538, 1992.

14. J. H. Brown and J. F. Gillooly. Ecological food webs: High-quality data facilitate. *PNAS*, 100(4):1467–1468, 2003.

15. J. H. Brown, J. F. Gillooly, A. P. Allen, V. M. Savage, and G. W. West. Toward a Metabolic Theory of Ecology. *Ecology*, 85(7):1771–1789, 2004.

16. W. A. Calder III. *Size, Function, and Life History.* Harvard University Press, 1984. ISBN 0-486-69191-8. A newer (1996) edition is available from Dover.

17. J. Camacho and R. V. Solé. Scaling in ecological size spectra. *Europhys. Lett.*, 55(6):774–780, 2001.

18. M.-F. Cattin, L.-F. Bersier, C. Banašek-Richter, R. Baltensperger, and J.-P. Gabriel. Phylogenetic constraints and adaptation explain food-web structure. *Nature*, 427:835–839, 2004.

19. D. Claessen and A. M. de Roos. Bistability in a size-structured population model of cannibalistic fish - a continuation study. *Theoretical Population Biology*, 64(1):49–65, 2003.

20. D. Claessen, A. M. de Roos, and L. Persson. Dwarfs and Giants: Cannibalism and Competition in Size-Structured Populations. *The American Naturalist*, 155(2):219–237, 2000.

21. D. Claessen, A. M. de Roos, and L. Persson. Population dynamic theory of size-dependent cannibalism. *Proc. R. Soc. Lond. B*, 271:333–340, 2004.

22. J. E. Cohen and C. M. Newman. A stochastic theory of community food webs: I. models and aggregated data. *Proc. R. Soc. Lond. B*, 224:421–448, 1985.

23. C. A. Darveau, R. K. Suarez, R. D. Andrews, and P. W. Hochachka. Allometric cascade as a unifying principle of body mass effects on metabolism. *Nature*, 417:166–170, 2002.

24. A. M. de Roos. Numerical methods for structured population models: The Escalator Boxcar Train. *Numerical Methods for Partial Differential Equations*, 4:173–195, 1988.

25. A. M. de Roos. A Gentle Introduction to Physiologically Structured Population Models. In S. Tuljaparker and H. Caswell, editors, *Structured-Population Models in Marine, Terrestrial, and Freshwater Systems*, number 18 in Population and Community Biology Series, pages 119–204. Chapman & Hall, 1996.

26. A. M. de Roos and L. Persson. Physiologically structured models – from versatile technique to ecological theory. *OIKOS*, 94:51–71, 2001.

27. A. M. de Roos and L. Persson. Competition in size-structured populations: mechanisms inducing cohort formation and population cycles. *Theoretical Population Biology*, 63(1):1–16, 2003b.

28. A. M. de Roos, J. A. J. Metz, E. Evers, and A. Leipoldt. A size dependent predator-prey interaction: who pursues whom? *J. Math. Biol.*, 28:609–643, 1990.

29. A. M. de Roos, O. Diekmann, and J. A. J. Metz. Studying the Dynamics of

Structured Population Models: A Versatile Technique and its Application to Daphnia. *The American Naturalist*, 139(1):123–147, 1992.

30. A. M. de Roos, L. Persson, and E. McCauley. The influence of size-dependent life-history traits on the structure and dynamics of populations and communities. *Ecology Letters*, 6:473–487, 2003a.
31. P. C. de Ruiter, V. Wolters, and J. C. Moore, editors. *Dynamic Food Webs*. Academic Press, 2005. ISBN 0-12-088458-5.
32. B. Drossel and A. J. McKane. Modelling Food Webs. In S. Bornholdt and H. G. Schuster, editors, *Handbook of Graphs and Networks: From the Genome to the Internet*. Wiley-VCH, 2003. ISBN 3-527-40336-1.
33. B. Ebenman and L. Persson, editors. *Size-Structured Populations: Ecology and Evolution*. Springer-Verlag, 1988. ISBN 3-540-50188-6.
34. J. H. Ferziger and M. Perić. *Computational Methods for Fluid Dynamics*. Springer-Verlag, 2002. ISBN 3-540-42074-6.
35. R. W. Fléron, M. Pedersen, J. H. Hales, P. R. Bidstrup, and A. Torp. Two-Axis MOEMS Sun Sensor and MEMS Electron Emitter developed at MIC for DTUsat. In *Proceedings of ESA's 4th Round Table on Micro/Nano Technologies for Space*, 2003.
36. W. M. Getz. An introspection on the art of modeling in population ecology. *BioScience*, 48(7):540–552, 1998.
37. J. F. Gillooly, E. L. Charnov, G. B. West, V. M. Savage, and J. H. Brown. Effects of size and temperature on developmental time. *Nature*, 417:70–73, 2002.
38. J. H. Hales and M. Pedersen. Two-Axis MOEMS Sun Sensor for Pico Satellites. In *Proceedings of the 16th Annual AIAA/USU Conference on Small Satellites*, 2002.
39. T. D. Havlicek and S. R. Carpenter. Pelagic species size distributions in lakes: Are they discontinuous? *Limnol. Oceanogr.*, 46(5):1021–1033, 2001.
40. R. HilleRisLambers, J. van de Koppel, and P. M. J. Herman. Persistence despite omnivory: benthic communities and the discrepancy between theory and observation. *OIKOS*, 113(1):23–32, 2006.
41. C. S. Holling. The Components of Predation as Revealed by a Study of Small-Mammal Predation of the European Pine Sawfly. *The Canadian Entomologist*, 91(7):293–320, 1959a.
42. C. S. Holling. Some Characteristics of Simple Types of Predation and Parasitism. *The Canadian Entomologist*, 91(7):385–398, 1959b.
43. R. D. Holt and G. A. Polis. A theoretical framework for intraguild predation. *The American Naturalist*, 149(4):745–764, 1997.
44. ICES. Report of the Study Group on Multispecies Assessment in the North Sea (SGMSNS). *ICES CM*, D/06, 2005.
45. S. Jennings and S. Mackinson. Abundance-body mass relationships in size-structured food webs. *Ecology Letters*, 6:971–974, 2003.
46. S. Jennings, J. K. Pinnegar, N. V. C. Polunin, and T. W. Boon. Weak cross-species relationships between body size and trophic level belie powerful

size-based trophic structuring in fish communities. *Journal of Animal Ecology*, 70:934–944, 2001.

47. S. Jennings, K. J. Warr, and S. Mackinson. Use of size-based production and stable isotope analyses to predict trophic transfer efficiencies and predator-prey body mass ratios in food webs. *Mar. Ecol. Prog. Ser.*, 240:11–20, 2002.
48. B. E. Kendall, J. Prendergast, and O. N. Bjørnstad. The macroecology of population dynamics: taxonomic and biogeographic patterns in population cycles. *Ecology Letters*, 1:160–164, 1998.
49. D. E. Kendall, C. J. Briggs, W. W. Murdoch, P. Turchin, S. P. Ellner, E. McCauley, R. M. Nisbet, and S. N. Wood. Why do populations cycle? a synthesis of statistical and mechanistic modeling approaches. *Ecology*, 80(6):1789–1805, 1999.
50. S. R. Kerr. Theory of Size Distribution in Ecological Communities. *J. Fish. Res. Board Can.*, 31:1859–1862, 1974.
51. S. R. Kerr and L. M. Dickie. *The Biomass Spectrum – A Predator-Prey Theory of Aquatic Production*. Columbia University Press, 2001. ISBN 0-231-08458-7.
52. M. Kleiber. Body size and metabolic rate. *Physiological Reviews*, 27(4): 511–541, 1947.
53. W. Kohn. 1998 Nobel Lecture: Electronic structure of matter - wave functions and density functional. *Reviews of Modern Physics*, 71(5):1253–1266, 1999.
54. S. A. L. M. Kooijman. *Dynamic Energy and Mass Budgets in Biological Systems*. Cambridge University Press, second edition, 2000. ISBN 0-521-78608-8.
55. E. G. Leigh. The Ecological Role of Volterra's Equations. In M. Gerstenhaber, editor, *Some Mathematical Problems in Biology*, pages 1–61. The American Mathematical Society, 1968. Providence, Rhode Island, USA.
56. N. P. Lester, B. J. Shutter, and P. A. Abrams. Interpreting the von bertalanffy model of somatic growth in fishes: the cost of reproduction. *Proc. R. Soc. Lond. B.*, 271:1625–1631, 2004.
57. P. Lewy. Personal conversation. Danish Institute for Fisheries Research (DIFRES), 2006.
58. N. Loeuille and M. Loreau. Evolutionary emergence of size-structured food webs. *PNAS*, 102(16):5761–5766, 2005.
59. A. J. Lotka. *Elements of physical biology*. Williams and Wilkins, Baltimore, 1925.
60. A. M. Makarieva, V. G. Gorshkov, and B.-L. Li. Ontogenetic growth: models and theory. *Ecological Modelling*, 176:15–26, 2004.
61. M. Mangel and C. W. Clark. Towards a unified foraging theory. *Ecology*, 67 (5):1127–1138, 1986.
62. P. A. Marquet, R. A. Quiñones, S. Abades, F. Labra, M. Tognelli, M. Arim, and M. Rivadeneira. Scaling and power-laws in ecological systems. *The Journal of Experimental Biology*, 208:1749–1769, 2005.

63. N. D. Martinez, R. J. Williams, and J. A. Dunne. Diversity, Complexity, and Persistence in Large Model Ecosystems. In M. Pascual and J. A. Dunne, editors, *Ecological Networks: Linking Structure to Dynamics in Food Webs*. Oxford University Press, 2005. ISBN 0-19-518816-0.

64. K. McCann, A. Hastings, and G. R. Huxel. Weak trophic interactions and the balance of nature. *Nature*, 395:794–798, 1998.

65. A. G. McKendrick. Applications of Mathematics to Medical Problems. *Proceedings of the Edinburgh Mathematical Society*, 44:98–130, 1926.

66. T. McMahon. Size and Shape in Biology. *Science*, 179:1201–1204, 1973.

67. T. A. McMahon and J. T. Bonner. *On size and life*. Scientific American Books, Inc., 1983. ISBN 0-7167-5000-7.

68. J. A. J. Metz and O. Diekmann, editors. *The Dynamics of Physiologically Structured Populations*, volume 68 of *Lecture Notes in Biomathematics*. Springer-Verlag, 1986. ISBN 3-540-16786-2.

69. MUMM. Management Unit of the North Sea Mathematical Models – North Sea facts, March 21, 2006. http://www.mumm.ac.be/EN/NorthSea/facts.php.

70. W. W. Murdoch, B. E. Kendall, R. M. Nisbet, C. J. Briggs, E. McCauley, and R. Bolser. Single-species models for many-species food webs. *Nature*, 417: 541–543, 2002.

71. S. D. Mylius, K. Klumpers, A. M. de Roos, and L. Persson. Impact of intraguild predation and stage structure on simple communities along a productivity gradient. *The American Naturalist*, 158(3):259–276, 2001.

72. R. M. Nisbet, E. B. Muller, K. Lika, and S. A. L. M. Kooijman. From molecules to ecosystems through dynamic energy budget models. *Journal of Animal Ecology*, 69:913–926, 2000.

73. D. Pauly and R. S. V. Pullin. Hatching time in spherical, pelagic, marine, fish eggs in response to temperature and egg size. *Environmental Biology of Fishes*, 22(4):261–271, 1988.

74. M. Pedersen, J. H. Hales, and R. W. Fléron. Linear Two-Axis MOEMS Sun Sensor and the Need for MEMS in Space. In *Proceedings of the 54th International Astronautical Congress of the International Astronautical Federation, the International Academy of Astronautics, and the International Institute of Space Law*, number IAC-03-U.2.b.02, 2003.

75. L. Persson, K. Leonardsson, A. M. de Roos, M. Gyllenberg, and B. Christensen. Ontogenetic Scaling of Foraging Rate and the Dynamics of a Size-Structured Consumer-Resource Model. *Theoretical Population Biology*, 54: 270–293, 1998.

76. L. Persson, D. Claessen, A. M. de Roos, P. Byström, S. Sjögren, R. Svanbäck, E. Wahlström, and E. Westman. Cannibalism in a Size-Structured Population: Energy Extraction and Control. *Ecological Monographs*, 74(1):135–157, 2004.

77. R. H. Peters. *The ecological implications of body size*. Cambridge University Press, 1983. ISBN 0-521-24684-9.

78. I. Peterson and J. S. Wroblewski. Mortality Rate of Fishes in the Pelagic

Ecosystem. *Can. J. Fish. Aquat. Sci.*, 41:1117–1120, 1984.

79. S. L. Pimm, J. H. Lawton, and J. E. Cohen. Food web patterns and their consequences. *Nature*, 350:669–674, 1991.
80. T. Platt and K. Denman. Organisation in the pelagic ecosystem. *Helgoländer wiss. Meeresunters.*, 30:575–581, 1977.
81. W. H. Press, B. P. Flannery, S. A. Teukolsky, and W. T. Vetterling. *Numerical Recipes in C : The Art of Scientific Computing*. Cambridge University Press, 1992. ISBN 0-521-43108-5. Also available at: http://www.nr.com/.
82. A. Pütter. Studien über physiologische Ähnlickkeit. VI. Wachtstumsähnlichkeiten. *Pflügers Archiv für die gesamte Physiologie des Menschen und der Tiere*, 180:298–340, 1920.
83. J. Rodriguez and M. M. Mullin. Relation between biomass and body weight of plankton in a steady state oceanic ecosystem. *Limnol. Oceanogr.*, 31(2): 361–370, 1986.
84. D. A. Roff. An Allocation Model of Growth and Reproduction in Fish. *Can. J. Fish. Aquat. Sci.*, 40:1395–1404, 1983.
85. M. L. Rosenzweig. Paradox of Enrichment: Destabilization of Exploitation Ecosystems in Ecological Time. *Science*, 171:385–387, 1971.
86. M. L. Rosenzweig and R. H. MacArthur. Graphical representation and stability conditions of predator-prey interactions. *The American Naturalist*, 97 (895):209–223, 1963.
87. V. M. Savage, J. F. Gillooly, J. H. Brown, G. B. West, , and E. L. Charnov. Effects of Body Size and Temperature on Population Growth. *The American Naturalist*, 163(3):429–441, 2004.
88. M. Scheffer and E. H. van Nes. Self-organized similarity, the evolutionary emergence of groups of similar species. *PNAS*, 103(16):6230–6235, 2006.
89. K. Schmidt-Nielsen. *Animal Physiology: Adaptation and environment*. Cambridge University Press, third edition, 1983. ISBN 0-521-25973-8. First edition: 1975.
90. K. Schmidt-Nielsen. *Scaling: Why is animal size so important?* Cambridge University Press, 1984. ISBN 0-521-26657-2.
91. K. P. Sebens. The Ecology of Indeterminate Growth in Animals. *Annual Review of Ecology and Systematics*, 18:371–407, 1987.
92. R. W. Sheldon and T. R. Parsons. A Continuous Size Spectrum for Particulate Matter in the Sea. *J. Fish. Res. Bd. Canada*, 24(5):909–915, 1967.
93. R. W. Sheldon, A. Prakash, and W. H. Sutcliffe, Jr. The size distribution of particles in the ocean. *Limnology and Oceanography*, 17(3):327–340, 1972.
94. W. Silvert and T. Platt. Dynamic Energy-Flow Model of the Particle Size Distribution in Pelagic Ecosystems. In W. C. Kerfoot, editor, *Evolution and Ecology of Zooplankton Communities*, pages 754–763. The University Press of New England, 1980.
95. J. W. Sinko and W. Streifer. A New Model For Age-Size Structure of a Population. *Ecology*, 48(6):910–918, 1967.
96. O. Sund. Torskebestanden i 1933. *Report on Norwegian Fishery and Marine*

Investigations, IV(7):3–12, 1934.

97. U. H. Thygesen, K. D. Farnsworth, K. H. Andersen, and J. E. Beyer. How optimal life history changes with the community size-spectrum. *Proc. R. Soc. B*, 272:1323–1331, 2005.
98. S. Tuljaparker and H. Caswell, editors. *Structured-Population Models in Marine, Terrestrial, and Freshwater Systems*. Number 18 in Population and Community Biology Series. Chapman & Hall, 1996. ISBN 0-412-07271-8.
99. E. Ursin. A Mathematical Model of Some Aspects of Fish Growth, Respiration, and Mortality. *J. Fish. Res. Bd. Canada*, 24(11):2355–2453, 1967.
100. E. Ursin. On the Prey Size Preferences of Cod and Dab. *Meddelelser fra Danmarks Fiskeri- og Havundersøgelser, N.S*, 7:85–98, 1973.
101. E. Ursin. Search Rate and Food Size Preference in Two Copepods. *ICES CM*, L/23:1–13, 1974.
102. P. F. Verhulst. Notice sur la loi que la population suit dans son accroissement. *Correspondance Mathématique et Physique*, 10:113–121, 1838.
103. H. K. Versteeg and W. Malalasekera. *An Introduction to Computational Fluid Dynamics: The Finite Volume Method*. Prentice Hall, 1995. ISBN 0-582-21884-5.
104. J. J. Videler and C. S. Wardle. Fish swimming stride by stride: speed limits and endurance. *Reviews in Fish Biology and Fisheries*, 1:23–40, 1991.
105. V. Volterra. Fluctuations in the Abundance of a Species considered Mathematically. *Nature*, 118:558–560, 1926.
106. L. von Bertalanffy. Untersuchungen über die Gesetzlichkeit des Wachtums. I. Allgemeine Grundlagen der Theorie: Mathematische und physiologische Gesetzlichkeiten des Wachtums bei Wassertieren. *Wilhelm Roux Archiv für Entwicklungsmechanik der Organism*, 131:613–652, 1934.
107. L. von Bertalanffy. Quantitative Laws in Metabolism and Growth. *Quarterly Review of Biology*, 32:217–231, 1957.
108. H. von Foerster. Some Remarks on Changing Populations. In F. Stohlman, editor, *The Kinetics of Cellular Proliferation*, pages 382–407. Grune & Stratton, 1959.
109. D. M. Ware. Bioenergetics of Pelagic Fish: Theoretical Change in Swimming Speed and Ration with Body Size. *J. Fish. Res. Board. Can.*, 35:220–228, 1978.
110. E. E. Werner and J. F. Gilliam. The Ontogenetic Niche and Species Interactions in Size-Structured Populations. *Annual Review of Ecology and Systematics*, 15:393–425, 1984.
111. G. B. West, J. H. Brown, and B. J. Enquist. A General Model for the Origin of Allometric Scaling Laws in Biology. *Science*, 276:122–126, 1997.
112. G. B. West, J. H. Brown, and B. J. Enquist. The Fourth Dimension of Life: Fractal Geometry and Allometric Scaling of Organisms. *Science*, 284: 1677–1679, 1999.
113. G. B. West, J. H. Brown, and B. J. Enquist. A general model for ontogenetic growth. *Nature*, 413:628–631, 2001.

114. G. B. West, J. H. Brown, and B. J. Enquist. Growth models based on first principles or phenomenology? *Functional Ecology*, 18:188–196, 2004.

115. R. J. Williams and N. D. Martinez. Simple rules yield complex food webs. *Nature*, 404:180–183, 2000.

116. R. J. Wootton. Energy Costs of Egg Production and Environmental Determinants of Fecundity in Teleost Fishes. *Symp. zool. Soc. Lond.*, 44:133–159, 1979.

117. P. Yodzis. *Introduction to Theoretical Ecology*. Harper & Row, 1989. ISBN 0-06-047369-X.

118. P. Yodzis and S. Innes. Body Size and Consumer-Resource Dynamics. *The American Naturalist*, 139(6):1151–1175, 1992.

119. E. Zeuthen. Oxygen uptake as related to body size in organisms. *The Quarterly Review of Biology*, 28(1):1–12, 1953.

120. M. Zijlema. On the construction of a third-order accurate monotone convection scheme with application to turbulent flows in general domains. *International Journal for Numerical Methods in Fluids*, 22:619–641, 1996.

A

Analytical Solutions

This appendix gives analytical solutions to some of the equations used in the models of the thesis. By using these results in the simulations substantial computation time can be avoided. This chapter contains mainly mathematical derivations, which means that the reader is referred to the model chapters for ecological interpretation of the equations.

A.1 Modelling the Background Spectrum

The populations growth functions (3.37a)–(3.37c) for the background spectrum are solved analytically in this section. To ease notation we carry out the derivations in the unstructured model domain.

A.1.1 Logistic Growth Model

The logistic growth model for a resource of size w is given by:

$$\dot{R}_w = R_w(t) r_w \left(1 - \frac{R_w(t)}{K_w}\right) - \mu(N, w) R_w(t) \tag{A.1}$$

$$N(w,t) = \sum_w R_w(t) + \sum_i n_i(t) \tag{A.2}$$

We may reduce $\mu(N, w)$ to $\mu(\sum_i n_i(t), w)$ if the background is not experiencing predation from the background. This is however not important for the problem at hand.

From time step t to $t + \mathrm{d}t$ the mortality may be assumed constant. I.e. in the PDE solution we do not vary it between steps either. However, remember to update the value of the mortality in each iteration.

With this simpler notation we obtain:

$$\begin{aligned} \dot{R}_w &= R_w(t) r_w \left(1 - \frac{R_w(t)}{K_w}\right) - \mu_w R_w(t) \\ &= R_w(t)(r_w - \mu_w) \left(1 - \frac{R_w(t)}{K_w \left(1 - \frac{\mu_w}{r_w}\right)}\right) \end{aligned} \tag{A.3}$$

$$= R_w(t)\tilde{r}_w\left(1 - \frac{R_w(t)}{\tilde{K}_w}\right) \tag{A.4}$$

where $\tilde{r}_w$ and $\tilde{K}_w$ are interpreted as the effective growth rate and carrying capacity. To find a solution by integration we reformulate the problem with the dimensionless variable $y = \frac{R_w}{\tilde{K}_w}$:

$$\begin{aligned} \frac{\mathrm{d}y}{\mathrm{d}t} &= y\tilde{r}_w\,(1-y) \qquad \Leftrightarrow \\ \int_0^t \frac{1}{y(1-y)}\frac{\mathrm{d}y}{\mathrm{d}t'}\,\mathrm{d}t' &= \int_0^t \tilde{r}_w\,\mathrm{d}t' \end{aligned} \tag{A.5}$$

and we get:

$$\begin{aligned} \tilde{r}_w t &= \int_{y_0}^{y(t)} \frac{1}{y(1-y)}\,\mathrm{d}y = \int_{y_0}^{y(t)} \frac{1}{y}\,\mathrm{d}y + \int_{y_0}^{y(t)} \frac{1}{1-y}\,\mathrm{d}y \\ &= \Big[\ln|y| - \ln|1-y|\Big]_{y_0}^{y(t)} = \left[\ln\left(\frac{|y|}{|1-y|}\right)\right]_{y_0}^{y(t)} = \ln\left(\frac{|y(t)||1-y_0|}{|1-y(t)||y_0|}\right) \end{aligned}$$

A population number is clearly positive so that $y(t) > 0$. With the dimensionless variable y we have effectively scaled the carrying capacity to 1, which means that $1 - y(t) > 0$. This gives us:

$$\begin{aligned} \frac{y(t)}{1-y(t)} &= \frac{y_0}{1-y_0}e^{\tilde{r}_w t} \qquad \Leftrightarrow \\ y(t) &= \frac{y_0}{(1-y_0)e^{-\tilde{r}_w t} + y_0} \end{aligned} \tag{A.6}$$

Solution:

$$R_w(t) = \tilde{K}_w \frac{R_{w,0}}{(\tilde{K}_w - R_{w,0})e^{-\tilde{r}_w t} + R_{w,0}} \tag{A.7}$$

Or in substituted form:

$$R_w(t) = K_w\left(1 - \frac{\mu_w}{r_w}\right)\frac{R_{w,0}}{\left(K_w(1-\frac{\mu_w}{r_w}) - R_{w,0}\right)e^{-(r_w-\mu_w)t} + R_{w,0}} \tag{A.8}$$

A.1.2 Parabolic Growth Model

Using the same procedure as for the logistic model:

$$\begin{aligned} \dot{R}_w &= R_w(t)r_w\left(1 - \frac{R_w(t)^2}{K_w^2}\right) - \mu_w R_w(t) \\ &= R_w(t)(r_w - \mu_w)\left(1 - \frac{r_w}{r_w - \mu_w}\frac{R_w(t)^2}{K_w^2}\right) \qquad \text{(A.9)} \\ &= R_w(t)\tilde{r}_w\left(1 - \frac{R_w(t)^2}{\tilde{K}_w^2}\right) \qquad \text{(A.10)} \end{aligned}$$

This can be solved using partial fraction decomposition as in the case for the logistic growth:

$$\begin{aligned}
\tilde{r}_w t &= \int_{y_0}^{y(t)} \frac{1}{y(1-y^2)}\,\mathrm{d}y \\
&= \int_{y_0}^{y(t)} \frac{1}{y}\,\mathrm{d}y + \frac{1}{2}\left(\int_{y_0}^{y(t)} \frac{1}{(1-y)}\,\mathrm{d}y - \int_{y_0}^{y(t)} \frac{1}{(1+y)}\,\mathrm{d}y\right) \\
&= \Big[\ln|y| - \frac{1}{2}\big(\ln|1-y| + \ln|1+y|\big)\Big]_{y_0}^{y(t)} \\
&= \left[\ln|y| - \frac{1}{2}\ln\left(1-y^2\right)\right]_{y_0}^{y(t)} = \left[\ln\left(\frac{|y|}{\sqrt{1-y^2}}\right)\right]_{y_0}^{y(t)} \\
&= \ln\left(\frac{|y(t)|}{|y_0|}\sqrt{\frac{1-y_0^2}{1-y(t)^2}}\right)
\end{aligned}$$

As in the case of the logistic growth we have $y(t) \in [0;1]$ which gives us:

$$\begin{aligned}
\frac{y_0^2}{1-y_0^2}e^{2\tilde{r}_w t} = \frac{y(t)^2}{1-y(t)^2} \qquad &\Rightarrow \\
y(t) = \sqrt{\frac{y_0^2}{(1-y_0^2)e^{-2\tilde{r}_w t} + y_0^2}} \qquad &\text{(A.11)}
\end{aligned}$$

Back-substituting we arrive at:

$$R_w(t) = \tilde{K}_w\sqrt{\frac{R_{w,0}^2}{(\tilde{K}_w^2 - R_{w,0}^2)e^{-2\tilde{r}_w t} + R_{w,0}^2}} \qquad \text{(A.12)}$$

$$= \sqrt{\frac{r_w - \mu_w}{r_w}}K_w\sqrt{\frac{R_{w,0}^2}{(\frac{r_w-\mu_w}{r_w}K_w^2 - R_{w,0}^2)e^{-2(r_w-\mu_w)t} + R_{w,0}^2}} \qquad \text{(A.13)}$$

A.1.3 Semi-chemostatic Growth Model

Again:

$$\begin{aligned}
\dot{R}_w &= r_w\big(K_w - R_w(t)\big) - \mu(N,w)R_w(t) \qquad \text{(A.14)} \\
&= (r_w + \mu_w)\left(\frac{r_w K_w}{r_w + \mu_w} - R_w(t)\right) \\
&= \tilde{r}_w\left(\tilde{K}_w - R_w(t)\right)
\end{aligned}$$

This integral is also easily solved by integration:

$$\begin{aligned}
&\int_0^t \frac{1}{\tilde{K}_w - R_w(t)}\frac{\mathrm{d}R_w}{\mathrm{d}t'}\,\mathrm{d}t' = \int_0^t \tilde{r}_w\,\mathrm{d}t' \qquad \Leftrightarrow \\
&\tilde{r}_w t = \int_{R_{w,0}}^{R_w(t)} \frac{1}{\tilde{K}_w - R_w}\,\mathrm{d}R_w = -\Big[\ln(\tilde{K}_w - R_w)\Big]_{R_{w,0}}^{R_w(t)} \qquad \Leftrightarrow \\
&R_w(t) = \tilde{K}_w - \left(\tilde{K}_w - R_{w,0}\right)e^{-\tilde{r}_w t} \qquad \text{(A.15)}
\end{aligned}$$

Or in substituted form:

$$R_w(t) = \frac{r_w K_w}{r_w + \mu_w} - \left(\frac{r_w K_w}{r_w + \mu_w} - R_{w,0} \right) e^{-(r_w + \mu_w)t} \tag{A.16}$$

For comparison with logistic growth model (A.3) we may formulate (A.14) as:

$$\dot{R}_w = K_w r_w \left(1 - \frac{R_w(t)}{K_w} \right) - \mu(N, w) R_w(t) \tag{A.17}$$

where we note that the semi-chemostatic regeneration rate is proportional with the carrying capacity and the logistic model is proportional with resource density. This gives faster regeneration times for the semi-chemostatic model.

A.2 Available Food from a Community Spectrum

The amount of available food for a predator w_p from the constant community spectrum $N_c(w)$ is found by solving the integral:

$$\begin{aligned} \phi_{i,c}(w_p) &= \int_0^\infty N_c(w) w s_i(w, w_p)\, \mathrm{d}w \\ &= \int_0^\infty \kappa w^{1-\lambda} \exp\left[-\ln^2 \left(\frac{w}{\beta w_p} \right) / (2\sigma^2) \right] \mathrm{d}w \end{aligned} \tag{A.18}$$

To ease notation we solve an equivalent integral by using the substitution $\ln w = x$:

$$\begin{aligned} \int_0^\infty K w^a e^{-b \ln^2(cw)}\, \mathrm{d}w &= K \int_0^\infty w^a e^{-b(\ln w + \ln c)^2}\, \mathrm{d}w \\ &= K \int_{-\infty}^\infty e^{x(a+1)} e^{-b(x+\ln c)^2}\, \mathrm{d}x = K \int_{-\infty}^\infty e^{-b\left((x+\ln c)^2 - \frac{a+1}{b} x\right)}\, \mathrm{d}x \\ &= K \int_{-\infty}^\infty \exp\left[-b\Big(x - \Big(\frac{a+1}{2b} - \ln c \Big) \Big)^2 + (a+1)\Big(\frac{a+1}{4b} - \ln c \Big) \right] \mathrm{d}x \\ &= K \exp\left[(a+1)\Big(\frac{a+1}{4b} - \ln c \Big) \right] \int_{-\infty}^\infty \exp\left[-b\Big(x - \Big(\frac{a+1}{2b} - \ln c \Big) \Big)^2 \right] \mathrm{d}x \\ &= K \sqrt{\frac{\pi}{b}} \exp\left[(a+1)\Big(\frac{a+1}{4b} - \ln c \Big) \right] \\ &= K \sqrt{\frac{\pi}{b}} \exp\left[\frac{(a+1)^2}{4b} \right] c^{-(a+1)} \end{aligned} \tag{A.19}$$

where the integration is carried out by realising that the integrand is a normal distribution with mean value $\frac{a+1}{2b} - \ln c$. By substituting into the variables from (A.18) we get:

$$\phi_{i,c}(w_p) = \sqrt{2\pi} \kappa \sigma \beta_i^{2-\lambda} \exp\left[\frac{1}{2} \sigma_i^2 (2-\lambda)^2 \right] w_p^{2-\lambda} \tag{A.20}$$

A.3 Predation Mortality in a Community spectrum

The size-dependent mortality for an individual of size w in a community spectrum $N_c = \kappa w^{-}\lambda$ is given by:

$$\begin{aligned}\mu(w) &= \int_0^\infty v(w_p) N_c(w_p) s(w, w_p)\,\mathrm{d}w_p \\ &= \kappa\zeta\gamma \int_0^\infty w^{q-\lambda} \exp\left[-\ln^2\left(\frac{w}{\beta w_p}\right)/(2\sigma^2)\right]\mathrm{d}w_p \end{aligned} \tag{A.21}$$

This integral can be evaluated with the use of (A.19):

$$\mu(w) = \sqrt{2\pi}\kappa\sigma\beta^{1+q-\lambda}\zeta\gamma \exp\left[\frac{1}{2}\sigma_i^2(1+q-\lambda)^2\right] w_p^{1+q-\lambda} \tag{A.22}$$

A.4 Steady-State of a Species in a Community

In the following we will solve:

$$\frac{\partial}{\partial w}\Big(g(w)n(w)\Big) = -\mu(w)n(w) \tag{A.23}$$

to obtain the steady-state spectrum equation $n(w)$ of a single species in the community spectrum. Equation (A.23) may also be formulated as:

$$\frac{1}{g(w)n(w)}\frac{\partial}{\partial w}\Big(g(w)n(w)\Big) = \frac{\partial}{\partial w}\ln\Big(c_u g(w)n(w)\Big) = -\frac{\mu(w)}{g(w)} \tag{A.24}$$

where c_u is a unity scalar with units that makes $g(w)n(w)$ unit free [m^3·year]. This can be integrated to obtain the solution:

$$\begin{aligned}\ln\Big(c_u g(w)n(w)\Big) = -\int \frac{\mu(w)}{g(w)}\,\mathrm{d}w + c \qquad &\Leftrightarrow \\ n(w) = \frac{K(w_\infty)}{g(w)} \exp\left(-\int \frac{\mu(w)}{g(w)}\,\mathrm{d}w\right) &\end{aligned} \tag{A.25}$$

where $K(w_\infty) = \exp(c)/c_u$ [m^{-3}/year] is the constant from the integration. We use the mortality and growth functions from (5.3) and (5.2). This allows us to write (A.25) as:

$$\begin{aligned}n(w) = \frac{K(w_\infty)}{\alpha h w^k - \alpha h w_\infty^{k-r} w^r} \exp\left(-\int \frac{\mu_p w^{k-1}}{\alpha h w^k - \alpha h w_\infty^{k-r} w^r}\,\mathrm{d}w\right) \\ \times \exp\left(-\int \frac{\mu_0}{\alpha h w^k - \alpha h w_\infty^{k-r} w^r}\,\mathrm{d}w\right)\end{aligned} \tag{A.26}$$

The challenge ahead is to solve the two integrals in the exponential functions.

Solving the First Integral

We start out by solving the first integral in a simpler notation:

$$\begin{aligned}\mu_p \int \frac{w^{k-1}}{aw^k - bw^r}\,\mathrm{d}w &= \frac{\mu_p}{a}\int \frac{w^{-1}}{1-\frac{b}{a}w^{r-k}}\,\mathrm{d}w = \frac{\mu_p}{a(r-k)}\int \frac{1}{x(1-\frac{b}{a}x)}\,\mathrm{d}x \\ &= \frac{\mu_p}{a(r-k)}\ln\left(\frac{x}{1-\frac{b}{a}x}\right) = \frac{\mu_p}{a(r-k)}\ln\left(\frac{w^{r-k}}{1-\frac{b}{a}w^{r-k}}\right)\end{aligned} \tag{A.27}$$

where the substitution $x = w^{r-k}$ has been used. If we switch back to the original notation the solution looks as:

$$\frac{\mu_p}{\alpha h(r-k)} \ln\left(\frac{w^{r-k}}{1-\left(\frac{w}{w_\infty}\right)^{r-k}}\right) \tag{A.28}$$

The first exponential function may now be evaluated to:

$$\begin{aligned}\exp\left(-\int \frac{\mu_p w^{k-1}}{\alpha h w^k - \alpha h w_\infty^{k-r} w^r}\,\mathrm{d}w\right) &= \exp\left(-\frac{\mu_p}{\alpha h(r-k)} \ln\left(\frac{w^{r-k}}{1-\left(\frac{w}{w_\infty}\right)^{r-k}}\right)\right) \\ = \left(\frac{w^{r-k}}{1-\left(\frac{w}{w_\infty}\right)^{r-k}}\right)^{-\frac{\mu_p}{\alpha h(r-k)}} &= w^{-\frac{\mu_p}{\alpha h}}\left(1-\left(\frac{w}{w_\infty}\right)^{r-k}\right)^{\frac{\mu_p}{\alpha h(r-k)}}\end{aligned} \tag{A.29}$$

Solving the Second Integral

The second integral we solve for $r = 1$ since the general solution is a long expression involving the β-function:

$$\begin{aligned}\mu_0 \int \frac{1}{aw^k - bw}\,\mathrm{d}w &= \frac{\mu_0}{a}\int \frac{w^{-k}}{1-\frac{b}{a}w^{1-k}}\,\mathrm{d}w = \frac{\mu_0}{a(1-k)}\int \frac{1}{1-\frac{b}{a}x}\,\mathrm{d}x \\ &= \frac{-\mu_0}{b(1-k)}\ln\left(1-\frac{b}{a}x\right) = \frac{-\mu_0}{b(1-k)}\ln\left(1-\frac{b}{a}w^{1-k}\right)\end{aligned} \tag{A.30}$$

where the substitution $x = w^{1-k}$ has been used. If we go back to the original notation we get:

$$\frac{-\mu_0}{\alpha h w_\infty^{k-1}(1-k)} \ln\left(1-\left(\frac{w}{w_\infty}\right)^{1-k}\right) \tag{A.31}$$

The second exponential function in (A.26) can be evaluated to:

$$\begin{aligned}&\exp\left(-\int \frac{\mu_0}{\alpha h w^k - \alpha h w_\infty^{k-r} w^r}\,\mathrm{d}w\right) \\ &= \exp\left(\frac{\mu_0}{\alpha h w_\infty^{k-1}(1-k)} \ln\left(1-\left(\frac{w}{w_\infty}\right)^{1-k}\right)\right) \\ &= \left(1-\left(\frac{w}{w_\infty}\right)^{1-k}\right)^{\frac{\mu_0}{\alpha h w_\infty^{k-1}(1-k)}}\end{aligned} \tag{A.32}$$

We may include the generality of r and avoid introducing the β-function by doing an approximation when deriving the integral (A.30):

$$\begin{aligned}\mu_0 \int \frac{1}{aw^k - bw^r}\,\mathrm{d}w &= \frac{\mu_0}{a}\int \frac{w^{-k}}{1-\frac{b}{a}w^{r-k}}\,\mathrm{d}w = \frac{\mu_0}{a(r-k)}\int \frac{x^{\frac{1-r}{r-k}}}{1-\frac{b}{a}x}\,\mathrm{d}x \\ &\approx \frac{\mu_0}{a(r-k)}\int \frac{1}{1-\frac{b}{a}x}\,\mathrm{d}x = \frac{-\mu_0}{b(r-k)}\ln\left(1-\frac{b}{a}x\right) \\ &= \frac{-\mu_0}{b(r-k)}\ln\left(1-\frac{b}{a}w^{r-k}\right)\end{aligned} \tag{A.33}$$

where the substitution $x = w^{r-k}$ has been used. The approximation used is $r \approx 1 \Rightarrow x^{\frac{1-r}{r-k}} \approx 1$. This result should clearly not be used far away from $r \approx 1$. When obtaining the spectrum equation in the next section we comment on the missing r generality in (A.30).

A.4.1 The Solution

Now we can write the solution (A.26) explicitly. First we find the solution with no background mortality ($\mu_0 = 0$) where the second exponential function naturally is 1. The equation for the single species spectrum with no background mortality thus becomes:

$$\begin{aligned} n(w) &= \frac{K(w_\infty)}{\alpha h w^k - \alpha h w_\infty^{k-r} w^r} w^{-\frac{\mu_p}{\alpha h}} \left(1 - \left(\frac{w}{w_\infty}\right)^{r-k}\right)^{\frac{\mu_p}{\alpha h(r-k)}} \\ &= \frac{K(w_\infty)}{\alpha h} w^{-k-\frac{\mu_p}{\alpha h}} \left(1 - \left(\frac{w}{w_\infty}\right)^{r-k}\right)^{\frac{\mu_p}{\alpha h(r-k)}-1} \end{aligned} \tag{A.34}$$

where we see that the spectrum has a scaling part that scales with $w^{-k-\frac{\mu_p}{\alpha h}}$, and a cut-off when w_∞ is approached. The solution where the mortality also includes a background mortality can only be derived in exact explicit form in the $r = 1$ case:

$$\begin{aligned} n(w) &= \frac{K(w_\infty)}{\alpha h} w^{-k-\frac{\mu_p}{\alpha h}} \left(1 - \left(\frac{w}{w_\infty}\right)^{1-k}\right)^{\frac{\mu_p}{\alpha h(1-k)}-1+\frac{\mu_0}{\alpha h w_\infty^{k-1}(1-k)}} \\ &= \frac{K(w_\infty)}{\alpha h} w^{-k-\frac{\mu_p}{\alpha h}} \left(1 - \left(\frac{w}{w_\infty}\right)^{1-k}\right)^{\frac{\mu_p+\mu_0 w_\infty^{1-k}}{\alpha h(1-k)}-1} \end{aligned} \tag{A.35}$$

The inclusion of a background mortality thus has the effect of changing the cut-off part of the spectrum. If $r \approx 1$ we get from the discussion in the previous section:

$$n(w) = \frac{K(w_\infty)}{\alpha h} w^{-k-\frac{\mu_p}{\alpha h}} \left(1 - \left(\frac{w}{w_\infty}\right)^{r-k}\right)^{\frac{\mu_p+\mu_0 w_\infty^{r-k}}{\alpha h(r-k)}-1} \tag{A.36}$$

We thus see that small deviations of r from $r = 1$ only has a minor effect on the shape of the cut-off of the spectrum. The solution (A.36) is thus the exact solution for $r = 1$ both with and without background mortality. It is also exact for $r \neq 1$ if background mortality is not included, but only approximate with added background mortality for $r \approx 1$.

A.4.2 Scaling of $K(w_\infty)$

$K(w_\infty)$ should be selected so that the summation of all species sum up to the community spectrum $N_c(w)$:

$$N_c(w) = \sum_{w_\infty} n(w; w_\infty) \tag{A.37}$$

Clearly only the scaling part of $n(w;w_\infty)$ is important in the summation. As shown in figure 5.1(b) the smaller species are dominating at smaller sizes. This means that we may use the approximation:

$$N_c(w)\Big|_{w=w_\infty} = \frac{K(w_\infty)}{\alpha h} w_\infty^{-k-\frac{\mu_p}{\alpha h}} \qquad \Leftrightarrow$$
$$K(w_\infty) = \kappa_c \alpha h w_\infty^{2k-q-2+\frac{\mu_p}{\alpha h}}$$

however, since we are clearly overestimating $K(w_\infty)$ when using $w = w_\infty$ where the cut-off has set in, the scaling should more correctly be written as:

$$K(w_\infty) \propto \kappa_c \alpha h w_\infty^{2k-q-2+\frac{\mu_p}{\alpha h}} \tag{A.38}$$

This scaling relation was used for figure 5.1(b), which qualifies the approximation.